POLITECNICO DI TORINO

Master of Science program in Physics of Complex Systems

Master Degree Thesis

Equilibrium model of fundamentalist and noise traders in a multi-asset framework

Supervisors:
Prof. Luca DALL'ASTA
Prof. Didier SORNETTE
Co-Supervisors:
Rebecca WESTPHAL

Candidate:
Emily DAMIANI
Matr. 253621

ACADEMIC YEAR: 2018 - 2019

To my parents
Anna and Domenico

Acknowledgements

I am really grateful to my supervisor Prof. Sornette for the opportunity to do the internship in his Chair. The meetings with him have been every time an occasion for learning and discussing. I really admire him and his extraordinary personality and work.
I really thank Rebecca Westphal, who helped me and guided me through the drafting of the Thesis. I could never thank her enough for her help and patience.

A special thank goes to my classmates. They have been my family in Trieste, Turin and Paris. A warmly thank is dedicated to Giuseppe, Alessio, Evelyn, Saverio, Giulia, Leonardo who have always encouraged me, made me laugh and hugged me when I needed. Naturally, infinite gratitude goes to Giovanni, Chiara, Costanza, Marco, Medea, Stefano, Fabio, Davide, Michele, Sebastiano and Giulia. You have always been there for me despite the distance to cheer me up, give me good advice and love me.

Finally, a heartfelt thanks to my parents and my sister Sara. I dedicate to them this Thesis because they have always encouraged me on the path I chose and support me to face the difficulties.

Abstract

Kaizoji et al. (2015) formulated an artificial market model which is able to reproduce financial bubbles with faster-than-exponential growth while fulfilling "stylized facts" of the financial market. Given the importance of bubbles and crashes in the financial market, research in the direction of understanding the mechanisms underlying such phenomena is more and more important. The present thesis contributes to this field of research by proposing an extension of the original market model to the multi-asset framework.

After a brief introduction of the original market model formulation, we aim at the comprehension of the reasons of the build-up of bubbles in the price trend and how they are related to the interplay between fundamentalists and noise traders. The former are rational and risk-averse traders whereas the latter are traders based on social imitation and trend following. In particular, we deepen the insight into the category of noise traders and the Ising-like structure of their class (Harras et al. (2012), Sornette (2014)). It is, indeed, the presence of an underlying phase transition from a disordered regime where the idiosyncratic opinion is determinant to the ordered phase where a manifested collective behavior of noise agents takes over that triggers the bubbles. Starting from a good comprehension of the original model, we move towards the enlargement of the original model to the case of multiple assets. In particular, our interest focuses on the case of two risky assets and one risk-free asset. We derive the new equations for the wealth dynamics, for the fundamentalists strategy and a complete new setup for the noise traders class. This latter is organized to be adherent to the original Ising-like scheme. For this reason, the class is divided into two sub-classes of traders. Each of them can trade only one type of risky asset and the risk-free asset. Each noise trader invests all his fortune in only one endowment. Thus, allowing the transitions between the two sub-classes, we can ensure the diversification of the noise traders portfolio at the aggregate level.

In the typical time series, bubbles are still present and the extended model is also able to reproduce some "stylized facts" of the financial market as far as regards the distributions of the returns. The theoretical insights into the model have been conducted in two different directions: the comprehension of the theoretical foundations at the origin of the bubbles and on the correlations between the two assets. In particular, we study the relationship between the correlation imposed a priori between the assets and the realised correlations found in the time series.

Contents

List of Figures

List of Tables

Chapter 1

Introduction

The present thesis aims to survey and extend an agent-based model of fundamentalists and noise traders proposed by Kaizoji et al. (2015), that is able to reproduce faster-than-exponential bubble growth. Indeed, as explained in Sornette (2014), Agent-based models (ABMs) furnish useful computational tools that can be used to explain the universal features of the Financial Market as the emergent phenomenon coming from the interactions of heterogeneous traders.
Indeed, a large body of the literature (Johansen et al. (2000), Sornette (2014), Lux and Marchesi (1999), Lux (1998), Chiarella et al. (2009)) agrees on the evidence that the well-known "stylised facts" of the financial market and other statistical properties of the time series cannot be explained by the classical economic assumptions, such as the "Efficient Market Hypothesis". According to Fama (1970), the latter assumes that the prices reflect the distribution of incoming news. On the contrary, in Lux (2009) it is argued that the financial market can be understood as a complex system of heterogeneous interacting traders. In other words, it is not the distribution of the news that really affects the market development, but the complex interactions among the traders, their heterogeneous expectations on the future that are decisive on the formation of the typical structure of the time series. According to Sornette (2014), this insight is able to capture more deeply how micro-interactions among traders can give origin to a more complex and sophisticated picture at the macro level. Moreover, Sornette (2014) suggests that Physics can offer useful computational tools to deal with complicated systems: agent-based models (ABMs) are the instruments for excellence in this field because they do not rely on intrinsic equilibrium assumptions. As pointed out by the author, the implementation of traders choices lead naturally to out-of-equilibrium states. This feature is remarkable and very useful, because it is a necessary condition to forecast extreme events, such as bubbles.

The literature on ABMs is very large and a complete review on it is beyond this

thesis, but we refer to Dieci and He (2018) and Hommes and LeBaron (2018) for an overvew on the argument. However, it is interesting to point out how many classical physical models have been used to understand financial time series. A great example is offered by the Ising Model. As explained in Sornette (2014), it was originally formulated to understand the transition from paramagnetism to ferromagnetism in statistical mechanics. Nevertheless, it quickly became the simplest representation of interacting agents that have to choose among a finite number of states. Indeed, the analogy between the magnetisation and the opinion polarization was already argued in the late '70s and it has been applied to many models to update the trader's opinion. In Sornette (2014), the author observes that "the Ising model is indeed one of the simplest models describing the competition between the ordering force of imitation or contagion and the disordering impact of private information or idiosyncratic noise..." (p. 8). Beyond the intuitive anology between the formation of the trader's opinion and the alignment of the spins, in Sornette (2014) a mathematical justification of the application of the Ising Model to social sciences is given. It is shown that from the models of discrete choice, in which a trader is asked to choose among a finite number of options it is possible to derive the optimal equation for the trader's choice. Surprisingly, it is exactly the same equation used to update the position of the spins (up or down) according to the Glauber dynamics. This fact does not provide only a justification to the use of a physical model in another discipline, but it gives also the oppurtunity to implement it in new models. The application of the Ising Model has been pursued by many authors (Sornette and Zhou (2006), Bornholdt (2001), Kaizoji (2000), Harras et al. (2012) etc) exploiting the idea of the spreading of social imitation among the traders. Furthermore, the intrinsic existence of a phase transition from a disordered regime to an ordered regime is the engine at the origin of many unstable states that lead to bubbles and crashes.

The model of Kaizoji et al. (2015) inherits the analogy with the Ising model. It is a model of fundamentalist and noise investors that can trade only two type of assets (risky and risk-free). Fundamentalists are rational and they trade the risky assets according to the optimal strategy given their risk aversion, that consists in the maximisation of their constant relative risk aversion expected utility function. On the contrary, noise traders are influenced by the majority opinion and the tendency to follow price momentum. The analogy of the noise traders' scheme with the Ising Model is cleared in Harras et al. (2012). According to the authors, the traders have to choose between two kind of assets and they are influenced by social imitation, which is the equivalent of the coupling interactions among the spins, and the trend-following nature that behaves as a time-varying magnetic field. As impressive result, the model of Kaizoji et al. (2015) is able to reproduce faster-than-exponential bubble growth. As shown in Kaizoji et al. (2015) and Sornette (2014), the formation of the bubbles are due to two key ingredients: the social imitation that enhances the

self-organized cooperativity and the presence of inner self-reinforcing loops created by momentum trading.

Beyond the objective to explain in details the original market model, this work aims to enlarge it to a more complex paradigm. In particular, our interest is focused in the introduction of a second risky asset against the risk-free asset and study how the traders deal with a richer problem in the asset allocation. In the following, we present the outline of the thesis.

Chapter 2 is dedicated to the formulation of the original market model. We pose the right focus on the underlying Ising-like structure of the noise traders class in order to explain the consequences of this assumption on the time series. In Chapter 3 we examine the typical time series resulting from the original model and we will give the formal explication at the origin of the bubbles and crashes. Chapter 4 introduces the formulation of the enlarged setup. We provide the derivation of the new equations for the allocation of wealth and the price dynamics. Moreover, we have updated the fundamentalists strategy to the new allocation problem and design a new set-up for the noise traders class. In Chapter 5 we show the typical time series originated from the model. We propose an explanation to the origin of the bubbles through a mean-value approach. In the second part, we deepen our insight into the model furnishing a detailed analysis on the correlations of the assets returns. The final part of the chapter is devoted to understanding if our model is able to grasp the typical behavior of real time series, whose fundamental characteristics are known as "stylized facts". Chapter 6 concludes the Thesis.

Chapter 2

The Market Model

This chapter aims to present the artificial market model, as formulated by Kaizoji et al. (2015) and further studied and modificated by Khort (2016), Ollikainen (2016) and Westphal and Sornette (2019). It consists of one risky asset and one risk-free asset at the disposal of two types of traders. The risk-free asset guarantees a fixed rate of return, whereas the risky asset pays a dividend and its return depends on past price changes.

In Kaizoji et al. (2015) the types of traders considered are fundamentalists and noise traders. The description of the fundamentalist class takes inspiration from the work of Chiarella et al. (2009): fundamentalists allocate a fraction of their wealth in the risky asset and the remaining in the risk-free asset according to a resulting optimal investment rule. The best strategy consists in the maximization of the expected utility function on future wealth according to their own level of risk. Since fundamentalists behave accordingly to a fixed rule and, thus, in the same manner, they can be represented by a single representative agent.
The description of the noise traders follows, instaed, the work of Lux and Marchesi (1999): noise traders rely on past price trends and are subjected to social imitation. Similarly to the work of Lux and Marchesi (1999), noise traders are distinguished among bearish and bullish investors on the basis of their attitude towards the future market development. According to Kaizoji et al. (2015) each noise trader invests all his fortune in only one endowment (the risky asset or the risk-free asset) according to the price trend and the influence of his acquaintances.

In Kaizoji et al. (2015) the market mechanism considered is similar to that of a Walrasian scenario (Walras (1926)), where, in case of not external supply, the net sell and buy of noise traders and fundamentalists are perfectly compensated at each period.

2.1 Dividend process and wealth dynamics

The original model of Kaizoji et al. (2015) is provided by a risky and risk-free asset. The risk-free asset pays a fixed interest rate r_f, or better, as specified in Kaizoji et al. (2015) it is in perfectly elastic supply. Hence, the wealth gained by the trader from the risk-free asset is given by the constant growth rate $R_f := 1+r_f$. At odds with the risk-free asset, the risky asset pays a dividend d_t to the shareholders that provides a element of stochasticity in the model. According to the modifications introduced first by Khort (2016), and further studied in Ollikainen (2016), Conti (2018) and Westphal and Sornette (2019), the dividend d_t is defined by a multiplicative growth process with a stochastic growth factor r_t^d.

$$d_t = (1 + r_t^d)d_{t-1}, \tag{2.1}$$

$$r_t^d := r_d + \sigma_r u_t, \tag{2.2}$$

where u_t is a RV drawn by the normal distribution $\mathcal{N}(0,1)$. In contrast with the original formulation, the dividend process does not depend on the price. Contrarily, the dividend effects the trading decisions of the fundamentalist agent. Therefore, taking into account the payment of the dividend, the total return of the risky asset over the time period $(t-1, t)$ is composed of two parts: the dividend yield d_t/P_{t-1} and the price return rate r_t, defined as

$$r_t := \frac{P_t}{P_{t-1}} - 1 = R_t - 1. \tag{2.3}$$

Since the total return rate depends on the price movements, the risky asset can be more remunerative with respect to the risk-free asset and thus be more appealing to the traders.

Following Kaizoji et al. (2015), at each time step $t-1$, each agent constructs his portfolio as a mix of risky-assets and risk-free assets, that they hold in the period $(t-1, t)$. In other words, each agent buys z_{t-1} risky assets and $z_{f,t-1}$ risk-free assets. In Kaizoji et al. (2015), the wealth dynamics is reformulated in terms of the portions of wealth invested in the risky asset, i.e. the risky fraction x_t:

$$x_t := \frac{z_t P_t}{W_t}. \tag{2.4}$$

According to the definition of the risky fraction, at time $t-1$ each trader invests x_{t-1} in the risky asset and $(1 - x_{t-1})$ in the risk-free asset. On the basis of this description, the total wealth dynamics reads:

$$W_t = W_{t-1}x_{t-1}\left[\frac{d_t}{P_{t-1}} + r_t + 1\right] + W_{t-1}(1 - x_{t-1})R_f, \tag{2.5}$$

or better

$$W_t = W_{t-1}\left[R_f + x_{t-1}\left(r_t - r_f + \frac{d_t}{P_{t-1}}\right)\right]. \tag{2.6}$$

In Kaizoji et al. (2015) the quantity in the parenthesis is defined as excess return r_{excess}:

$$r_{excess,t} := r_t - r_f + \frac{d_t}{P_{t-1}}. \tag{2.7}$$

Indeed, this quantity reflects the difference between the risky asset gain against the constant risk-free rate. The chance of gaining over the difference makes clearly the risky asset more desirable by the traders.

2.2 Fundamentalist trader

The first group of traders is composed of fundamentalists. The setup of these investors follows very closely the related work of Chiarella et al. (2009) and Brock and Hommes(1999). As described in Kaizoji et al. (2015), fundamentalists are essentially myopic risk-averse investors. They are rational traders and at each time implement the best strategy according to their own level of risk. Basically, according to Chiarella et al. (2009), fundamentalists consider the constant relative risk aversion utility function (CRRA) $U(t)$ to evaluate their propensity to the risk. The CRRA utility function is characterized by a constant risk aversion γ defined as

$$\gamma(W) = -W\frac{U''(W)}{U'(W)}, \tag{2.8}$$

from which follows the CRRA definition:

$$U(W) = \begin{cases} log(W) & \gamma = 1 \\ \frac{W^{1-\gamma}}{1-\gamma} & \gamma \neq 1 \end{cases} \tag{2.9}$$

According to the previous definition of the wealth in terms of the risky fraction (eq. 2.5), the best strategy for fundamentalists consists in maximizing the expected value of the utility function of the future wealth in terms of the risky fraction:

$$x_t^f = \max_{x_t} \mathbb{E}_t[U(W_{t+1}^f)]. \tag{2.10}$$

As explained in Chiarella et al. (2009), the maximization problem is not trivial and the dynamics of the prices is affected by the dynamics of the wealth with the result that wealth and prices co-evolve. Eq. 2.10 is equal for all fundamentalist traders. That is the reason why it is valid the hypothesis of considering one single representative fundamentalist trader that simply invests the totality of the wealth

of the group W_t^f. The maximization problem has been solved in Chiarella and He (2001). The proof is omitted here, but the solution is considered as given,

$$x_t^f = \frac{1}{\gamma} \frac{\mathbb{E}_t[r_{excess,t+1}]}{Var_t[r_{excess,t+1}]}. \tag{2.11}$$

The expected value of the excess return is computed over all available information up to time t and using the equation for the dividend process, eq. 2.11 becomes

$$\mathbb{E}_t[r_{excess,t+1}] = \mathbb{E}_t[r_{t+1}] - r_f + \frac{d_t(1+r_d)}{P_t}. \tag{2.12}$$

In order to compute the optimal value x_t^f it is necessary for the fundamentalist trader to update his belief on the expected value of the future return and on the variance of r_{excess} at time $t+1$, knowing only the information up to time t. As adopted in Khort (2016), Ollikainen (2016) and Westphal and Sornette (2019), the fundamentalist expects a constant return rate $\mathbb{E}_t[r_{t+1}] := \mathbb{E}_{rt}$ and for the sake of simplicity assumes the variance on the return to be constant in time $Var_t[r_{t+1}] = \sigma^2$. As argued in Westphal and Sornette (2019), the value of $\mathbb{E}_{rt}$ should equal the expected return in the long run and the optimal risky fraction x_t^f is approximated at the first order considering $d_t << P_t$. According to these assumptions, eq. 2.11 becomes:

$$x_t^f \simeq \frac{\mathbb{E}_{rt} - r_f + \frac{d_t(1+r_d)}{P_t}}{\gamma\sigma^2}. \tag{2.13}$$

As pointed out in Ollikainen (2016), it is evident the net separation between the long term behavior represented by $\frac{\mathbb{E}_{rt}-r_f}{\gamma\sigma^2}$ and the short term behavior, determined by the dividend-price ratio that changes in time. According to the fundamentalist philosophy, the "fundamental" value of the risky-asset is obtained by discounting the stream of dividends and thus, the fundamentalists believe that $R_{avg} \sim (1+r_d)$ on the long term. As explained by the author, any deviation from the fundamental value created by the dividend-price ratio represents an opportunity of gain. In addition, from the previous formula it is clear that the strategy of the fundamentalist traders is buying the risky asset when the dividend-price ratio is high (and thus the fundamental value is higher than actual price) and selling when the dividend-price ratio is low (and thus the actual price is higher than the fundamental value).

2.3 Noise Trader

In Kaizoji et al. (2015), noise traders' behavior is characterized by the tendency to imitate other individuals and to rely on chart trading (Lux and Marchesi (1999)). They do not diversify their portfolios allocating a portion of their wealth in the risky

asset and following a precise maximization rule, but they invest all their wealth in the risky asset or in the risk-free asset at each period. As remarked in Kaizoji et al. (2015), the lack-of-diversification behavior has been documented in Kelly (1995) and it is not far from the reality. Therefore, their contribution can be considered only at the aggregate level: noise traders behave as a unique group trading a total wealth W_t^n, that is equally distributed among the traders. Thus, the portion of wealth invested in the risky asset x_t^n is accounted as the fraction of noise traders investing in it. Therefore, the reason why the noise traders can be considered a unique agent is subtly different from fundamentalists: each noise trader acts differently, but only the impact of the whole class really matters in the allocation of the total wealth.

Essentially, noise traders are subjected to social imitation and trend-following attitude. Each investor is pushed by the majority opinion and from the past price changes. The former is the easiest form of human conditioning, the latter is the conviction that is possible to extract information from the past price trend to predict the future development of the market. The general setup of the noise trader class is organized as follows.

The group is divided into two subgroups denoted as N_t^+ if they holds the risky asset and N_t^- otherwise. Needless to say, the sum of the two gives the total number of noise traders $N_n = N_t^+ + N_t^-$. Given the lack of diversification, the noise traders can be seen as a unique group where the fraction of invested wealth in the risky asset is given by

$$x_t^n := \frac{N_t^+}{N_n}. \tag{2.14}$$

Following the suggestion given in Lux and Marchesi (1999), in Kaizoji et al. (2015) it is introduced the opinion index s_t:

$$s_t := \frac{N_t^+ - N_t^-}{N_n} \in [-1,1], \tag{2.15}$$

which measures the attitude of the class towards the risky asset. According to Kaizoji et al. (2015), a positive value indicates a bullish attitude, while a negative value a bearish one.

According to Kaizoji et al. (2015), the total number of noise traders is fixed, but the opinion of each noise traders changes continuously in time: during the period $(t-1,t)$ each noise trader may decide to invest in the risky asset if he holds the risk-free asset or decide to maintain his previous investment strategy. The switching between the two sub-group is regulated by the following set of probabilities: p_t^- represents the probability that a noise trader out of N_t^- decides to buy the risky asset,

whereas p_t^+ represents the probability that a trader of N_t^+ decides to sell the risky asset. Each binary decision is represented by a Bernoulli RV $\xi(p)$. Each noise trader in N_t^- at time t, can either stay within the group ($\xi = 0$) with probability $1 - p_t^-$ or can buy the risky asset ($\xi = 1$) with probability p_t^-. Similarly, any trader of N_t^+ can decide to sell the risky asset with probability p_t^+ ($\xi = 1$). According to these rules, the number of traders in each subgroup at time t is given by

$$N_t^- = \sum_{j=1}^{N_{t-1}^+} \xi_j(p_{t-1}^+) + \sum_{j=1}^{N_{t-1}^-} [1 - \xi_j(p_{t-1}^-)], \tag{2.16a}$$

$$N_t^+ = \sum_{j=1}^{N_{t-1}^-} \xi_j(p_{t-1}^-) + \sum_{j=1}^{N_{t-1}^+} [1 - \xi_j(p_{t-1}^+)]. \tag{2.16b}$$

Obviously, the switching probabilities depend on the two factors that can influence the noise traders. The effect of the opinion of the majority of the traders is accounted mathematically by the opinion index s_t, whereas, the "chartist" attitude of the noise traders is caught by an indicator of the price trend, called price momentum H_t. According to Kaizoji et al. (2015), the latter is define as the exponential moving average of the past price changes:

$$H_t = \theta H_{t-1} + (1 - \theta) r_{t-1} = \theta H_{t-1} + (1 - \theta) \left(\frac{P_t}{P_{t-1}} - 1 \right). \tag{2.17}$$

Here, $\theta \in [0,1[$ is an exogenous parameter controlling the time window over which the noise traders compute the exponential moving average of past returns: $\tau_{memory} \sim 1/(1 - \theta)$.
For the sake of simplicity, the relationship between the probabilities and performance factor of the risky asset ($s_t + H_t$) is taken to be linear:

$$p_t^{\pm} = \frac{1}{2} \left(p_{\pm} \mp \frac{p_{\pm}}{p_+} \kappa_t (s_t + H_t) \right). \tag{2.18}$$

The formulation of eq. 2.18 is taken from Khort (2016) and slightely differs from the original equations in Kaizoji et al. (2015). Eq. 2.18 introduces the new parameter κ_t. It is called herding propensity and its sign and magnitude reflects the strength of social herding and momentum trading. Kaizoji et al. (2015) explains that in the case when $\kappa_t > 0$, the probability p_t^- increases and so increases the possibility that a new trader buys the risky asset, wheres the probability p_t^+ to buy the risk-free asset decreases. In the absence of social herding or momentum influence, the probabilities assume the values of the exogenous parameters $p_{\pm}$ that represent a measure of the time window over which the same decision is maintained ($\sim 2/p_{\pm}$ time steps).

Having all the quantities defined, one can eventually write down the equation for the noise risky fraction at the next time step from eq. 2.14

$$x_t^n = \frac{1}{N_n} \sum_{j=1}^{N_{t-1}^+} [1 - \xi_j(p_{t-1}^+)] + \frac{1}{N_n} \sum_{j=1}^{N_{t-1}^-} \xi_j(p_{t-1}^-). \tag{2.19}$$

2.4 Market clearing conditions and price dynamics

This section completes the model with the derivation of price equation, which is obtained by the definition of the market clearing condition. In the following we will mark any quantity as "f" if it refers to fundamentalists and with "n" if it refers to noise traders.

Fundamentalists are represented by a unique trader with total wealth W_t^f. Instead, noise investors must be considered at their aggregate level trading a total wealth W_t^n. Thus, it is possible to calculate the aggregate excess demand for each group $i = \{f, n\}$, considering the number of risky assets z_{t-1} bought by each category:

$$\Delta D_{t-1\to t}^i = z_t^i P_t - z_{t-1}^i P_t. \tag{2.20}$$

The same equation can be expressed in terms of the risky fraction through eq. 2.4 as

$$\Delta D_{t-1\to t}^i = W_t^i x_t^i - W_{t-1}^i x_t^i \frac{P_t}{P_{t-1}}. \tag{2.21}$$

Eq. 2.21 is re-written, expliciting the dependence of the wealth dynamics on the price (eq. 2.5):

$$\Delta D_{t-1\to t}^i = W_{t-1}^i \left\{ x_t^i \left[1 + r_f + x_{t-1}^i \left(r_t - r_f + \frac{d_t}{P_{t-1}} \right) \right] - x_{t-1}^i \frac{P_t}{P_{t-1}} \right\}. \tag{2.22}$$

In the original model, the market clearing conditions are set according the Walresian auctioneer scenario (Walras (1926)): at each period, in absence of external supply, the excess demand of fundamentalists and noise traders are perfectly compensated. In other words, the equilibrium condition is given by

$$\Delta D_{t-1\to t}^f + \Delta D_{t-1\to t}^n = 0. \tag{2.23}$$

However, before inserting in eq. 2.23 the excess demands in eq. 2.21, it is necessary to further manipulate eq. 2.21 for fundamentalists because the fundamentalist risky fraction (eq. 2.11) depends on the price P_t, which makes the resolution of eq. 2.23

not trivial.
Inserting eq. 2.11 for fundamentalist risky fractions into eq. 2.22, in Khort (2016) it is shown that is possible to obtain a quadratic expression in the price P_t:

$$a_t P_t^2 + b_t P_t + c_t = 0, \tag{2.24}$$

where the parameters are given by:

$$a_t = \frac{1}{P_{t-1}} \left[W_{t-1}^n x_{t-1}^n (x_t^n - 1) + W_{t-1}^f x_{t-1}^f \left(\frac{\mathbb{E}_{rt} - r_f}{\gamma \sigma^2} - 1 \right) \right], \tag{2.25a}$$

$$b_t = \frac{W_{t-1}^f}{\gamma \sigma^2} \left\{ x_{t-1}^f \frac{d_t(1+r_d)}{P_{t-1}} + (\mathbb{E}_{rt} - r_f) \left[x_{t-1}^f \left(\frac{d_t}{P_{t-1}} - R_f \right) + R_f \right] \right\} \tag{2.25b}$$

$$+ W_{t-1}^n x_t^n \left[x_{t-1}^n \left(\frac{d_t}{P_{t-1}} - 1 - r_f \right) + R_f \right],$$

$$c_t = W_{t-1}^f \frac{d_t(1+r_d)}{\gamma \sigma^2} \left[x_{t-1}^f \left(\frac{d_t}{P_{t-1}} - R_f \right) + R_f \right]. \tag{2.25c}$$

From simple inspection, one can see that $x_t^n - 1 < 0$ and $x_{min}^f - 1 < 0 \ \forall t$, so that the coefficient $a_t < 0 \ \forall t$. On the other hand, b_t and c_t are always positive because

$$x_{t-1}^i \left[\left(\frac{d_t}{P_{t-1}} - R_f \right) + R_f \right] > 0.$$

Given that $a_t < 0, \ b_t > 0, \ c_t > 0$, the unique physical solution for the quadratic price equation is:

$$P_t = \frac{-b_t - \sqrt{b_t^2 - 4 a_t c_t}}{2 a_t}. \tag{2.26}$$

Chapter 3

Time series description and theoretical analysis

In the previous chapter we have introduced the description of the model based on the work of Kaizoji et al. (2015) with the modifications further studied in Khort (2016), Ollikainen (2016), Conti (2018) and Westphal and Sornette (2019). It consists of two types of traders, fundamentalist and noise investors trading a risky asset or a risk-free asset.
Fundamentalists are myopic rational traders, that maximize their expected utility function on future wealth according to their own level of risk. Their strategy is rational, but depends on their initial assumption on the long-term rate of return and the typical volatility of the risky asset.
On the contrary, noise traders are influenced by social imitation and the heuristic belief that the past price changes can be a useful indicator of the performance of the asset. The choice of each noise trader has probabilistic nature, introducing an inherit element of stochasticity in the model.
As mentioned in Kaizoji et al. (2015), the model does not allow the switching between the fundamentalist and noise trader strategy. At odds with other models, for instance in Lux and Marchesi (1999), the strategy switching is permitted and the emergence of bubbles is explained as the growth in the number of "chartist" traders. On the contrary, in Kaizoji et al. (2015) the emergence of bubbles are explained by the random fluctuations of the herding propensity κ_t.

In the original article, the authors speculate that the varying herding propensity can be interpreted as a changing in the economic or geopolitical environment by which noise traders are subjected. Specifically, Kaizoji et al. (2015) proposes the herding propensity to follow a discretized Ornstein-Uhlenbeck process of the type:

$$\kappa_t = \kappa_{t-1} + \eta_\kappa(\mu_\kappa - \kappa_{t-1}) + \sigma_\kappa \upsilon_t, \tag{3.1}$$

where $\eta_\kappa > 0$ represents the mean reversion rate, μ_κ is the mean and $\sigma_\kappa > 0$ is the standard deviation of the Wiener process identified by $v_t \sim N(0,1)$. The previous parameters can be computed using the assumption that on the long run κ_t has a Gaussian stationary distribution

$$\kappa_t \sim N\left(\mu_\kappa, \frac{\sigma_\kappa}{\sqrt{2\eta_\kappa}}\right). \tag{3.2}$$

In Kaizoji et al. (2015) are shown the details for the derivation of η_κ and σ_κ, the final results are:

$$\eta_\kappa = \frac{1}{\Delta T} log\left(\frac{0.2\frac{p_-}{p_+}}{\frac{p_-}{p_+} - \mu_\kappa}\right), \sigma_\kappa = 0.2p_-\sqrt{2\eta_\kappa}. \tag{3.3}$$

The aim of the chapter is to show the typical time series obtained by the market model of Kaizoji et al. (2015) and discuss the emergence of faster-than-exponential growth in price time series, benchmark of bubbles. The understanding of the emergence of bubbles is accounted trough the theoretical explanations given in Kaizoji et al. (2015) and the relationship between the noise traders class and the Ising model (Harras et al. (2012)).

3.1 Choice of parameters

This section is focused on the description of the parameters of the model and on the simulations details. We have used the code originally written by Khort (2016), Ollikainen (2016) and Westphal and Sornette (2019) and which has been furnished by the co-advisor, Rebecca Westphal. Moreover, we adopt the same set of parameters used in Westphal and Sornette (2019).

In all simulations, a unique set of the parameters is used and their values are listed in table 3.1. The reasons behind the parameters choice is found in Khort (2016) and in Ollikainen (2016). As already mentioned, fundamentalists have to make assumptions on the constant expected value of future returns and volatility. On the basis of empirical observations, the expected standard deviation of the risky asset returns is $\sigma = 0.02$, while the expected return of the risky asset is set to $\mathbb{E}_{rt} = 0.00016$. The fundamentalists' attitude towards the risk is determined by the relative constant aversion γ. Nevertheless, in Westphal and Sornette (2019), γ is not chosen a priori but imposed endogenously by the equation

$$\gamma = \frac{\mathbb{E}_{rt} + \frac{d_0}{P_0}(1 + r_d) - r_f}{x_0^f \sigma^2}. \tag{3.4}$$

	Parameters		
Assets	$r_d = 0.00016$ $\sigma_d = 0.000016$	$r_f = 0.00004$ $P_0 = 1$	$d_0 = 0.00016$ $\sigma^2 = 0.0004$
Fundamentalists	$x_0^f = 0.3$	$\mathbb{E}_{rt} = 0.00016$	$W_0^f = 10^9$
Noise Traders	$x_0^n = 0.3$ $\theta = 0.95$	$p_+ = 0.199375$ $H_0 = 0.00016$	$p_- = 0.200625$ $W_0^n = 10^9$
Herding propensity	$\mu_\kappa = 0.98 \cdot p_+$	$\eta_\kappa = 0.11$	$\sigma_\kappa = 0.001$

Table 3.1: Table of parameters used for the simulations of the agent based model formulated in Kaizoji et al. (2015). The meaning of the parameters have been explained in Chapter 2. We use the code constructed by Khort (2016), Ollikainen (2016) and Westphal and Sornette (2019).

Thus, the fundamentalists tendency to the risk is accounted in a indirect way, as a function of the initial investment into the risky asset $x_0^f = 0.3$. As far as concerns the assets, the dividend process is characterized by a growth rate of $r_d = \frac{0.04}{250} = 0.00016$, which corresponds to an annual interest rate of the 4%, whereas the standard deviation is one order magnitude smaller. Hence, the initial value of the dividend process is set to the same value $d_0 = 0.00016$. The risk-free asset is characterized, instead, by a smaller interest rate $r_f = 0.00004$. Eventually, the parameters relative to the noise traders class are chosen as follows. The time window τ_{memory} used by noise traders to compute the price momentum is linked to the parameter θ, since $\tau_{memory} = 1/(1-\theta)$. In our simulations, θ is chosen to guarantee a memory length of $\tau_{memory} \sim 100$ time steps. The parameters used for the switching probabilities $p_\pm$ are not equal, but $p_+ < p_-$. As remarked by Khort (2016), this choice ensures that in absence of trading momentum and herding behavior, the probability to sell the risk-free asset is higher than the probability of the contrary action. This choice is arbitrary but ensure the presence of more positive bubbles than negative ones.

Eventually, it is necessary to give an idea of the typical time scale τ of the simulations according to the real volatility of the financial market, which is around the 1%. In order to find the typical length of the simulation, we use the same method adopted in Ollikainen (2016). In loose words, the approach consists in deriving the time length of the simulation imposing the equality between the realised standard deviation of the returns and the empirical one. First, Ollikainen (2016) considers the return time series as a realization of a Wiener process. Therefore, between to

points α and β the following equation is valid:

$$\sigma_{T_\alpha} = \sigma_{T_\beta} \sqrt{\frac{T_\alpha}{T_\beta}}. \tag{3.5}$$

According to this equation, one can deduce the length of the time simulation T_N imposing $\sigma_{sim} = \sigma_{real}$ and thus the time scale $\tau = 1/T_N$:

$$\tau = \left(\frac{\sigma_{sim}}{0.01} \right)^2. \tag{3.6}$$

3.2 Time series description

In this section, we present the qualitative description of the time series obtained for constant herding propensity $\kappa = \mu_\kappa$ and the Ornstein-Uhlenbeck herding propensity κ_t, respectively in figure 3.1 and 3.2. The analysis follows the same formulation used in Kaizoji et al. (2015) and in Ollikainen (2016).

Figure 3.1 shows the typical time series obtained for the constant κ. The eight frames presents from above the time series of the price P_t in a semilog plot, the price return r_t, the price momentum H_t, the dividend-price ratio d_t/P_t, the noise traders switching probabilities, the risky fractions, the wealth ratio $\nu_t = W_t^n/W_t^f$ and the constant herding behavior $\mu_\kappa = \kappa = 0.98$. Along the x-axis, it is specified the time scale τ of the simulation, obtained by eq. 3.6.

The price track in the semi-log plot shows a linear increment, which corresponds to the average rate of interest $R_{avg} \sim R_d$ obtained by the dividend payments. The price fluctuates around the linear line, but without particular deviations from it. In the second frame, the price return shows fluctuations of the entity of $\sim 2\%$, which by sight alone seems to be in agreement with realistic returns time series. In the third frame it is represented the price momentum H_t and the constant initial value $H_0 = 0.00016$. From the comparison with the price, it is easy to check that the momentum development follow a similar track and when the price shows a peak, the momentum increases. This is, obviously, due to the fact that the momentum is computed as the exponential moving average of the past returns. The fourth frame shows the dividend-price ratio d_t/P_t. Obviously its development is the mirror image of the price track, but it is useful to compare it with the fundamentalist fraction x_t^f shown in the sixth frame. Indeed, as noticed by Ollikainen (2016), the optimal strategy for fundamentalists rely on eq. 2.11 that implies a linear relationship between x_t^f and d_t/P_t. From the figure it is not easy to catch the relationship, because x_t^f is maintained almost constant for the whole simulation. The fifth frame, instead, shows the noise trader switching probabilities p_t^- and p_t^+. The immediate characteristics

to notice is the mirroring effect between p_t^+, the probability to sell the risky asset and p_t^-, the probability to buy it. Naturally from their definition (eq. 2.18), when p_t^+ increases, p_t^- decreases in order to maintain fixed their sum, equal to $\frac{p^+ + p^-}{2}$. The behavior of the noise probabilities effects directly the number of traders investing in the risky asset and then, the risky fraction. Actually, the development of p_t^- mirrors the track of x_t^f very closely as we can expect from the fact that the number of traders in N_t^+ is determined linearly by p_t^- by eq. 2.14. Finally, the last frames show the wealth ratio ν_t and the herding propensity, which in this case is simply constant. In the simulations, noise and fundamentalist traders begin with the same amount of wealth ($\nu_0 = 1$), but the track shows clearly huge deviations from the initial value. The peaks correspond to the moments when noise traders wealth is much higher than the fundamentalist one. The lucky periods for noise traders coincide with when noise traders polarization, i.e. when the majority of them holds the risky fraction. As a matter of fact, the noise traders class is considered at the aggregate level and they gains more when they invest in the risky asset.

Figure 3.2 shows the results of the simulation with the Ornstein-Uhlenbeck κ_t. The plot reproduces the same scheme and shows similarities with the previous discussion, with the due differences. First, the price track shows evidence of huge deviations from the fundamental value. These are clear benchmarks of bubbles, followed by crashes that bring the price back to its fundamental. The bubbles are marked by super-exponential growth behavior. The same result was already presented in the original formulation of the market model in Kaizoji et al. (2015) and it is still present in the modificated version used by Khort (2016), Ollikainen (2016) and Westphal and Sornette (2019). As explained in Kaizoji et al. (2015), the emergence of the bubbles is related to the herding propensity κ_t that changing its value make the system pass from the sub-critical regime to the critical regime. In order to understand better the origin of bubbles in the price track, it is necessary to compare the price development with the other plots. First, it is evident that the bubbles regimes are followed by high return rates and turbulent activity, alternated by tranquil periods of quiescence. This phenomenon is called volatility clustering and it is reflected also in huge deviations in the price momentum H_t. Moreover, along with the bubbles, the noise trader risky fraction x_t^n reaches the upper limit, which means that the pool of noise traders is entirely investing in the risky asset. Once reached the complete polarization of the entire class, the situation is no more sustainable and the price falls. For a brief period, the noise fraction maintains polarized and the price dynamics shows a plateau at the end of the faster-than-exponential growth. In this moment, the noise traders experience what is called the lock-in effect. As explained in Ollikainen (2016), along the plateau, the probability to sell the risky asset becomes

zero, because of the non-negative value constraint and the dividend-price ratio becomes roughly constant. Furthermore, in the presence of bubbles, the wealth ratio ν_t shows relevant deviations. which indicates periods in which the fortune of the noise traders overcomes that of fundamentalists. However, despite the peaks of luck for the noise traders, the general trend is downwards. Thus, at the end of the simulation, the fundamentalist's strategy results to be more remunerative than the noise traders one.

In conclusion, from the comparison between the two plots, it is evident that the origin of the super-exponential growth is the presence of a time-varying herding propensity and the formation of an unstable regime (Kaizoji et al. (2015)). The underlying phenomenon will be studied deeply in the next section. Here, we propose to notice how many features are shared by the two plots, such as the mirroring effect between the risky fractions and the switching probabilities, the linear relationship between the dividend-price ratio and the fundamentalist risky fraction. However, volatility clustering, lock-in effects and bubbles are peculiarity emerging only in the case of the Ornstein-Uhlenbeck κ_t.

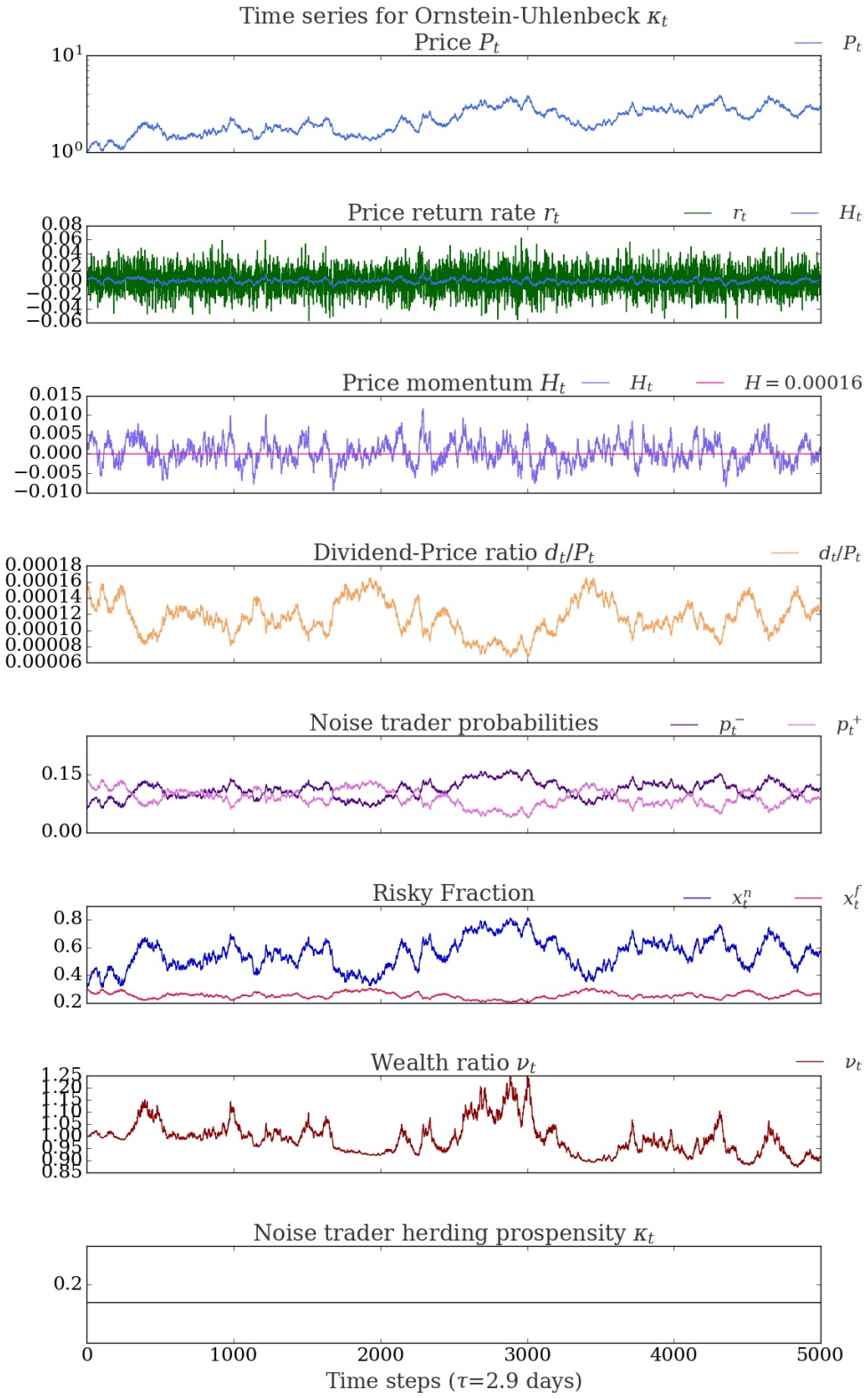

Figure 3.1: The figure shows in 8 panels the typical time series of the simulation obtained with constant κ. The plot shows in order: the price track P_t in a semilog plot, the returns r_t, the momentum H_t, the dividend-price ratio d_t/P_t, the noise trader switching probabilities $p_t^{\pm}$, the risky fractions $x_t^{f,n}$, the wealth ratio ν_t and the constant herding propensity $\kappa_t = \kappa = 0.98$. The time scale τ of the simulation is specified in x-axis and derived using eq. 3.6.

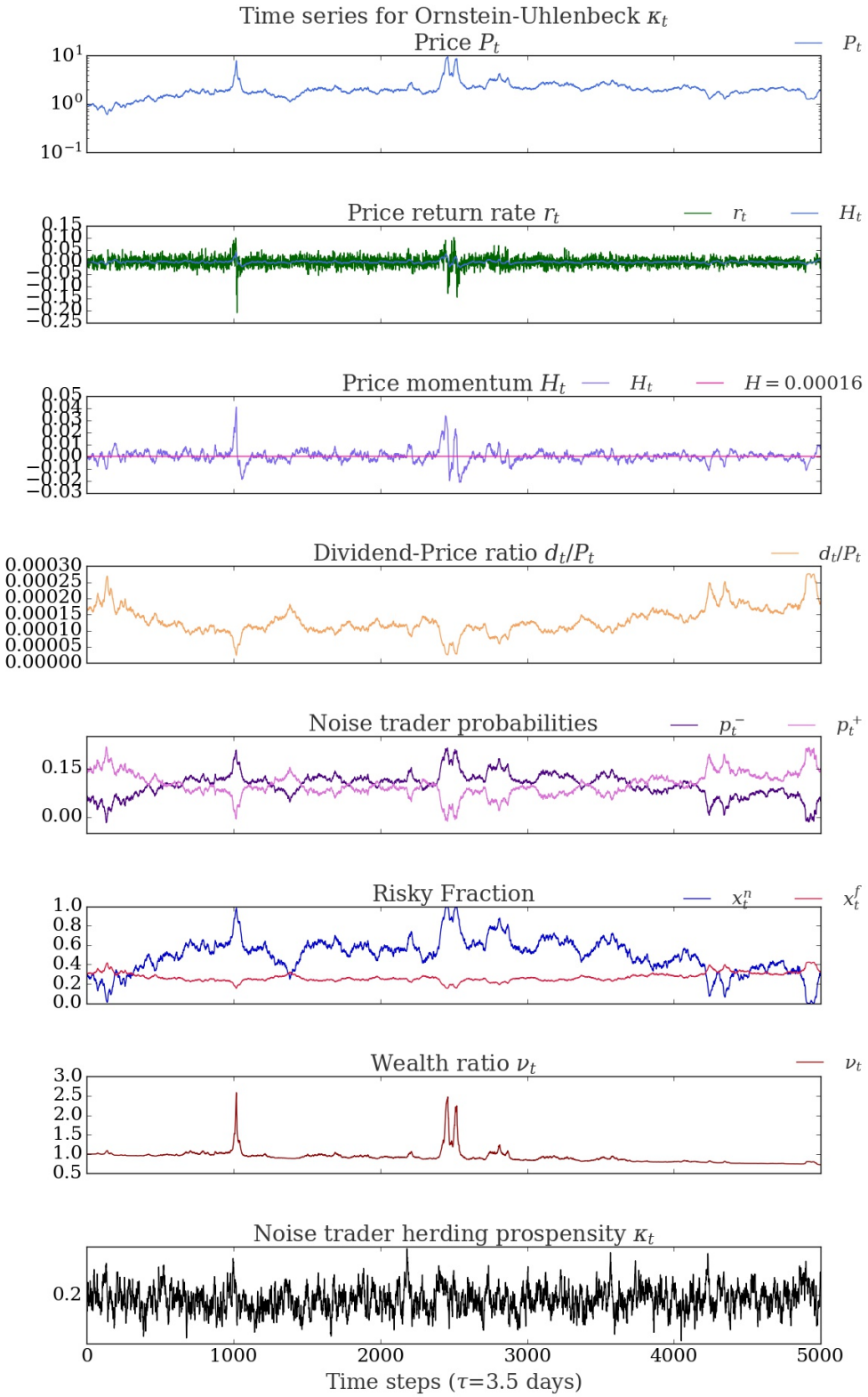

Figure 3.2: The figure shows in 8 panels the typical time series of the simulation obtained with the Ornstein-Uhlenbeck κ. The plot shows in order: the price track P_t in a semilog plot, the returns r_t, the momentum H_t, the dividend-price ratio d_t/P_t, the noise trader switching probabilities $p_t^{\pm}$, the risky fractions $x_t^{f,n}$, the wealth ratio ν_t and the constant herding propensity κ_t. The time scale τ of the simulation is specified in x-axis and derived using eq. 3.6.

3.3 Theoretical Analysis

In this section the theoretical explanation of the numerical simulations presented in section 3.2 is given. In particular, we focus on the role of the underlying Ising model presented in the artificial market and the reasons at the origin of the build-up of the bubbles. The current analysis is based on a large research conducting by Sornette and collaborators on the argument (Harras and Sornette (2011), Harras et al. (2012), Kaizoji et al. (2015), Sornette (2014)).

The market model formulated by Kaizoji et al. (2015) is characterized by heterogeneous traders, among which noise traders are influenced by social imitation and trend-following attitude. This type of investors allocates their resources on the basis of the majority opinion and of the development of the price track, signaled by the momentum. Their decisions are of probabilistic nature but the form of the equations of the switching probabilities $p_t^{\pm}$ (eq. 2.18) is not given by chance. Indeed, they represent the linearised version of the traditional switching probabilities used in the Glauber dynamics of the Ising Model (Harras et al. (2012)).

In Harras et al. (2012) the equivalence between the kinetic Ising model and the Glauber dynamics is cleared up. In the framework of the kinetic Ising model, the update of the sign of the spin s_i is given by

$$s_i(t+\delta) = sign\left(f(t) + \xi_i(t) + \sum_j K_{ij} s_j(t)\right), \tag{3.7}$$

where $f(t)$ is interpreted as the time-varying external field, K_{ij} represents the coupling constant between the spins that takes into account the nature of the magnetic interaction and ξ_i represents the noise. In contrast, the Glauber dynamics is a useful tool to update the spins of an Ising Model, provided by a probability of switching of the type

$$p = \frac{1}{e^{\beta \Delta E_i} + 1}, \tag{3.8}$$

where ΔE_i is the variation of energy given by the update of a spin. In particular, the update of the sign of the spin s_i for the Ising model is

$$s_t(t+\delta) = \begin{cases} +1 \; with \; p = (e^{-2\beta\Lambda} + 1)^{-}1 \\ -1 \; with \; p = (e^{2\beta\Lambda} + 1)^{-}1 \end{cases} \tag{3.9}$$

where $\Lambda = \sum_j K_{ij} s_j + f$. Harras et al. (2012) has demonstrated that eq. 3.7 and eq. 3.9 are equivalent if the noise $\xi_i(t)$ follow the Logistic distribution. The authors of the article point out that the sign of the spin s_i can be interpreted as the trader

decision between buying or selling the risky asset. The choice of the trader is influenced by the opinion of the neighbors, the price momentum and his opinion. Along to the analogy in Harras et al. (2012), the mean-field coupling constant is replaced by the herding propensity κ_t, whereas the magnetization is replaced by the opinion index s_t. Finally, the momentum H_t replaces the role of the external field f varying in time and the noise $\xi_i(t)$ replaces the idiosyncratic opinion of the trader.

Overall, the relationship between the noise traders class and the spins of the Ising model is now clear: the trader decision (buy or sell) follows the same dynamics. Nevertheless, the analogy does not stop to the updating rules of traders decisions, but it is reflected also in the emergence of many statistical features of the time series. The Ising model is characterized by a critical value K_c of the coupling constant that signals the separation between the ordered and disordered regime. As explained in Kaizoji et al. (2015), in the disordered regime, the private information or the idiosyncratic opinion wins over the imitative tendency of the noise traders. On the contrary, when the value of the herding propensity is greater than its critical value κ_c, the imitative behavior is so strong to overcome the opinion of the individual and the majority of the noise traders behaves in the same way causing the emergence of a collective behavior.
The consequences of the underlying kinetic Ising model have been explored in many publications, such as in Harras et al. (2012), Johansen et al. (2000), Harras and Sornette (2011) and in Sornette (2014). The principal idea in the literature is that the emergence of bubbles and crashes is linked to the following features presented in the market formulation:

1. the presence of the noise traders influenced by social imitation,

2. the emergence of cooperativity created by imitation,

3. the positive feedbacks that create reinforcing internal loops.

Specifically, Kaizoji et al. (2015) explains that the feedback internal loops are not due only to the herding behavior, but also to the trend-following attitude of the noise traders. Indeed, the momentum H_t does not act only as a time varying external field, but it depends itself on past price changes. In fact, higher is the momentum, higher is the percentage of noise traders investing in the risky asset and thus higher the price leading by the noise traders strategy. In summary, according to Kaizoji et al. (2015), the emergence of bubbles are triggered mainly by the noise traders strategy and the time varying herding propensity κ_t: following the Ornstein-Uhlenbeck dynamics, the Ising-like control parameter can move in the critical ordered regime and trigger a uniform response of the noise traders. The majority of the traders buys the risky asset, creating a self-reinforcing growth of the price, well beyond its fundamental

and thus an increasing number of traders willing to buy the risky asset. Eventually, as explained in Ollikainen (2016), during the build-up of the bubbles, more and more noise traders invest until the exhaustion of the pool of traders. At this point the regime of the price is no more sustainable and the noise traders are found in the lock-in conditions. During lock-in effects, the switching probabilities would become negative, but this eventuality is prohibited by the non-negativity condition and the probabilities are set to zero in this occasion and the only actors in the market are the fundamentalists. In response to the fundamentalists strategy, the prices begin to decrease again to reset on its fundamental value and so the fraction of noise traders involved in the risky asset decreases again.

On a final note, it is important to remark that in Kaizoji et al. (2015), Harras and Sornette (2011) and Sornette (2014) the emergence of the bubbles is due to the presence of a critical point in the underlying Ising-like structure of the noise trader class. The system passes from the critical to the sub-critical regime through the time varying control parameter (the herding propensity in this case), along to a phenomenon called the "sweeping of the instability" (see Sornette (1994)). The internal positive feedback loops created by social imitation and trend-following at the micro-level gives origin to the emergence of cooperativity among the whole noise traders class at the macro-level and to the build-up of bubbles, or better the faster-than exponential growth of the price.

Chapter 4

Market Model with two risky assets

In the previous chapters, we have analyzed in details the artificial market model elaborated by Kaizoji et al. (2015) with the modifications introduced by Khort (2016), from the model setup to the investigation of its typical time series and their theoretical explanations. Especially, we have emphasized the role of the Ising-like structure underlying the noise traders class and we have deepened our insight into the phenomena at the origin of the bubbles.

This chapter enters in the heart of the question: the introduction of a multi-asset framework. Indeed, the framework with only one asset and one risk-free asset is only the first step towards the real comprehension of the financial market. In a real situation, the traders have to face the difficult task of allocating their wealth into multiple assets and create efficient portfolios. This creates dependence between the assets. The original market model shares many features with a large part of the ABM literature such as the distinction between the risky and a risk-free asset and the presence of heterogeneity among boundedly rational traders. For example, we can cite Lux and Marchesi (1999), Brock and Hommes (1998), Chiarella and He (2001) and Chiarella and He (2002). These models investigate how the heterogeneous beliefs and the asset pricing dynamics can give origin to the statistical description of the financial time series without taking in consideration the arrival of external random news. However, the paradigm of one risky asset and one risk-free asset is far from the reality. Reason why a large part of the literature has already taken into account the allocation problem among multiple assets (Chiarella et al. (2007), Bohm and Chiarella (2005)).

The present chapter aims to introduce the problem of the asset allocation in the contest of two different risky assets and only one risk-free asset. This problem is the

immediate generalization of the original one. Nevertheless, already with two risky assets the allocation problem is not trivial. The major difficulty is the adaptation and the extension of the previous strategies for fundamentalists and noise traders to two different risky assets. Despite the difficulties, this approach let us to test the limits of the original market models, verify if it still predicts the emergence of bubbles and study the correlation between the build-up of bubbles in two different assets .

Following the original framework, the present model conserves the heterogeneous composition of boundedly rational traders. They are mainly divided into two classes: fundamentalist and noise traders, that differ for beliefs and expectations on the future development of the financial market. However, the formulation of the strategies for fundamentalists and noise traders have to be revisited.
Fundamentalists behave exactly as in the original model, but they face the issue of possible correlations between the assets (Chiarella et al. (2009), Chiarella et al. (2007)). Indeed, the traders have to deal with the possibilities of co-movements between the two assets. However, fundamentalists have now the possibility to diversify their portfolios between two risky assets and they can now invest a larger total fraction of wealth in the risky assets.
The definition of the noise traders class is more delicate and not easily suitable to an extension while maintaining the Ising structure. Our approach consists in the separation of the noise traders class into two sub-classes of traders that can trade only one type of risky asset. Enabling the switching from one subgroup to the other, each trader can decide to trade the first risky asset, the second risky asset or the risk-free asset.
Finally, the market clearing mechanism is the Walresian auctioneer (Walras (1926)) as in the original market model. The price dynamics will be derived by the equilibrium condition between noise traders and fundamentalists excess demands for both of the risky assets independently.

4.1 The multi-asset framework

The aim of this section is to enlarge the original market model of Kaizoji et al. (2015) to the multi-asset framework. The present discussion is based on a large body of literature that has studied the problem of the portfolio allocation among multiple risky assets. In particular, we can cite the work of Chiarella et al. (2009), Chiarella et al. (2007) and Bohm and Chiarella (2005). Among the vast literature, we refer to Chiarella et al. (2009) for the derivation of the wealth dynamics and the portfolio optimization problem in the case of multiple assets.

Our enlarged model is provided of two risky assets and one risk-free asset. In analogy to the original framework: the risk-free asset pays a fixed interest rate r_f, which defines a constant growth rate $R_f = 1 + r_f$. In contrast, the risky assets pay the dividends $d_{1,t}$ and $d_{2,t}$. The dividends follow the description given in Khort (2016) and Westphal and Sornette (2019), i.e. they are defined by two multiplicative growth processes with stochastic rates r_1^d and r_2^d:

$$\begin{cases} d_{1,t} = (1 + r_t^{1,d}) d_{1,t-1} \\ r_t^{1,d} = r_1^d + \sigma_1^d u_t \end{cases} \qquad \begin{cases} d_{2,t} = (1 + r_t^{2,d}) d_{2,t-1} \\ r_t^{2,d} = r_2^d + \sigma_2^d u_t \end{cases} \tag{4.1}$$

where u_t is a RV extracted from the Normal distribution $\mathcal{N}(0,1)$, whereas $\sigma_{1,2}^d$ are the standard deviations of the stochastic processes for the dividend rates.
Following the reasoning in Chiarella et al. (2009), the wealth dynamics of a trader type is given by three main contributions: $W_t^{r.f.a}$ is the wealth invested in the risk-free asset, whereas $W_t^{r.a.1}$ and $W_t^{r.a..2}$ are the wealth invested in the risky assets. Respectively they are defined as follows

$$W_t^{r.f.a} = W_{t-1}^{r.f.a} R_f, \tag{4.2}$$

$$W_t^{r.a.1} = W_{t-1}^{r.f.1} \left[\frac{d_{1,t}}{P_{1,t-1}} + r_{1,t} + 1 \right], \tag{4.3}$$

$$W_t^{r.a.2} = W_{t-1}^{r.a.2} \left[\frac{d_{2,t}}{P_{2,t-1}} + r_{2,t} + 1 \right], \tag{4.4}$$

where $r_{1,t}$ and $r_{2,t}$ represent the price returns for the two risky assets, given by the usual definitions

$$r_{1,t} := \frac{P_{1,t}}{P_{1,t-1}} - 1 \qquad r_{2,t} := \frac{P_{2,t}}{P_{2,t-1}} - 1, \tag{4.5}$$

while $d_{1,t}/P_{1,t-1}$ and $d_{2,t}/P_{2,t-1}$ identify the dividend yields. The total wealth is given by the sum of the three contributions:

$$\begin{aligned} W_t = W_{t-1} \Big[& R_f (1 - x_{1,t-1} - x_{2,t-1}) + x_{1,t-1} \left(\frac{d_{1,t}}{P_{1,t-1}} + r_{1,t} + 1 \right) + \\ & + x_{2,t-1} \left(\frac{d_{2,t}}{P_{2,t-1}} + r_{2,t} + 1 \right) \Big], \end{aligned} \tag{4.6}$$

$$W_t = W_{t-1} \left[R_f + x_{1,t-1} \left(\frac{d_{1,t}}{P_{1,t-1}} + r_{1,t} - r_f \right) + x_{2,t-1} \left(\frac{d_{2,t}}{P_{2,t-1}} + r_{2,t} - r_f \right) \right]. \tag{4.7}$$

Here, as $x_{1,t-1}$ and $x_{2,t-1}$ we intend the risky fractions, i.e. the portions of wealth invested in the risky assets. In Chiarella et al. (2009) the wealth dynamics is rewritten

using the vectorial notation to simplify the equations. Thus, we adopt the vector of prices $\mathbf{P}_t = (P_{1,t}, P_{2,t})^\intercal$, the vector of the dividends $\mathbf{d}_t = (d_{1,t}, d_{2,t})^\intercal$, the vector of the returns $\mathbf{r}_t = (r_{1,t}, r_{2,t})^\intercal$ and the vector of the risky fractions $\mathbf{x}_{t-1} = (x_{1,t-1}, x_{2,t-1})^\intercal$. Therefore, eq. 4.7 is rewritten as:

$$W_t = W_{t-1}\left[R_f + \mathbf{x}_{t-1}^\intercal\left(\mathbf{r}_t + \frac{\mathbf{d}_t}{\mathbf{P}_{t-1}} - r_f\right)\right]. \tag{4.8}$$

Following the analogy with the case of the single risky asset, it is possible to define the excess returns $r_{excess,1,t}$ and $r_{excess,2,t}$ for the two risky assets as in the following:

$$r_{excess,1,t} := r_{1,t} + \frac{d_{1,t}}{P_{1,t-1}} - r_f, \tag{4.9}$$

$$r_{exces,2,t} := r_{2,t} + \frac{d_{2,t}}{P_{2,t-1}} - r_f. \tag{4.10}$$

Using the new variables, eq. 4.7 can be recast into

$$W_t = W_{t-1}\left[R_f + x_{1,t-1}r_{excess,1,t} + x_{2,t-1}r_{excess,2,t}\right]. \tag{4.11}$$

The vectorial notation is not only useful, but it allows also to generalize the current equations to the case of N assets more easily, as shown in Chiarella et al. (2009).

4.2 Fundamentalist trader

The present model is collocated in the same paradigm of the original market model and of a large part of the ABMs based on the bounded rationality of the traders and their heterogeneity. Therefore, the model inherits the classical division of the pool of traders into fundamentalists and noise traders.
The objective of the paragraph is the introduction to the fundamentalists class. As in the original model, they are rational and risk-averse traders. Their strategy consists in maximizing the expected utility function on the future wealth for a given level of risk in terms of the risky fractions. However in the case of the multiple asset framework the maximization problem is not trivial because of the possible correlation among the risky assets (Chiarella et al. (2009)).

Following mainly the work of Chiarella et al. (2009) and the related work of Chiarella et al. (2007) and Bohm and Chiarella (2005), basically, the problem of the fundamentalist trader is to maximize the expected utility of the wealth on next period choosing the right portion of wealth to invest in each risky asset, namely

$$\max_{x_{1,t},x_{2,t}} \mathbb{E}_t[U(W_{t+1}(x_{1,t}, x_{2,t})]. \tag{4.12}$$

In the formula, U represents the CRRA utility function, defined as in eq. 2.9 with constant risk aversion γ (defined in eq. 2.8).
The maximization problem has been solved by Chiarella and He (2001) only in the framework of one risky asset. Nevertheless, its extension has already been proposed by Xu et al. (2014). In the following we derive the solution to the maximization problem, following an analogous solution to Xu et al. (2014) with the restriction to only two risky assets.
First, it is necessary to develop further the utility function U as a function of the wealth. On this purpose, it is useful to think of the wealth as a continuous function of time $W(t)$ and assume that it follows a continuous stochastic differential equation of the type

$$dW = \mu(W)dt + \sigma(W)dz, \tag{4.13}$$

where $z(t)$ is a Wiener process. Consider, now, the new variable $X = U(W)$ and assume G to be the inverse function of the utility U, such that $W = G(X)$. Using the Ito formula, we can derive the stochastic differential equation for the new variable X:

$$dX = \left[U'(W)\mu(W) + \frac{1}{2}\sigma(W)^2 U''(W)\right] dt + \sigma(W)U'(W)dz, \tag{4.14}$$

which can be re-casted into

$$dX = \mu(X)dt + \sigma(X)dz. \tag{4.15}$$

The definitions of $\mu(X)$ and $\sigma(X)$ can be simply obtained by comparison with eq. 4.14 and substitution with $W = G(X)$:

$$\mu(X) := U'(G(X))\mu(G(X)) + \frac{1}{2}\sigma^2 U''(G(X)), \tag{4.16}$$

$$\sigma(X) := \sigma(G(X))U'(G(X)). \tag{4.17}$$

Discretizing eq. 4.15, one obtains

$$X(t + \Delta t) = X(t) + \mu(X(t))\Delta t + \sigma(X(t))\Delta z, \tag{4.18}$$

with

$$\mathbb{E}_t[X(t + \Delta t)] = X(t) + \mu(X(t))\Delta t, \tag{4.19}$$

$$\mathbb{V}_t[X(t + \Delta t)] = \sigma^2(X(t)). \tag{4.20}$$

Increasing the time step to the unity, eq. 4.19 becomes

$$\mathbb{E}[X_{t+1}] = X_t + \mu(X_t). \tag{4.21}$$

Given the equality $X_{t+1} = U(W_{t+1})$, one obtains exactly the formula for the expected utility function of next period wealth:

$$\mathbb{E}_t[U(W_{t+1})] = U(W_t) + \mu_t(W_t)U'(W_t) + \frac{1}{2}\sigma_t^2(W_t)U''(W_t). \tag{4.22}$$

Nevertheless, the last equation is not already the solution, because it is necessary to work out the form for $\sigma_t(W_t)$ and $\mu(W_t)$ as functions of the two risky fractions. For this purpose, it is necessary to rewrite the wealth dynamics in eq. 4.8 as a function of the new variables $\rho_{1,t+1}$ and $\rho_{2,t+1}$, defined as the total return of each asset

$$\rho_{i,t+1} = r_{i,t+1} + \frac{d_{i,t+1}}{P_{i,t}}, \tag{4.23}$$

for $i = \{1,2\}$. The final result is

$$W_{t+1} - W_t = W_t r_f\,(1 - x_{1,t} - x_{2,t}) + W_t(x_{1,t}\rho_{1,t+1} + x_{2,t}\rho_{2,t+1}). \tag{4.24}$$

Assume that the variables $\rho_{i,t+1}$, with $i = \{1,2\}$, can be expressed in the form of stochastic discrete differential equations:

$$\rho_{1,t+1} = \mathbb{E}_t[\rho_{1,t+1}] + \sqrt{\mathbb{V}_t[\rho_{1,t+1}]}\xi_{1,t}, \tag{4.25}$$

$$\rho_{2,t+1} = \mathbb{E}_t[\rho_{2,t+1}] + \sqrt{\mathbb{V}_t[\rho_{2,t+1}]}\xi_{2,t}, \tag{4.26}$$

where $\xi_{1,t}$ and $\xi_{2,t}$ are simply RVs drawn from a Normal distribution $\mathcal{N}(0,1)$. Plugging eq. 4.26 into the wealth dynamics (eq. 4.24) leads to

$$\begin{aligned} W_{t+1} - W_t =& W_t\Big[r_f(1 - x_{1,t} - x_{2,t}) + x_{1,t}\mathbb{E}_t[\rho_{1,t+1}] + x_{2,t}\mathbb{E}_t[\rho_{2,t+1}]\Big] + \\ &+ W_t\Big(x_{1,t}\sqrt{\mathbb{V}_t[\rho_{1,t+1}]}\xi_{1,t} + x_{2,t}\sqrt{\mathbb{V}_t[\rho_{2,t+1}]}\xi_{2,t}\Big). \end{aligned}$$

The last step consists in rewriting the previous equation into a discrete stochastic differential equation

$$W_{t+1} - W_t = \mu_t(W) + \sigma_t(W)\xi_t. \tag{4.27}$$

The definition of $\mu_t(W)$ and $\sigma_t(W)$ can be obtained as the definition of mean value and standard deviation of the sum of two variables. Therefore

$$\mu_t = r_f(1 - x_{1,t} - x_{2,t}) + x_{1,t}\mathbb{E}_t[\rho_{1,t+1}] + x_{2,t}\mathbb{E}_t[\rho_{2,t+1}], \tag{4.28}$$

$$\begin{aligned} \sigma_t^2 &= \mathbb{V}\left[W_t\left(x_{2,t}\sqrt{\mathbb{V}_t[\rho_{1,t+1}]}\xi_{1,t} + x_{2,t}\sqrt{\mathbb{V}_t[\rho_{2,t+1}]}\xi_{2,t}\right)\right], \\ &= W_t^2\Big[x_{2,t}^2\mathbb{V}_t[\rho_{1,t+1}] + x_{2,t}^2\mathbb{V}_t[\rho_{2,t+1}] + 2Cov_t[\rho_{1,t+1},\rho_{2,t+1}] \\ &\quad x_{1,t}x_{2,t}\sqrt{\mathbb{V}_t[\rho_{1,t+1}]}\sqrt{\mathbb{V}_t[\rho_{2,t+1}]}\Big]. \end{aligned} \tag{4.29}$$

Plugging, thus, the equations for $\mu_t(W)$ and $\sigma_t(W)$ into eq. 4.22 leads to

$$\mathbb{E}_t[U(W_{t+1})] = U(W_t) + U'(W_t)W_t\Big(- r_f x_{1,t} + E_t[\rho_{1,t+1}]x_{1,t} - r_f x_{2,t} + \mathbb{E}_t[\rho_{2,t+1}]x_{2,t}\Big) + \frac{U''(W_t)}{2}x_{1,t}^2 W_t^2 \mathbb{V}_t[\rho_{1,t+1}] + \frac{U''(W_t)}{2}x_{2,t}^2 W_t^2 \mathbb{V}_t[\rho_{2,t+1}] + Cov_t[\rho_{1,t+1}, \rho_{2,t+1}]x_{1,t}x_{2,t}W_t^2 U''(W_t). \tag{4.30}$$

Given the expression of $\mathbb{E}_t[U(W)]$, the demonstration in Xu et al. (2014) proceeds with the resolution of the optimization problem and finds the optimal risky fractions. The usual procedure of maximization imposes the derivation of $x_{1,t}$ and $x_{2,t}$ as solution of the following system:

$$\begin{aligned}\frac{\partial \mathbb{E}_t[U(W_{t+1})]}{\partial x_{1,t}} =& W_t U'(W_t)\Big(- r_f + \mathbb{E}_t[\rho_{1,t+1}]\Big) + U''(W_t)W_t^2\Big(Cov_t[\rho_{1,t+1}, \rho_{2,t+1}]x_{2,t} + \\ &+ \mathbb{V}_t[\rho_{1,t+1}]x_{1,t}\Big) = 0\end{aligned}$$

$$\begin{aligned}\frac{\partial \mathbb{E}_t[U(W_{t+1})]}{\partial x_{2,t}} =& W_t U'(W_t)\Big(- r_f + \mathbb{E}_t[\rho_{2,t+1}]\Big) + U''(W_t)W_t^2\Big(Cov_t[\rho_{1,t+1}, \rho_{2,t+1}]x_{1,t} + \\ &+ \mathbb{V}_t[\rho_{2,t+1}]x_{2,t}\Big) = 0\end{aligned}$$

The solutions $x_{1,t}^f$ and $x_{2,t}^f$ of the maximization problem can be rewritten pointing out the dependence on the constant risk aversion γ (eq. 2.8):

$$\begin{pmatrix} x_{1,t}^f \\ x_{2,t}^f \end{pmatrix} = \frac{1}{\gamma}\begin{pmatrix} \mathbb{V}_t[\rho_{1,t+1}] & Cov_t[\rho_{1,t+1}, \rho_{2,t+1}] \\ Cov_t[\rho_{1,t+1}, \rho_{2,t+1}] & \mathbb{V}_t[\rho_{2,t+1}] \end{pmatrix}^{-1}\begin{pmatrix} \mathbb{E}_t[\rho_{1,t+1}] - r_f \\ \mathbb{E}_t[\rho_{2,t+1}] - r_f \end{pmatrix} \tag{4.31}$$

The expected value of the variables $\rho_{i,t+1}$ can be further worked out using their definitions in eq. 4.26, the definition of the dividend processes in eq. 4.1 and the assumption that fundamentalists expectations on future returns are constant, i.e. $\mathbb{E}_t[r_{i,t}] := \mathbb{E}_{rt,i}$ for $i = \{1,2\}$. This assumption is already present in the original model and it is based on the idea that fundamentalists do not learn from previous data, but form a fixed expectation on the rate of return. Therefore, we have:

$$\mathbb{E}_t[\rho_{1,t+1}] = \mathbb{E}_{rt,1} + \frac{d_{1,t}(1 + r_1^d)}{P_{1,t}}, \tag{4.32a}$$

$$\mathbb{E}_t[\rho_{2,t+1}] = \mathbb{E}_{rt,2} + \frac{d_{2,t}(1 + r_2^d)}{P_{2,t}}. \tag{4.32b}$$

Moreover, it is worthy noticing that the optimal fractions of wealth to invest depend on the inverse of the covariance matrix. Assuming the independence between the

feature returns and the dividends, it can be assumed that the contribution of the dividends is negligible and then evaluate the variance and the covariance elements of the matrix on expectations on future returns. Usually, in literature (see for instance Chiarella et al. (2009)) the following notation is adopted:

$$\begin{cases} \mathbb{V}_t[r_{j,t+1}] := \bar{\sigma_j}^2, \\ Cov_t[r_{j,t+1}, r_{k,t+1}] := \rho\bar{\sigma_k}\bar{\sigma_j}, \end{cases} \tag{4.33}$$

for $j,k = \{1,2\}$. The parameter $\rho \in [0,1]$ is understood as the correlation coefficient between the two risky assets. Eventually, the equations for the optimal risky fractions become

$$\begin{pmatrix} x^f_{1,t} \\ x^f_{2,t} \end{pmatrix} = \frac{1}{\gamma} \begin{pmatrix} \bar{\sigma_1}^2 & \rho\bar{\sigma_1}\bar{\sigma_2} \\ \rho\bar{\sigma_1}\bar{\sigma_2} & \bar{\sigma_2}^2 \end{pmatrix}^{-1} \begin{pmatrix} \mathbb{E}_{rt,1} + \frac{d_{1,t}(1+r^d_1)}{P_{1,t}} - r_f \\ \mathbb{E}_{rt,2} + \frac{d_{2,t}(1+r^d_2)}{P_{2,t}} - r_f \end{pmatrix} \tag{4.34}$$

Fortunately, finding the inverse of a 2×2 matrix is an easy task and the equations can be reformulated into

$$\begin{pmatrix} x^f_{1,t} \\ x^f_{2,t} \end{pmatrix} = \frac{1}{\gamma\bar{\sigma_1}^2\bar{\sigma_2}^2(1-\rho^2)} \begin{pmatrix} \bar{\sigma_2}^2 & -\rho\bar{\sigma_1}\bar{\sigma_2} \\ -\rho\bar{\sigma_1}\bar{\sigma_2} & \bar{\sigma_1}^2 \end{pmatrix} \begin{pmatrix} \mathbb{E}_{rt,1} + \frac{d_{1,t}(1+r^d_1)}{P_{1,t}} - r_f \\ \mathbb{E}_{rt,2} + \frac{d_{2,t}(1+r^d_2)}{P_{2,t}} - r_f \end{pmatrix} \tag{4.35}$$

$$x^f_{1,t} = \frac{1}{\gamma\bar{\sigma_1}^2(1-\rho^2)}\Big[\mathbb{E}_{rt,1} - r_f + \frac{d_{1,t}(1+r^d_1)}{P_{1,t}}\Big] - \frac{\rho}{\gamma\bar{\sigma_1}\bar{\sigma_2}(1-\rho^2)}\Big[\mathbb{E}_{rt,2} + \frac{d_{2,t}(1+r^d_2)}{P_{2,t}} - r_f\Big], \tag{4.36a}$$

$$x^f_{2,t} = \frac{1}{\gamma\bar{\sigma_2}^2(1-\rho^2)}\Big[\mathbb{E}_{rt,2} - r_f + \frac{d_{2,t}(1+r^d_2)}{P_{2,t}}\Big] - \frac{\rho}{\gamma\bar{\sigma_1}\bar{\sigma_2}(1-\rho^2)}\Big[\mathbb{E}_{rt,1} + \frac{d_{1,t}(1+r^d_1)}{P_{1,t}} - r_f\Big]. \tag{4.36b}$$

It is evident that each risky fractions depends on both the dividend processes and price tracks. This fact is due to the correlation factor ρ. In case of zero correlation between the two assets, the formulas reduce to eq. 2.11 valid in the 1 risky asset/1 risk-free asset framework. Nevertheless, the relative aversion constant γ is computed in a different way in the enlarged model, thus the fraction invested in each asset is smaller. Essentially, for $\rho = 0$, each risky fraction depends uniquely on the respective price development and the strategy for the fundamentalist trader is essentially buying low and selling high. However, when $\rho \neq 0$, the risky fractions are influenced by the correlation between the two assets. Indeed, eq. 4.36a and 4.36b are essentially given by two contributions weighted by the factors $1/(1-\rho^2)$ and $-\rho/(1-\rho^2)$.

The fundamentalists strategy can be analysed further, separating two different cases:

- $\rho > 0$: the first factor $1/(1-\rho^2)$ is positive and greater than 1, whilst the second factor $-\rho/(1-\rho^2)$ is negative. Thus, the risky fraction $x^f_{1,t}$ is characterized by the competition between the gain given by deviation of the price of asset 1 with respect to its fundamental value against the gain given by the second asset. The analogous analysis is valid for $x^f_{2,t}$.

- $\rho < 0$: the first factor $1/(1-\rho^2)$ is greater than 1, whereas the second term $-\rho/(1-\rho^2)$ is positive. Hence, both the two factors contribute positively to the determination of the risky fractions but with different weights. For instance, for $x_{1,t}$, any positive deviation of the price $P_{1,t}$ (or $P_{2,t}$) from it fundamental value decreases the risky fractions (i.e. induce the fundamentalists to sell the risky assets) and any negative deviation from the fundamental value increases the risky fractions (i.e. induce the fundamentalists to buy the risky assets). Analogously for $x_{2,t}$.

In conclusion, each fundamentalist trader at time t computes the optimal values of the fractions of wealth to invest in the risky assets in order to obtain the highest profit on the next period for a given level of risk. In contrast with what happens in the one risky asset paradigm, in the case of multiple assets, the optimization problem is more complicated and the optimal risky fractions are correlated. Therefore, the fundamentalist trader can now diversify more and gain or loose on the possible correlations between the two assets.

As in the original model, the choice of every fundamentalist trader is the same, thus, the entire class can be represented by a unique agent.

4.3 Noise traders

According to the tradition in the ABM literature and the original formulation by Kaizoji et al. (2015), the noise traders represent the part of the investors that are led by social imitation and the impulse to believe in "charts", such as the past price performance.
In the previous chapter, we have deepened the understanding of the similarities between the noise traders class and the Kinetic Ising model. Following Sornette (2014) and Harras et al. (2012), we have shown how the usage of the Ising model can be justified in the paradigm of social models. As far as concerns the noise traders class, the Ising-like structure consists in the possibility to choose to buy or to sell the risky asset. The opinion index s_t represents the analogous of the magnitization in the Ising model and measures the majority opinion of the traders, whereas the momentum H_t plays the role of the external field that tends to align the opinions. In contrast to the original formulation of the Ising model, the control parameter,

the herding propensity κ, is a time-varying. The continuous change in time of the herding propensity allows the system to pass from the sub-critical regime to the critical regime in which the opinion of the traders is polarized. The phenomenon of the "sweeping of the instability" is at the origin of the build-up of the bubbles in price time series (Sornette (1994)).

Given the link between the present construction of the noise traders class with the Ising model, its extension to the multi-assets framework is not trivial. Reason why, our approach tries to conserve the original set-up, but adapting it to the new framework.
The first approach consists in dividing the pool of N_n traders into two sub-classes that can trade only one type of risky asset. For simplicity, the two subgroups are denoted with numbers 1 and 2 and the total number of traders in each subgroup is $N_{1,t}$ and $N_{2,t}$, according to the risky asset they trade. Inside each subgroup, the agents can trade only the risky asset or the risk-free asset. The traders investing respectively in the latter are denoted as $N^-_{1,t}$ or $N^-_{2,t}$ and in the former as $N^+_{1,t}$ and $N^+_{2,t}$. Despite the division between the two pools of traders, they have the possibility to switch from one subgroup to the other with a certain probability that represents how the noise traders perceive the difference in performance of the assets. The possible switching are the following:

- switching between the subgroup of $N^-_{1,t}$ investors holding the risk-free asset to the subgroup of investors $N^+_{1,t}$ holding the risky asset 1,
- switching between the subgroup of $N^-_{2,t}$ investors holding the risk-free asset to the subgroup of $N^+_{2,t}$ investors holding the risky asset 2,
- switching between the subgroups $N^+_{1,t}$ and $N^+_{2,t}$ of traders holding the risky assets.

In this scheme, we assume that the risk-free asset is exactly the same, or in other words that it guarantees exactly the same rate of interest. In this case, there is no real reason for allowing switching between the subgroup $N^+_{1,t}$ and $N^-_{2,t}$ or $N^+_{2,t}$ and $N^-_{1,t}$. The switching are mediated by the following set of probabilities: $p^+_{11,t}$ and $p^+_{22,t}$ denote the possibility that a trader from the subgroup of investors holding the risky asset 1 or 2 decides to buy the bond, analogously $p^-_{11,t}$ and $p^-_{22,t}$ determine the number of traders holding the bond that decide to buy the risky asset 1 or 2. The probabilities $p^+_{12,t}$ and $p^+_{21,t}$ regulate the switching between the subgroup of $N^+_{1,t}$ and $N^+_{2,t}$ traders. In particular on $p^+_{12,t}$ depends the number of traders that decide to sell the risky asset 1 and buy the risky asset 2 and $p^+_{21,t}$ regards the inverse operation. Figure 4.1 shows the scheme of all possible transitions between the two sub-classes of noise traders. In order to define the set of probabilities according to the parameters

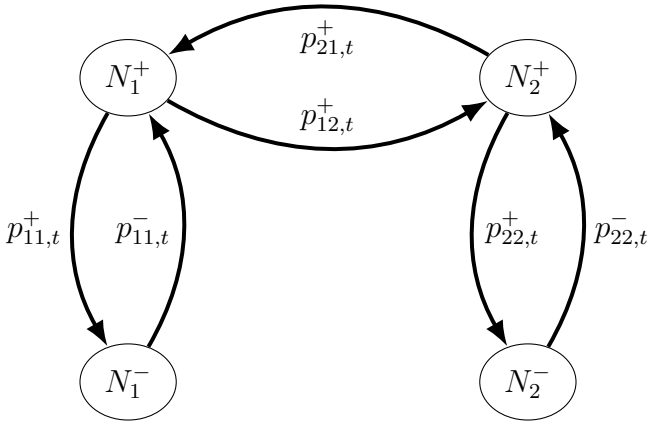

Figure 4.1: The figure shows the scheme of all possible transitions between the two sub-classes of traders. The subgroups marked as $N^+_{1,t}$ and $N^+_{2,t}$ denote respectively the numbers of traders holding the risky asset 1 and 2, whereas $N^-_{1,t}$ and $N^-_{2,t}$ indicate the traders holding the risk-free asset. The arrows indicate, instead, all possible types of switching between the subgroups.

of the model and the description of the class, it is necessary to analyse every possible type of switching

1. *Switching between the risk-free asset group and the risky asset subgroup*
   This type of transition involves the probabilities $p^{\pm}_{11,t}$ and $p^{\pm}_{22,t}$ and do not involve a change in the total number of traders for the two sub-classes. Inside each sub-class, the scheme respects perfectly the original noise traders structure. Therefore, the probabilities depends on the social imitation among traders and on their "chartist" nature. In the case of the two sub-classes, we compute the risky fractions $x_{1,t}$ and $x_{2,t}$ respectively as the relative fraction of traders investing in the risky assets 1 and 2:

$$x_{1,t} = \frac{N^+_{1,t}}{N_{1,t}}, \qquad x_{2,t} = \frac{N^+_{2,t}}{N_{2,t}}. \tag{4.37}$$

   Therefore, the opinion indices for the two assets are defined as in the original model as:

$$s_{1,t} = \frac{N^+_{1,t} - N^-_{1,t}}{N_{1,t}} = 2x_{1,t} - 1, \tag{4.38}$$

$$s_{2,t} = \frac{N^+_{2,t} - N^-_{2,t}}{N_{2,t}} = 2x_{2,t} - 1. \tag{4.39}$$

   They indicate which is the major opinion inside each sub-class: if the majority of the traders is investing into the respective risky asset or if the majority is

investing in the bond. The form of contagion of the same opinion goes along with the trend-following tendency. As a matter of fact, noise traders do no believe only that the opinion of their acquaintance counts, but also the past performance of the risky asset does. That is the reason why, the investors of each sub-class rely on the price momentum indicators $H_{1,t}$, $H_{2,t}$ defined as the exponential moving average for each asset on past returns:

$$H_{1,t} = \theta H_{1,t-1} + (1-\theta) r_{1,t}, \tag{4.40}$$

$$H_{2,t} = \theta H_{2,t-1} + (1-\theta) r_{2,t}. \tag{4.41}$$

Here, the parameter θ is assumed equal for all noise traders and determine the time window $\tau_{memory} = 1/(1-\theta)$ used by the investors to compute the moving average. According to the original formulation, the probabilities to switch are assumed to be a linear combination of the opinion index and momentum weighted by the herding propensity κ_t. The probabilities can be formulated in a similar way, considering, though, the due differences. At each time t, the traders holding the risky asset 1 (or 2) can decide to sell it and buy the bond or the risky asset 2 (or 1). Thus, the probability to sell the risky asset must take into account the two contributions. Therefore, for the probabilities $p^-_{11,t}$ and $p^-_{22,t}$, it is possible to maintain the original formulation (eq. 2.18):

$$p^-_{11,t} = \frac{1}{2}\Big[p^- + \kappa_t(s_{1,t} + H_{1,t})\Big], \tag{4.42}$$

$$p^-_{22,t} = \frac{1}{2}\Big[p^- + \kappa_t(s_{2,t} + H_{2,t})\Big]. \tag{4.43}$$

In contrast, the probabilities $p^+_{11,t}$ and $p^+_{22,t}$ depend on the switching probabilities between the risky assets.

2. *Switching between the two risky assets groups*
The noise traders holding a risky asset has the opportunity at each time t to sell their risky asset and buy the other one. This possibility is regulated by the set of probabilities $p^+_{12,t}$ and $p^+_{21,t}$ for switching from $N^+_{1,t}$ to $N^+_{2,t}$ and vice-versa. According to the previous reasoning, the performance of each asset is measured in the noise traders evaluation as the sum of two indicators: the opinion index and the momentum. Thus, the choice of the traders must rely on the difference between the two assets performances: $s_{1,t} + H_{1,t} - s_{2,t} - H_{2,t}$. Obviously, when the quantity is positive the performance of the risky asset 1 is better than the the performance of the second, whist in case of negativity it is the contrary. The difference on the performance is weighted naturally by the herding propensity κ_t that regulates how much the social index and the past trends can influence the traders. When the herding propensity is zero, there

is no motivation for each noise trader to change his strategy. In summary, according to the reasoning, we can write the equations of the transition rates as

$$\tilde{p}^{+}_{12,t} = \frac{1}{2}\kappa_t f\left(s_{2,t} + H_{2,t} - s_{1,t} - H_{1,t}\right), \tag{4.44}$$

$$\tilde{p}^{+}_{21,t} = \frac{1}{2}\kappa_t f\left(-s_{2,t} - H_{2,t} + s_{1,t} - H_{1,t}\right). \tag{4.45}$$

The parameter $f \in [0,1]$ has been added to motivate the natural tendency that perceive each individual to maintain the previous or the current decison in a decision making problem. The "status quo bias" has been confirmed in behavioral Economics as a prominent phenomenon effecting traders decisions (Samuelson and Zechauser (1988)). Here, the tendency to be stick to the previous decision is represented by the magnitude of the parameter f: the larger is f, the smaller is the status quo bias and vice-versa. Analysing better eq. 4.45 and 4.44, one can observe than when the risky asset 1 performs better than the second, $\tilde{p}^{+}_{12,t}$ is positive, but vice-versa $\tilde{p}^{+}_{21,t}$ would end up to be negative. In order to avoid this problem and switch to a probabilistic definition, we impose the non-negativity condition on $\tilde{p}^{+}_{12,t}$ and $\tilde{p}^{+}_{21,t}$ imposing that

$$p^{+}_{12,t} = \begin{cases} 0.5\kappa_t f\left(s_{2,t} + H_{2,t} - s_{1,t} - H_{1,t}\right), & \text{if } s_{2,t} + H_{2,t} - s_{1,t} - H_{1,t} > 0 \\ 0, & \text{otherwise} \end{cases} \tag{4.46a}$$

$$p^{+}_{21,t} = \begin{cases} 0.5\kappa_t f\left(s_{1,t} + H_{1,t} - s_{2,t} - H_{2,t}\right), & \text{if } s_{1,t} + H_{1,t} - s_{2,t} - H_{2,t} > 0 \\ 0, & \text{otherwise} \end{cases} \tag{4.46b}$$

Given that in eq. 4.46 the condition is exclusive, when $p^{+}_{12,t}$ is positive, $p^{+}_{21,t}$ is set to zero and vice-versa. Therefore, there is always a net flux of traders going from $N^{+}_{1,t}$ to $N^{+}_{2,t}$ or vice-versa.

3. *Switching between the risky asset subgroup and the risk-free asset group*
According to the previous definitions, we can construct the probabilities $p^{+}_{11,t}$ and $p^{+}_{22,t}$ such that $p^{+}_{11,t} = p^{-}_{11,t} + p^{+}_{21,t}$ and similarly $p^{+}_{22,t} = p^{-}_{22} + p^{+}_{12,t}$. Using the definition of the transition rates $\tilde{p}^{+}_{12}$ and $\tilde{p}^{+}_{21}$ we can easily write the transition rates as

$$\tilde{p}^{+}_{11,t} = \frac{1}{2}\Big\{p^{+} - \kappa_t\Big[s_{1,t} + H_{1,t} + f(s_{2,t} + H_{2,t} - s_{1,t} - H_{1,t})\Big]\Big\}, \tag{4.47}$$

$$\tilde{p}^{+}_{22,t} = \frac{1}{2}\Big\{p^{+} - \kappa_t\Big[s_{2,t} + H_{2,t} + f(s_{1,t} + H_{1,t} - s_{2,t} - H_{2,t})\Big]\Big\}. \tag{4.48}$$

Considering now to the definitions of the probabilities $p^+_{12,t}$ and $p^+_{21,t}$ implemented in eq. 4.44 and 4.45, the correct way to express the previous equations as probabilities is the following:

$$p^+_{11,t} = \begin{cases} \frac{1}{2}\Big\{p^+ - \kappa_t\Big[(s_{1,t}+H_{1,t})(1-f)+f(s_{2,t}+H_{2,t})\Big]\Big\}, & \text{if } s_{2,t}+H_{2,t}-s_{1,t}-H_{1,t}>0 \\ \frac{1}{2}\Big[p^+ - \kappa_t(s_{1,t}+H_{1,t})\Big], & \text{otherwise} \end{cases} \tag{4.49}$$

$$p^+_{22,t} = \begin{cases} \frac{1}{2}\Big\{p^+ - \kappa_t\Big[(s_{2,t}+H_{2,t})(1-f)+f(s_{1,t}+H_{1,t})\Big]\Big\}, & \text{if } s_{1,t}+H_{1,t}-s_{2,t}-H_{2,t}>0 \\ \frac{1}{2}\Big[p^+ - \kappa_t(s_{2,t}+H_{2,t})\Big]. & \text{otherwise} \end{cases} \tag{4.50}$$

With the previous definition we ensure the conditions

$$p^+_{11,t} = p^-_{11,t} + p^+_{12,t}, \tag{4.51}$$

$$p^+_{22,t} = p^-_{22,t} + p^+_{21,t}. \tag{4.52}$$

Once defined the set of switching probabilities, the implementation of the transitions is done through the number of investors for each subgroup. Nevertheless, we can derive the dynamical evolutions of the average values of $N^\pm_{1,t}$ and $N^\pm_{2,t}$. In order to implement the mean-values equations through the discrete Master equation, we denote as $n^\pm_{1,t}, n^\pm_{2,t}$ the mean values of the number of noise traders $N^\pm_{1,t}$ and $N^\pm_{2,t}$. Moreover, it is necessary to switch from probabilities to transitions rates. Eventually, the equations are

$$n^+_{1,t} = n^+_{1,t-1} + n^-_{1,t-1}\tilde{p}^-_{11,t-1} - n^+_{1,t-1}\tilde{p}^+_{11,t-1} + n^+_{2,t-1}\tilde{p}^+_{21,t-1} - n^+_{1,t-1}\tilde{p}^+_{12,t-1}, \tag{4.53a}$$

$$n^-_{1,t} = n^-_{1,t-1} + n^+_{1,t-1}\tilde{p}^+_{11,t-1} - n^-_{1,t-1}\tilde{p}^-_{11,t-1}, \tag{4.53b}$$

$$n^+_{2,t} = n^+_{2,t-1} + n^+_{2,t-1}\tilde{p}^+_{22,t-1} - n^+_{2,t-1}\tilde{p}^+_{22,t-1} + n^-_{2,t-1}\tilde{p}^+_{12,t-1} - n^+_{2,t-1}\tilde{p}^+_{21,t-1}, \tag{4.53c}$$

$$n^-_{2,t} = n^-_{2,t-1} + n^+_{2,t-1}\tilde{p}^+_{22,t-1} - n^-_{2,t-1}\tilde{p}^-_{22,t-1}, \tag{4.53d}$$

Overall, the formulation of the noise traders class preserves the original formulation and the Ising-like structure. The noise traders do not diversify their portfolios as fundamentalists do, but each noise trader chooses at each period if investing all his wealth in the bond or in one of the risky assets. Nonetheless, we are interested in the aggregate impact of the noise traders accounting the portions of investors holding the risky asset 1 and the risky asset 2 as risky fractions.

4.4 Market clearing conditions and price dynamics

In the original market formulation, the price dynamic is determined by setting the sum of the excess demand for fundamentalists and noise traders equal to zero. In

short, the model assumes a Walresian auction scenario (Walras (1926)) where at each period the supply and the demand is perfectly compensated. The same equilibrium condition is extended to the multi-assets formulation. Though, the equilibrium conditions needs to hold for each asset.
In the following we are going to derive the excess demands for the two assets and the equilibrium price equations. Besides, every quantity will be denoted with the apex "f" for fundamentalists and "n" for the noise traders.

The excess demand for the period $(t-1,t)$ is defined as in eq. 2.20 for $i=\{f,n\}$:

$$\Delta D^i_{t-1\to t} = z^i_t P_t - z^i_{t-1} P_t = W^i_t x^i_t - W^i_{t-1} x^i_{t-1} \frac{P_t}{P_{t-1}}. \tag{4.54}$$

The unique difference with the previous framework is that in this case the number of assets are two. In this contest, the equilibrium prices are obtained posing the aggregate excess demand for each stock equal to zero. Thus, a system of two equations of unknowns $P_{1,t}$ and $P_{2,t}$ is obtained.

For fundamentalist traders, the excess demands for the two risky assets are immediate from eq. 2.20:

$$\Delta D^{1,f}_{t-1\to t} = W^f_t x^f_{1,t} - W^f_{t-1} x^f_{1,t-1} \frac{P_{1,t}}{P_{1,t-1}}, \tag{4.55}$$

$$\Delta D^{2,f}_{t-1\to t} = W^f_t x^f_{2,t} - W^f_{t-1} x^f_{2,t-1} \frac{P_{2,t}}{P_{2,t-1}}. \tag{4.56}$$

Plugging, now, the equations of the wealth dynamics (eq. 4.7), one obtains

$$\begin{aligned}\Delta D^{f,1}_{t-1\to t} =& x^f_{1,t} W^f_{t-1} \Big[(P_{1,t}+d_{1,t}) \frac{x^f_{1,t-1}}{P_{1,t-1}} + (P_{2,t}+d_{2,t}) \frac{x^f_{2,t-1}}{P_{2,t-1}} + (1-x^f_{1,t-1}-x^f_{2,t-1}) R_f) \Big] \\ & - x^f_{1,t-1} W^f_{t-1} \frac{P_{1,t}}{P_{1,t-1}},\end{aligned} \tag{4.57a}$$

$$\begin{aligned}\Delta D^{f,2}_{t-1\to t} =& x^f_{2,t} W^f_{t-1} \Big[(P_{1,t}+d_{1,t}) \frac{x^f_{1,t-1}}{P_{1,t-1}} + (P_{2,t}+d_{2,t}) \frac{x^f_{2,t-1}}{P_{2,t-1}} + (1-x^f_{1,t-1}-x^f_{2,t-1}) R_f \Big] \\ & - x^f_{2,t-1} W^f_{t-1} \frac{P_{2,t}}{P_{2,t-1}}.\end{aligned} \tag{4.57b}$$

The excess demands contain an implicit dependence on the equilibrium prices $P_{1,t}$ and $P_{2,t}$. Therefore, the next step consists in making explicit the dependence, inserting into the previous equations the definitions of the values of the optimal risky

fractions $x^f_{1,t}$ and $x^f_{2,t}$ (eq. 4.34). On this purpose, we rewrite the optimal fractions in this way, explicating the dependence on the equilibrium prices:

$$x^f_{1,t} = \frac{A_{1,t}}{P_{1,t}} - \frac{B_{1,t}}{P_{2,t}} + C_{1.t},$$
$$x^f_{2,t} = \frac{A_{2,t}}{P_{1,t}} - \frac{B_{2,t}}{P_{2,t}} + C_{2,t}.$$

The parameters $A_{i,t}, B_{i,t}$ and $C_{i,t}$ are obtained by direct comparison with eq. 4.34:

$$A_{1,t} = \frac{d_{1,t}(1+r^d_1)}{\gamma\bar{\sigma}^2_1(1-\rho^2)}, \tag{4.58a}$$
$$B_{1,t} = \frac{d_{2,t}\rho(1+r^d_2)}{\gamma\bar{\sigma}_1\bar{\sigma}_2(1-\rho^2)}, \tag{4.58b}$$
$$C_{1,t} = \frac{\bar{\sigma}^2_2(E_{rt,1}-r_f) - \rho\bar{\sigma}_1\bar{\sigma}_2(\mathbb{E}_{rt,2}-r_f)}{\gamma\bar{\sigma}^2_1\bar{\sigma}^2_2(1-\rho^2)}, \tag{4.58c}$$

$$A_{2,t} = \frac{d_{2,t}(1+r^d_2)}{\gamma\bar{\sigma_2}^2(1-\rho^2)}, \tag{4.58d}$$
$$B_{2,t} = \frac{d_{1,t}\rho(1+r^d_1)}{\gamma\bar{\sigma}_1\bar{\sigma}_2(1-\rho^2)}, \tag{4.58e}$$
$$C_{2,t} = \frac{\bar{\sigma}^2_1(\mathbb{E}_{rt,2}-r_f) - \rho\bar{\sigma}_1\bar{\sigma}_2(\mathbb{E}_{rt,1}-r_f)}{\gamma\bar{\sigma}^2_1\bar{\sigma}^2_2(1-\rho^2)}. \tag{4.58f}$$

The derivation of the excess demands for noise traders is more involved. Indeed, the noise traders are separated into two distinct sub-classes which admit transitions between them. Therefore, the excess demands have to be adapted to the scheme and take into account the exchange of traders from one group to the other.
A good solution is to divide the total wealth W^n_t between the two sub-classes, in the manner that the sub-class with $N_{1,t}$ agents trade a total amount of wealth $W_{1,t}$ and the sub-class with $N_{2,t}$ traders has the total quantity $W^n_{2,t}$. Naturally, $W^n_{1,t} + W^n_{2,t} = W^n_t$ gives the total amount of wealth of the noise traders class. However, the possibility to exchange traders mean also the possibility to decrease or increase the wealth of each subgroup. As a consequence, the procedure to consider the exchange of wealth at time $t-1$ is to take into account the quantity of wealth traded ΔW

$$\Delta W = \frac{N_{2\to1}W_2}{N_{2,t-1}} - \frac{N_{1\to2}W_1}{N_{1,t-1}}, \tag{4.59}$$

where $N_{1\to2}$ is the number of traders that sell the risky asset 1 and buys the asset 2 and $N_{2\to1}$ is the analogous quantity. Then, the amounts of wealth for each subgroup become:

$$W^*_{1,t-1} = W_{1,t-1} + \Delta W, \tag{4.60}$$
$$W^*_{2,t-1} = W_{2,t-1} - \Delta W. \tag{4.61}$$

The two amounts of wealth are updated after the noise traders decisions and before the computation of the excess demands for noise traders. Consequently, it is sufficient to consider the updated wealth in the equations

$$\Delta D^{1,n}_{t-1\to t} = W^n_{1,t}x^n_{1,t} - W^n_{1,t-1}x^n_{1,t-1}\frac{P_{1,t}}{P_{1,t-1}}, \tag{4.62}$$
$$\Delta D^{2,n}_{t-1\to t} = W^n_{2,t}x^n_{2,t} - W^n_{t-1}x^n_{2,t-1}\frac{P_{2,t}}{P_{2,t-1}}. \tag{4.63}$$

The evolution of the two amounts of wealth of the two subgroups differs from eq.4.7, because now the noise traders sub-classes can be considered separately. Therefore, we can express $W^n_{1,t}$ and $W^t_{2,t}$ simply as

$$W^n_{1,t} = W^n_{1,t-1}\Big[x^n_{1,t-1}\Big(\frac{P_{1,t}}{P_{1,t-1}} + \frac{d_{1,t}}{P_{1,t-1}} - r_f - 1\Big) + R_f\Big], \tag{4.64}$$
$$W^n_{2,t} = W^n_{2,t-1}\Big[x^n_{2,t-1}\Big(\frac{P_{2,t}}{P_{2,t-1}} + \frac{d_{1,t}}{P_{2,t-1}} - r_f - 1\Big) + R_f\Big]. \tag{4.65}$$

Inserting eq. 4.65 into the excess demands equations for noise traders (eq. 4.63) leads to

$$\Delta D^{n,1}_{t-1\to t} = W^n_{1,t-1}x^n_{1,t}\Big[\Big(P_{1,t} + d_{1,t}\Big)\frac{x^n_{1,t}}{P_{1,t-1}} + (1 - x^n_{1,t-1})(1 + r_f)\Big] - x^n_{1,t-1}W^n_{1,t-1}\frac{P_{1,t}}{P_{1,t-1}}, \tag{4.66}$$

$$\Delta D^{n,2}_{t-1\to t} = W^n_{2,t-1}x^n_{2,t}\Big[\Big(P_{2,t} + d_{2,t}\Big)\frac{x^n_{2,t}}{P_{2,t-1}} + (1 - x^n_{2,t-1})(1 + r_f)\Big] - x^n_{2,t-1}W^n_{2,t-1}\frac{P_{2,t}}{P_{2,t-1}}. \tag{4.67}$$

The aggregate excess demand for the two assets is defined by the sum of the excess demands of fundamentalists and noise traders. Eventually, the equilibrium conditions are obtained posing the aggregate excess demands equal to zero:

$$\Delta D^{f,1}_{t-1\to t} + \Delta D^{n,1}_{t-1\to t} = 0, \tag{4.68}$$
$$\Delta D^{f,2}_{t-1\to t} + \Delta D^{n,2}_{t-1\to t} = 0, \tag{4.69}$$

The two equations can be re-casted into two explicit equations of the equilibrium prices $P_{1,t}$ and $P_{2,t}$. The full computation is described in appendix A, but here we provide only the the final results:

$$a_{1,t}P_{1,t}^2 + b_{1,t}P_{2,t}^2 + c_{1,t}P_{1,t}^2P_{2,t} + d_{1,t}P_{1,t}P_{2,t}^2 + e_{1,t}P_{1,t}P_{2,t} + f_{1,t}P_{1,t} + g_{1,t}P_{2,t} = 0, \quad (4.70)$$

$$a_{2,t}P_{2,t}^2 + b_{2,t}P_{1,t}^2 + c_{2,t}P_{2,t}^2P_{1,t} + d_{2,t}P_{2,t}P_{1,t}^2 + e_{2,t}P_{1,t}P_{2,t} + f_{2,t}P_{2,t} + g_{2,t}P_{1,t} = 0. \quad (4.71)$$

The price equations are non-linear and coupled. The list of parameters are listed in appendix A in eq. A.6 and A.7. It is worthy noticing that it is possible to retrieve the second order equation of the original model if we assume that only one of the two risky fraction is not zero. This confirms that our derivation is correct. The solution of the coupled system cannot be found analytically and only numerical solutions are possible. Thus, we will leave the solutions implicit.

Chapter 5

Time series description and theoretical analysis

In the previous chapter, we have introduced the extension of the original market model (Kaizoji et al. (2015), Khort (2016), Westphal and Sornette (2019)) to the multi-asset framework. As in the original formulation, the structure of the model is based on the bounded rationality of the traders and their heterogeneous composition into fundamentalists and noise traders.

In this chapter we present the main results of the extended model. The first part is devoted to a detailed description of the typical time series and to the detection of possible faster-than-exponential growth of the prices, signature of financial bubbles. We show that our model is able to reproduce bubbles and we try to explain their emergence from a theoretical point of view. Our approach consists in the analysis of the mean-values equations of relevant quantities. Similar approach is not rare in literature and even in the original article, Kaizoji et al. (2015) have explained the emergence of the bubbles studying the behavior of the mean-value opinion index. Furthermore, the extended model is able to reproduce in time series the synchronous build-up of bubbles in the two assets. This feature cannot be grasped in the simpler framework with only one risky asset and it is in line with empirical observations.
The second point of our analysis regards the presence of correlations between the two assets returns. We investigate the emergence of correlations among assets in two different directions. First, we analyse how the fundamentalists expectations on the correlation between the two assets can effect their realization. Second, we study the effect of the noise traders class on the distribution of the returns and how they depend on the parameter f.
Eventually, the analysis concludes checking if the simulated data manifest the typical regularities of the financial market, the well-known "stylized facts".

5.1 Choice of parameters

In this section, we present the complete set of parameters used in the simulations in tab. 5.1. The parameters are divided in two columns per type of risky asset, whereas the general parameters are listed in the last row.

Risky asset 1			Risky asset 2		
$x^f_{1,0} = 0.3$	$d_{1,0} = 0.00016$	$r^d_1 = 0.00016$	$x^f_{2,0} = 0.3$	$d_{2,0} = 0.00016$	$r^d_2 = 0.00016$
$H_{1,0} = 0.00016$	$\theta = 0.99$	$\mathbb{E}_{rt,1} = 0.00016$	$H_{2,0} = 0.00016$	$\theta = 0.99$	$\mathbb{E}_{rt,2} = 0.00016$
$P_{1,0} = 1.0$	$\bar{\sigma}^2_1 = 0.0004$	$N_{1,0} = 500$	$P_{2,0} = 1.0$	$\bar{\sigma}^2_2 = 0.0004$	$N_{2,0} = 500$
$x^n_{1,0} = 0.3$	$\sigma^d_1 = 0.000016$		$x^n_{2,0} = 0.3$	$\sigma^d_2 = 0.000016$	
Common values					
$p^+ = 0.199375$	$p^- = 0.200625$	$N_n = 1000$	$r_f = 0.00008$	$\nu^{nf}_0 = 1$	$\kappa = 0.98 p_+$

Table 5.1: The table reports the values of the parameters used in the simulations. In the event that different values are used, it will specifically highlighted.

It is worthy noticing that the most of the parameters are used also in the original market model. In this way the comparison with the framework of 1 risky asset/free-risk is easier. Furthermore, for the moment we have taken the decision to design the two risky assets with the same parameters as far as concerns the growth rates of the dividends, the expected values of future returns and the initial values $P_{1,0} = P_{2,0} = 1.0$, $H_{1,0} = H_{2,0} = 0.00016$, $d_{1,0} = d_{2,0} = 0.00016$. In table 5.1, the parameters ρ and f are not specified, since they are used as control parameters and their values will be specified when needed.

For fundamentalists, the variances of the future returns are set equal to $\bar{\sigma}_1 = \bar{\sigma}_2 = 0.002$ so that they can be comparable with realistic fluctuations of the returns. Finally, the relative risk aversion constant γ is obtained as an endogenous parameter depending on the initial risky fractions $x^f_{1,t}$ and $x^f_{2,t}$. From eq. 4.34 at time $t = 0$, we can derive the value of γ as

$$\gamma = \frac{\left[\mathbb{E}_{rt,1} - r_f + \frac{d_{1,0}(1+r^d_1)}{P_{1,0}}\right]}{x^f_{1,0}\bar{\sigma_1}^2 + \rho\bar{\sigma}_1\bar{\sigma}_2 x^f_{2,0}}. \tag{5.1}$$

Actually, the value of γ is set in this way in order to maintain almost constant the fraction of fundamentalists investing in the risky assets.

Eventually, let us give some clarifications about the implementation of the noise traders class. As one can notice in tab. 5.1, the parameter p^- is slightly bigger than

p^+. This choice is arbitrary, but inherited from the previous model setup. It ensures the fact that in absence of social factors, the noise traders invest in the risky assets more often than in the risk-free one and thus the positive bubbles happen more frequently than negative bubbles, as observed in real data. The initial number of traders $N_n = 1000$ is distributed equally at the beginning of the simulations, such as $N_{1,0} = N_{2,0} = 500$. Once the simulation is started, the number of the traders is updated using the transition probabilities presented in section 4.3. The difference to the original market formulation is that the dynamics cannot be formulated using the Bernouilli RVs simulating the random decisions (buy or sell) of each noise trader. Actually, the traders that hold the risky asset 1 (or 2) can decide to sell it and buy the bond or the risky asset 2 (or 1) or they can even decide to do nothing. For this reason it is necessary to implement a new type of RV drawn by a probability distribution that take account of the three possibilities. For the traders in the subgroup holding the risky asset 1, the number can be updated using the following probability distribution

$$P(p^+_{12,t}, p^+_{11,t}) = \begin{cases} \text{risky asset 2} & \text{with probability } p^+_{12,t} \\ \text{risk-free asset} & \text{with probability } p^+_{11,t} \\ \text{risky asset 1} & \text{with probability } 1 - p^+_{11,t} - p^+_{12,t} \end{cases} \tag{5.2}$$

Whereas, the number of traders belonging to $N^+_{2,t}$, or better holding the the risky asset 2, can be updated using the following distribution

$$P(p^+_{21,t}, p^+_{22,t}) = \begin{cases} \text{risky asset 1} & \text{with probability } p^+_{21,t} \\ \text{risk-free asset} & \text{with probability } p^+_{22,t} \\ \text{risky asset 2} & \text{with probability } 1 - p^+_{22,t} - p^+_{21,t} \end{cases} \tag{5.3}$$

In contrast, for risky assets, we adopt the Bernoulli RVs as in the original model. We conclude with a brief annotation on the herding propensity κ_t. For noise traders, the herding propensity measures how much social factors as the opinion index and the charts-following tendency influence the decisions of the traders. First, we take into account only one herding propensity κ_t, making no difference between the two subclasses. Second, as in the original paper, we consider the case of constant $\kappa_t = \kappa$ and the case in which it follows the Ornstein-Uhlenbeck process. This latter is defined as in Chapter 3 from eq. 3.1 to eq. 3.3.

5.2 Time series description

This section is devoted to the description of the typical time series of the market model with two risky assets. Figure 5.1 shows the results of a simulation with constant herding propensity κ, whereas figure 5.2 shows the results of a simulation for the Ornstein-Uhlenbeck κ_t. Both the plots are organized as follows: the first column contains the time series corresponding to the first risky asset, whilst the second column contains the realizations of the second risky asset. The first line contains the time series of the prices $P_{1,t}$ and $P_{2,t}$, the second line shows the time series of the returns $r_{1,t}$ and $r_{2,t}$ respectively for the price track of the first asset and second asset. The third line shows the comparison between the momentum series $H_{1,t}$ and $H_{2,t}$ and the fourth line the comparison between the dividend-price ratios $d_{1,t}/P_{1,t}$ and $d_{2,t}/P_{2,t}$. In the fifth line each frame represents the switching probabilities for the noise traders class: on the left it is represented the developments of $p^{+}_{11,t}$ and $p^{-}_{11,t}$, on the right the probabilities $p^{+}_{22,t}$ and $p^{-}_{22,t}$. The sixth line shows the development in time of the risky fractions for both fundamentalists and noise traders. The four last panels show the common variables. In the seventh line there is the representation of the number of traders selling the risky asset 1 and buying the risky asset 2 ($N_{1\to 2}$) and vice-versa ($N_{2\to 1}$). In the eight frame, we have represented z_t, the fraction of noise traders in the first sub-class:

$$z_t := \frac{N_1}{N}, \quad z_t \in [0,1]. \tag{5.4}$$

The last two frames show the wealth ratio ν_t and the herding propensity κ_t process. In order to make the comparison between the two prices track more clearly, we have plotted the prices time series in figure 5.3 relative to the previous simulations.

Let us start with the description of the time series in figure 5.1 for constant κ. From comparison between the prices series (fig. 5.3)(a), one can immediately notice that the prices show significant deviations from the linear growth (naturally expected in the semilog plot) and that the two time series are very similar and they show peaks approximately at the same time or with a certain lag. Indeed, we can expect that the price have on average the same linear trend because they have the same dividend growths. However the presence of similar peaks and apparently correlations between the two prices series is to be searched in the equilibrium prices equations and in the interplay between the fundamentalists and noise traders, as we will explain later. In order to enter in the heart of the question, it is useful to observe the price returns. The price returns of both the two assets show evidence of volatility clustering. In other words, the returns series interval periods of turbulence to periods of tranquility. According to Lux (2009), this is an immediate evidence of the fact that the distribution of returns is not Gaussian, but a more leptokurtic distribution, since huge deviations happen more often than the Gaussian distribution

predicts. These phenomena are reproduced also in real returns time series. Some of these empirical observations seem to be so ubiquitous in the financial market that they have been called "stylized facts". Here, we simply say that the returns alternates between periods of huge deviations to periods of calm, but the the argument will be re-discussed later.
Immediately related to the signed returns is the price momentum. It is calculated as the moving average over the past price returns. Thus, the momentum is higher in the presence of huge fluctuations in the returns time series and lower during tranquil periods (as we can see in fig. 5.1). The exponential average is calculated over a time window of $\tau_{memory} \sim 100$ time steps, large enough to catch the typical trends of the returns. Furthermore, the momentum influences the choices of the noise traders through the transition probabilities. On the other hand, the noise traders strategies can effect the price trends and thus the momentum. This dependence can create self-reinforcing loops that sustain the build-up of high deviations of the returns.
The fourth line shows instead the development of the dividend-price ratios $d_{1,t}/P_{1,t}$ and $d_{2,t}/P_{2,t}$. The important aspect of this quantity is that the fundamentalist risky fractions $x^f_{1,t}$ and $x^f_{2,t}$ are a linear combination of the two. Even though the fundamentalist risky fractions stay almost constant, we can observe that the deviations follow the peaks and the drawbacks of the respective dividend-price ratios process. In case of positive correlation factor ρ, the effect of the opposite risky asset is to lower the magnitude of the risky asset. Eventually, in the third line we can appreciate the development of the noise trader probabilities. On the left, the frame represents the transition probabilities $p^-_{11,t}$ and $p^+_{11,t}$, i.e. the probabilities to sell the free-risk asset and buy the risky asset 1 and vice-versa. The two probabilities seems to be one the mirroring image of the other. However, this is not exactly true, given that only the sum $p^+_{11,t} + p^+_{12,t}$ equals the probability $p^-_{11,t}$. The analogous analysis can be conducted for the frame on the right with the switching probabilities $p^-_{22,t}$ and $p^+_{22,t}$, i.e. the probabilities to sell the bond and buy the risky asset 2. The noise risky fractions $x^n_{1,t}$ and $x^n_{2,t}$ depend directly on the switching probabilities through the fractions of noise traders investing in the risky assets: $N^+_{1,t}/N_{1,t}$ and $N^+_{2,t}/N_{2,t}$. On the other hand, the number of traders $N^+_{1,t}$ and $N^+_{2,t}$ depend on the probability that some investors decide to buy the risky assets, which happens with probability $p^+_{11,t}$ and $p^+_{22,t}$.
With a comparison with the fundamentalist risky fractions, it is immediate that the noise fractions are more fluctuating and and they even reach in certain occasion the upper bound, i.e. the complete polarization of the sub-class.
The noise traders' risky fractions are relative quantities that can take into account the distribution of the population only inside each sub-class. Consequently, it is useful to consider how much larger is a sub-class with respect to the other, in order to understand better the flux of traders between the two sub-classes. The flux of

traders is represented in terms of investors that at each time decide to sell a risky asset and buy another one according to the switching probabilities $p^+_{12,t}$ and $p^+_{21,t}$. Quantitatively, the change is represented by the fraction of traders in the first sub-class N_1. When the flux of noise traders $N_{1\to 2}$ grows, the percentage of people in the first sub-class decreases and so z_t. On the contrary, when there are periods where there is an intense flux of traders $N_{2\to 1}$, the fraction z_t arises. The latter plots are very useful to understand which risky asset is more attractive and how the role of the leading asset changes in time and how it depends on the control parameter f. The last consideration regards the wealth ratio $\nu_t = W^n_t/W^f_t$. The last frame shows that in the long run the wealth of the noise trader class overcome the total wealth of the fundamentalist class. Even though the fundamentalists have the opportunity to diversify their portfolios and thus exploits the gains of two assets, noise traders are more likely to hold the risky assets, namely they have in average higher risky fractions than fundamentalists.

Figure 5.2 shows the typical time series obtained by the ABM with Ornstein-Uhlenbeck κ_t. The frames are organized as in the previous simulation. At first glance, in fig. 5.3(b) one can notice the emergence of bubbles in the price trends, marked by a super-exponential growth. Even if in different measure, they are present in both the prices time series. In particular, we can see evidence of the build-up of two bubbles at $t \sim 3500 - 4000$ time steps. The most important feature to notice is that the build-up of bubbles is synchronous. The synchronization is shown in figure 5.4 by the comparison with the moving window Pearson correlation. The moving window Pearson coefficient is obtained for two different time windows $w = 25$ and $w = 50$ time steps, whereas the horizontal line shows the Pearson correlation coefficient computed over the whole simulation ($T = 5000$ time steps). The plot offers an illustrative example of the synchronization between the prices: during the bubble regimes the Pearson coefficient is almost 1, or better there exists perfect linear correlation between the time series. In contrast, during normal regimes the moving window is nearer the value of the Pearson coefficient calculated over the entire time series. In order to underline that it is a common feature for different simulated time series, in Appendix B, figure B.1 shows the same results for different bubbles regimes. Furthermore, it is worthy noticing that the synchronous build-up of bubbles constitutes a new result that in the simpler 1 risky asset/1 risk-free asset cannot be predicted.
The presence of the bubbles is illustrated also in the returns series with more volatile periods. As a consequence of increasing prices, the momentum series show large peaks in correspondence of bubbles. This means also that the momentum becomes more competitive against the opinion index in determining the decisions of the traders. Furthermore, after careful analysis, one can recognize a correspondence between the peaks of polarization of the risky fractions and the price tracks. Strictly

speaking, the growth of the noise traders and the prices are reciprocally sustained: when the noise risky fractions grow, there is more cohesion among noise traders and the emergence of a collective behavior influences the prices and thus the momentum trends. Higher is the momentum, higher the probability that people will invest in the risky fractions. The self-reinforcing loop lasts until the exhaustion of the pool of the noise traders in the two sub-classes. At this point, the prices experience a drawback that reduce the noise risky fraction, but encourage the risk-avoid traders to come forward and invest when they deem the prices is lower than its fundamental value. In the original market model, during financial bubbles, noise traders experience the so-called lock-in effects and cannot buy the bond because the relative probability is zero (see Ollikainen (2016)). In the multi-asset framework the probability to switch to the bond goes equally to zero, but the possibility to buy the other risky fraction is still available. This is the motivation why the flux of traders does not cease during bubbles.
As far as regards the fundamentalist risky fractions, they depend on the dividend-price ratios, that are now more fluctuating because of the high deviations of the price trends. Thus, also the fundamentalist risky fractions are more fluctuating and show better the dependence on the dividend-price ratios.
Eventually, we can notice from the wealth ratio ν_t that during the bubbles noise traders have enormous peaks of fortune (their wealth become almost 5 times greater than the wealth of the fundamentalists), nonetheless they are transient. As in the case of constant κ_t the long term behavior is upwards, i.e. noise traders gain more.

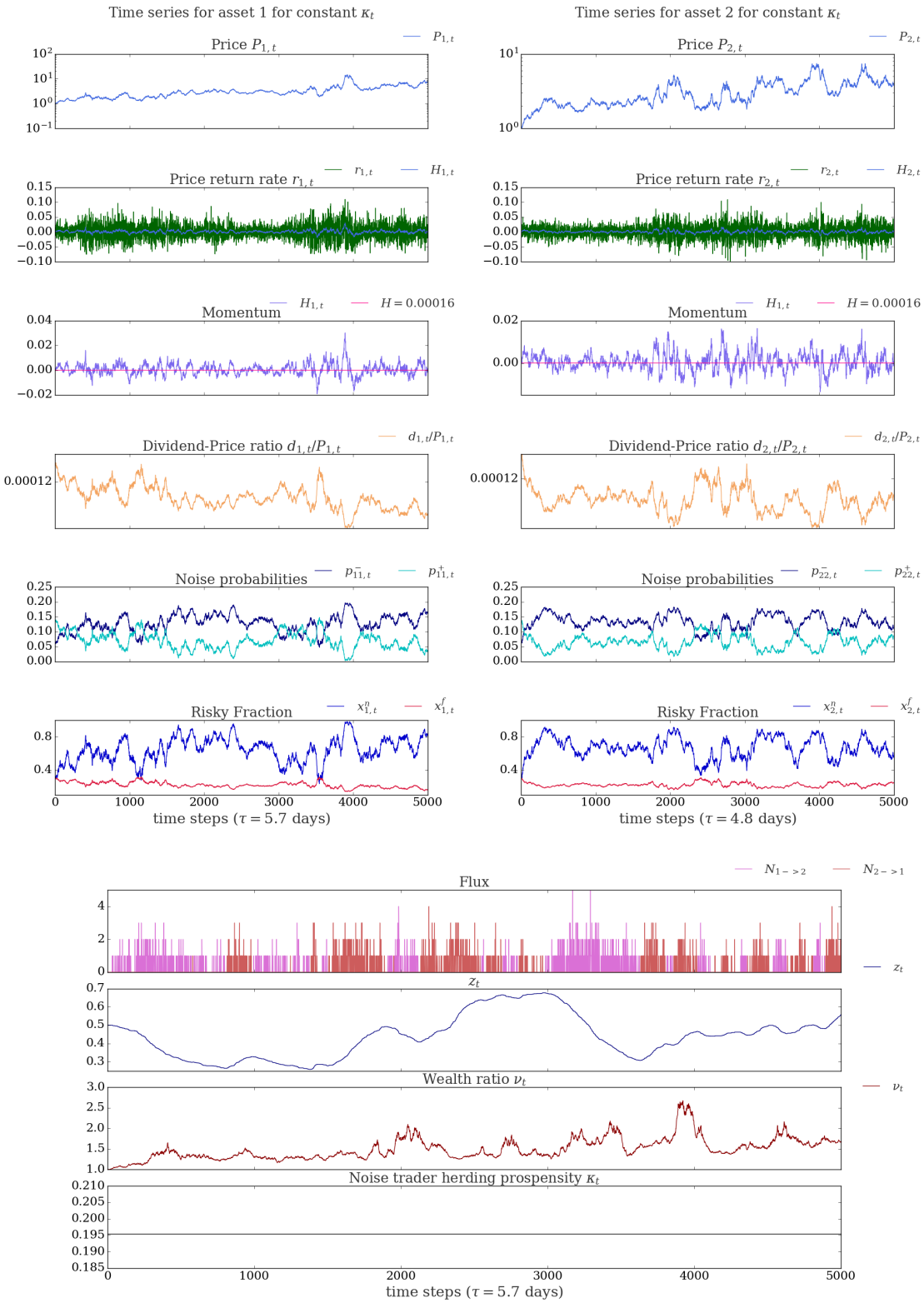

Figure 5.1:
The figure shows the typical time series obtained with constant herding propensity κ and $\rho = 0.3$ and $f = 0.05$. The frames are divided into two columns according to asset 1 and asset 2. The final four frames represent common time series.

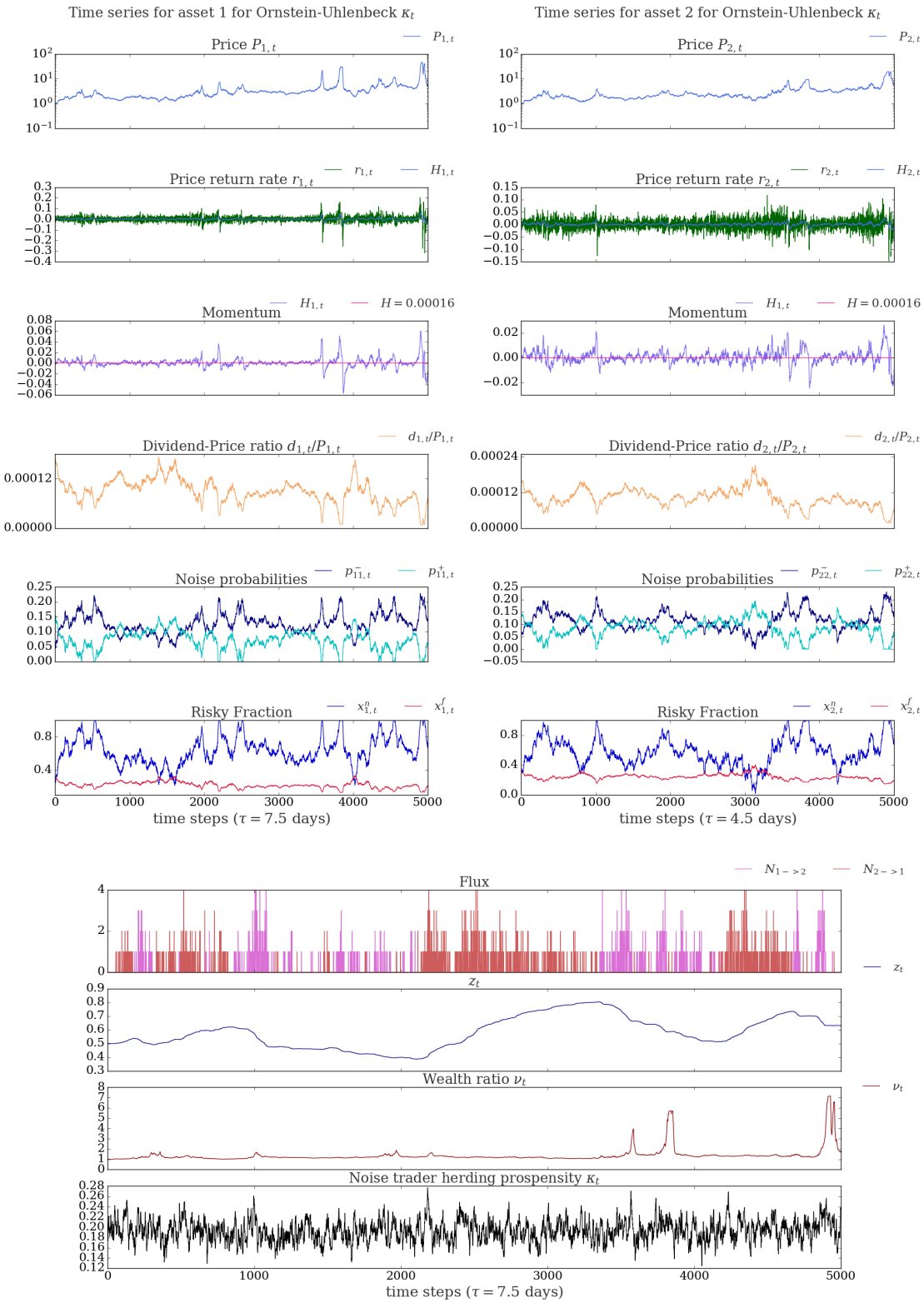

Figure 5.2:
The figure shows the typical time series obtained with Ornstein-Uhlenbeck herding propensity κ_t and $\rho = 0.3$ and $f = 0.05$. The frames are divided into two columns according to asset 1 and asset 2. The final four frames represent common time series.

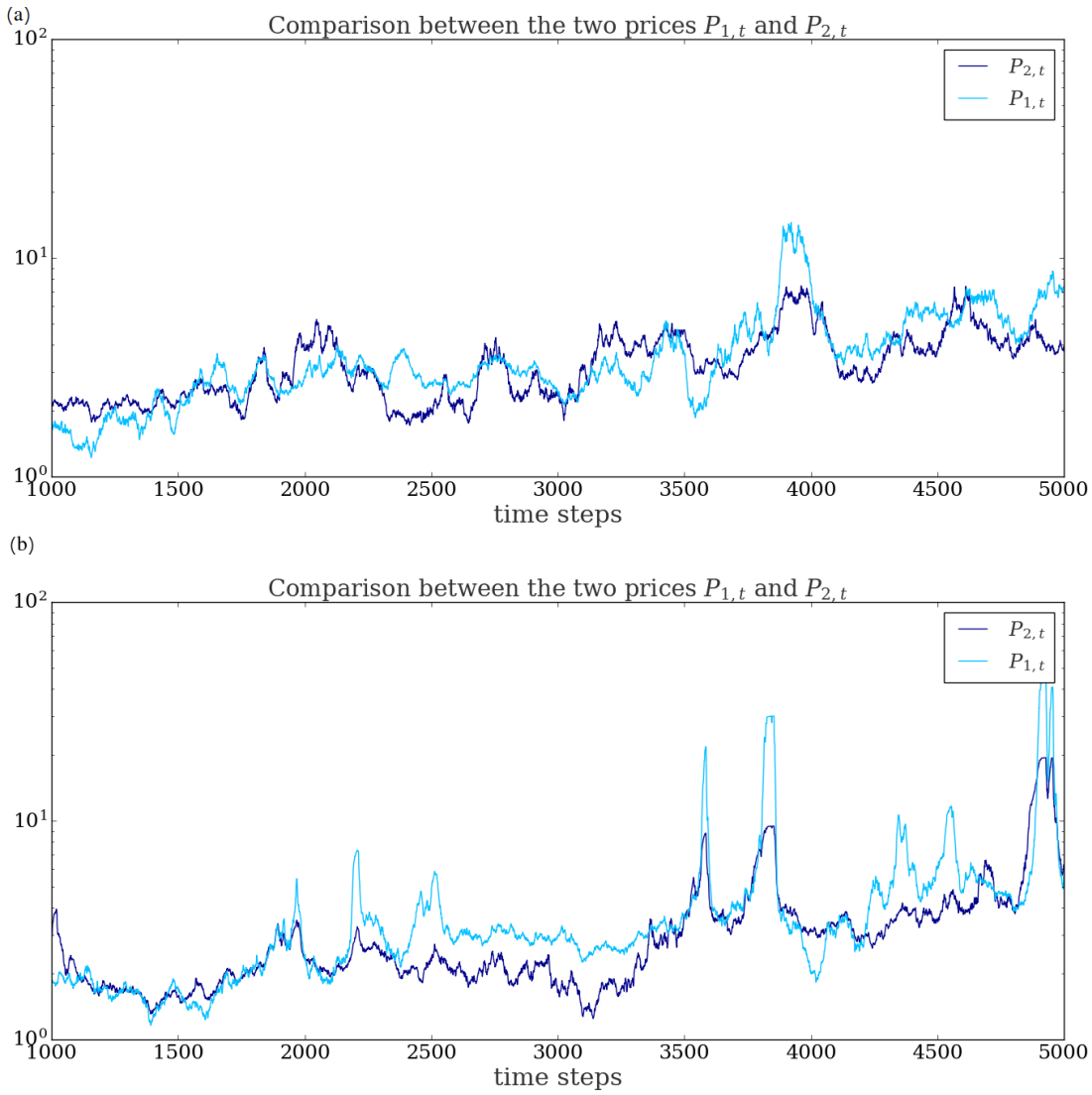

Figure 5.3:
(a) The figure shows the comparison between the prices time series $P_{1,t}$ and $P_{2,t}$ in case of constant κ for the previous simulation for $\rho = 0.3$ and $f = 0.05$.
(b) The figure shows the comparison between the prices time series $P_{1,t}$ and $P_{2,t}$ in case of Ornstein-Uhlenbeck κ for the previous simulation for $\rho = 0.3$ and $f = 0.05$.

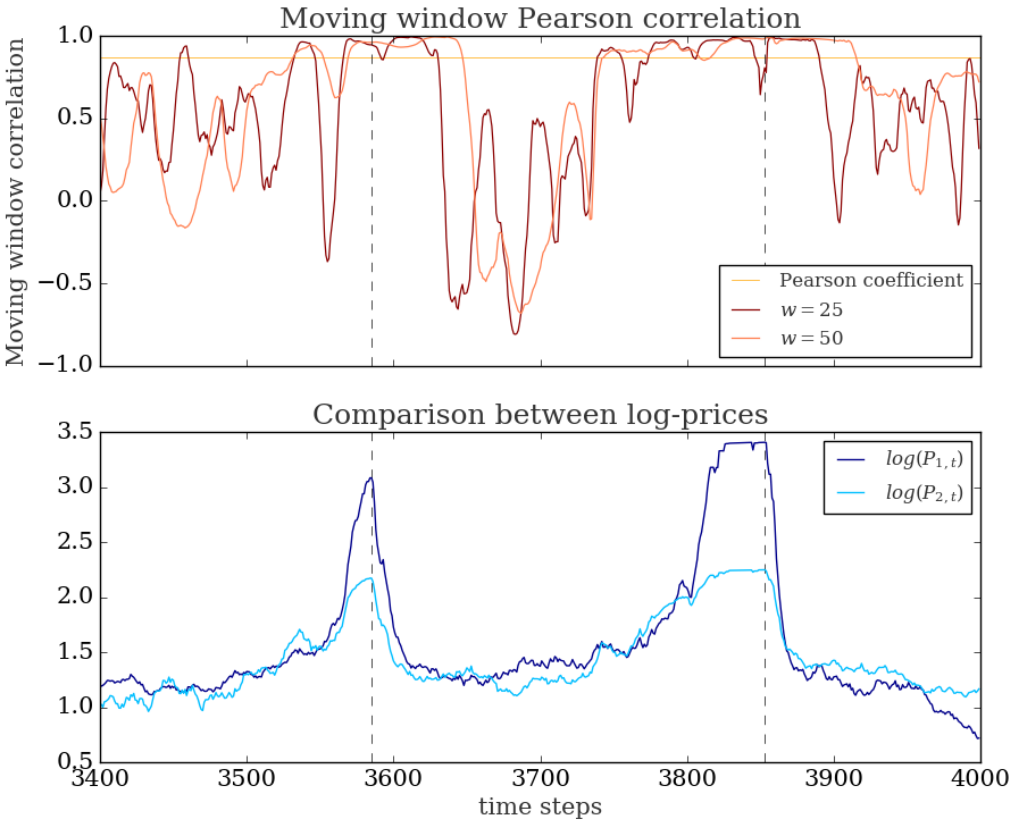

Figure 5.4: The figure shows the comparison between the log-prices (lower panel) and the moving window Pearson correlation coefficient (upper panel), obtained for two windows of length $w = 25$ time steps and $w = 50$ time steps. The horizontal line shows the Pearson correlation coefficient calculated for the whole time series. It is immediate that the correlation between the two series is nearly 1 during bubbles regime, but it detaches during stable regimes.

5.3 Origin of bubbles

This section aims to understand the process at the origin of faster-than-exponential growth bubbles from a theoretical point of view. The description of the model through all equations is quite complicated and it is characterized by stochastic elements (in the dividends processes, in the updating the number of noise traders and in the Ornstein-Uhlenbeck κ_t). However, we can limit our observations on the dynamical equations of the mean values of z_t and the opinion indices $s_{1,t}$ and $s_{2,t}$. It is possible to decouple the equations of the noise traders class from the others considering the fixed point of the momentum for both the assets equal to $H^* = H = 0.00016$. Certainly, this simplifies the picture but the behavior of the mean-value quantities can be useful for the comprehension of the whole dynamics and the emergence of bubbles. The derivation of the mean-value equations follows a similar approach used by Lux and Marchesi (2000) and Lux (1998) .

The dynamical equations of the mean values of $z, s_{1,t}$ and $s_{2,t}$ can be derived from the mean-value equations of the number of noise traders in each subgroup in eq. 4.53. For the sake of simplicity, it is better to consider the variables in the continuous time limit. Thus, in the following we denote as $n_1^{\pm}$ and $n_2^{\pm}$ the average values of $N_1^{\pm}$ and $N_2^{\pm}$ and with $p_{11}^{\pm}$, $p_{22}^{\pm}$, p_{12}^{+}, p_{21}^{+} the set of transitions rates. Eventually, the dynamical equations can be rewritten in the following way:

$$\frac{dn_1^+}{dt} = n_1^- p_{11}^- - n_1^+ p_{11}^+ + n_2^+ p_{21}^+ - n_1^+ p_{12}^+, \tag{5.5}$$

$$\frac{dn_1^-}{dt} = n_1^+ p_{11}^+ - n_1^- p_{11}^-, \tag{5.6}$$

$$\frac{dn_2^+}{dt} = n_2^- p_{22}^- - n_2^+ p_{22}^+ - n_2^+ p_{21}^+ + n_1^+ p_{12}^+, \tag{5.7}$$

$$\frac{dn_2^-}{dt} = n_2^+ p_{22}^+ - n_2^- p_{22}^-. \tag{5.8}$$

Analogously, we can think the mean values of z, s_1 and s_2 as continuous functions. Moreover, in the following we will intend as z, s_1 and s_2 the mean values of the respective variables. It follows that their definitions are:

$$z = \frac{n_1}{N_n}, \qquad s_1 = 2\frac{n_1^+}{n_1} - 1, \qquad s_2 = 2\frac{n_2^+}{n_2} - 1. \tag{5.9}$$

The derivation of the mean-value equations for z, s_1 and s_2 is obtained recasting the previous set of equations using only the interested variables. Thus, from eq. 5.9, we

can rewrite the mean values of the number of traders as:

$$n_1 = zN_n, \qquad n_2 = (1-z)N_n, \tag{5.10}$$

$$n_1^+ = \frac{1+s_1}{2}zN_n, \qquad n_2^+ = \frac{1+s_2}{2}(1-z)N_n, \tag{5.11}$$

$$n_1^- = \frac{1-s_1}{2}zN_n, \qquad n_2^- = \frac{1-s_2}{2}(1-z)N_n. \tag{5.12}$$

1. *Mean-value equation of z*
   Given the definition of z, we can write:

$$\frac{dz}{dt} = N_n\frac{dn_1}{dt} = N_n\Big(\frac{dn_1^+}{dt} + \frac{dn_1^-}{dt}\Big) = N_n\Big(n_2^+p_{21}^+ - n_1^+p_{12}^+\Big). \tag{5.13}$$

   Plugging the equations for the transition probabilities in eq. 5.13 leads to

$$\frac{dz}{dt} = \begin{cases}(1+s_2)(1-z)\frac{\kappa f}{4}(s_2-s_1) & \text{if } s_2-s_1<0\\ -(1+s_1)z\frac{\kappa f}{4}(s_2-s_1) & \text{if } s_2-s_1>0\end{cases} \tag{5.14}$$

2. *Mean-value equation of s_1*
   The dynamics of s_1 can be derived from its definition:

$$\frac{ds_1}{dt} = \frac{2}{zN}\frac{dn_1^+}{dt} - \frac{2n_1^+}{z^2N_n}\frac{dz}{dt}.$$

   By substitution of eq. 5.12 and eq. 5.6, one can obtains

$$\begin{aligned}\frac{ds_1}{dt} &= \frac{2}{zN}\Big[n_1^-p_{11}^- - n_1^+p_{11}^+n_2^+p_{21}^+ - n_1^+p_{12}^+\Big] - \Big(\frac{1+s_1}{z}\Big)\frac{dz}{dt},\\ &= [(1-s_1)p_{11}^- - (1+s_1)p_{11}^+ + \frac{1-z}{z}(1+s_2)p_{21}^+ - (1+s_1)p_{12}^+] - \frac{dz}{dt}\Big(\frac{1+s_1}{z}\Big).\end{aligned}$$

   Substituting the equations of the transition probabilities and separating the cases, we have

$$\frac{ds_1}{dt} = \begin{cases}\frac{1}{2}[(p^- - p^+) - s_1(p^- + p^+)] + \kappa(s_1+H) + \Big(\frac{1-z}{z}\Big)\frac{\kappa f}{2}(1+s_2)(s_1-s_2)\\ -\frac{1+s_1}{z}\frac{dz}{dt} \quad \text{if } s_2-s_1<0,\\ \\ \frac{1}{2}[(p^- - p^+) - s_1(p^- + p^+)] + \kappa(s_1+H) - \frac{1+s_1}{z}\frac{dz}{dt} \quad \text{if } s_2-s_1>0.\end{cases} \tag{5.15}$$

3. *Mean-value equation of s_2*
   The procedure for deriving the equation of s_2 is similar:

$$\begin{aligned}\frac{ds_2}{dt} &= \frac{2}{(1-z)N_n}\frac{dn_2^+}{dt} + \frac{2n_2^+}{(1-z)^2N_n}\frac{dz}{dt},\\ &= \frac{2}{(1-z)N_n}\Big[n_2^- p_{22}^- - n_2^+ p_{22}^- n_2^+ p_{21}^+ + n_1^+ p_{12}^+\Big] + \Big(\frac{1+s_2}{1-z}\Big)\frac{dz}{dt},\\ &= \Big[(1-s_2)p_{22}^- - (1+s_2)p_{22}^+ + \Big(\frac{z}{1-z}\Big)(1+s_1)p_{12}^+ - (1+s_2)p_{21}^+\Big] + \frac{dz}{dt}\Big(\frac{1+s_2}{1-z}\Big).\end{aligned}$$

   Plugging, now, the transition probabilities, one obtains

$$\frac{ds_2}{dt} = \begin{cases} \frac{1}{2}[(p^- - p^+) - s_2(p^- + p^+)] + \kappa(s_2 + H) + \frac{1+s_2}{1-z}\frac{dz}{dt} & \text{if } s_2 - s_1 < 0,\\ \frac{1}{2}[(p^- - p^+) - s_2(p^- + p^+)] + \kappa(s_2 + H) + \frac{\kappa f}{2}(1+s_1)(s_2 - s_1)(\frac{z}{1-z}) & \\ +\frac{1+s_2}{1-z}\frac{dz}{dt} \quad \text{if } s_2 - s_1 > 0. & \end{cases} \tag{5.16}$$

The mean-value equations of z, s_1 and s_2 are non-linear and the analysis of the stability for the continuum of the steady states is done in appendix B. The line of fixed points is

$$s_1^* = s_2^* = s = \frac{p^+ - p^- - 2\kappa H}{2\kappa - (p^+ + p^-)} \quad \text{for arbitrary} \quad z^*. \tag{5.17}$$

Thus, the stationary states are characterized by the same value s for the opinion indices and they depend on the herding propensity κ. The equilibrium line ($s_1^* = s, s_2^* = s, z^*$) is stable if z^* is comprehended in the interval $[z_b, z_a]$ for $\kappa < \kappa_c$, with z_a and z_b defined as

$$z_a = \frac{\frac{\kappa f}{4}(1+s)^2 + \frac{p^+ + p^-}{2} - \kappa}{\frac{\kappa f}{2}(1+s) + \frac{p^+ + p^-}{2} - \kappa}, \tag{5.18}$$

$$z_b = \frac{\frac{\kappa f}{4}(1+s)(1-s)}{\frac{\kappa f}{2}(1+s) + \frac{p^+ + p^-}{2} - \kappa}. \tag{5.19}$$

In contrast, for $\kappa > k_c$, the continuum of fixed points is unstable for $\forall z^* \in [0,1]$. The critical value of the herding propensity is $\kappa_c = \frac{p^+ + p^-}{2} = 0.2$. From eq. 5.19, one can notice that the critical values z_a and z_b depend on the herding propensity κ and the parameter f. Figure 5.5 reproduces the range $[z_b, z_a]$ of values for which the line of fixed points is stable as a function of the herding propensity κ for different values of f. It is evident that for larger values of f, the range is narrower.

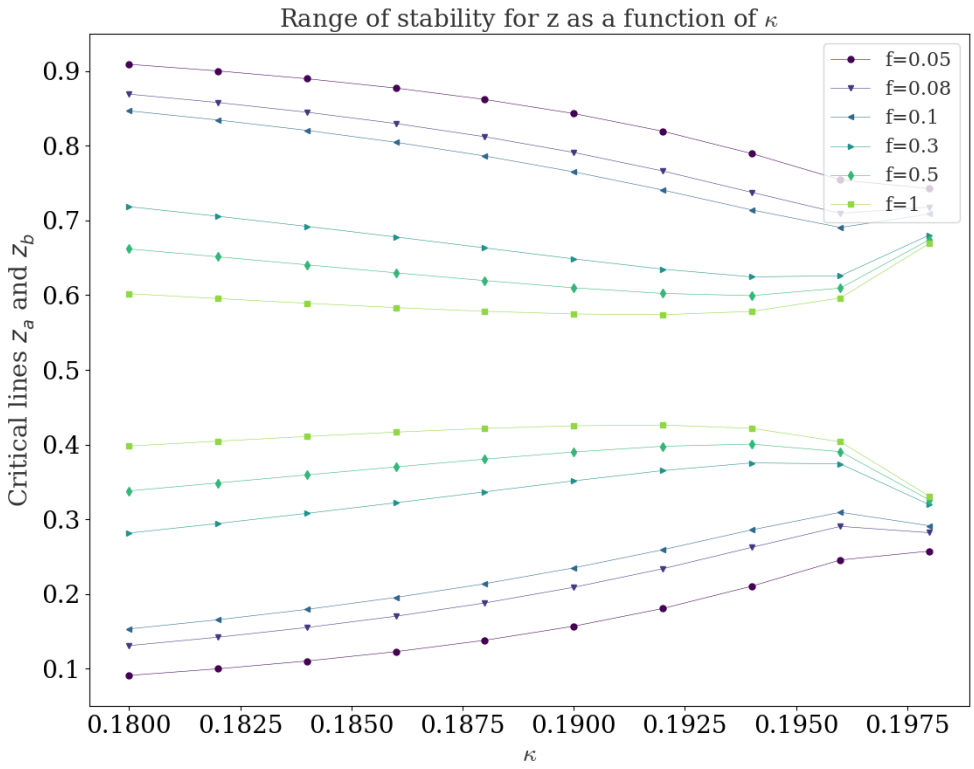

Figure 5.5: The figure shows the lines z_a (in the upper part) and z_b (in the lower part) for different values of κ and f. The range of z-values between the two curves are stable. The interval of stable values becomes narrower, higher the parameter f.

The theoretical insight can be very useful to understand the time series with constant herding propensity. At odds with the case with only one risky asset, the continuum of stationary states is stable only for a restricted range of z values, depending on κ and f. As long as z_t moves randomly in the stable range, no instabilities can arise. However, because of the random fluctuations, the values of z can exit from the stable regime and causes the deviations of the opinion indices that tend to diverge exponentially from the unstable fixed point s. As a consequence, the growth in the opinion indices determines deviations in the price trends, thus, higher fluctuations and volatility clustering in the returns. Since for higher values of f, the range of stability is tighter, the possibiWhestphallity of instability is higher.
In the previous theoretical explanation, the momentum is thought as constant. In reality, the momentum changes in time and its fluctuations are determined by the

past returns. Its behavior enhances the emergence of possible instabilities creating a self-reinforcing loop. The phenomenon is not far from what is denoted in Kaizoji et al. (2015) as a "self-fulfilling prophecy"(p. 291). More noise traders believe in the upward trend of the price, more people will invest in the risky assets, effecting positively the upward trends of the prices.

Eventually, in order to understand better the relationship between the theoretical explanation with the simulated data, we propose to study the transition between the different regimes examining the behavior of the empirical average values of the opinion indices for different values of κ and f. Following the same strategy in Harras et al. (2012), we study the opinion indices mean values computed over the simulated time series and their normalized standard deviations scaled by the amplitude of the momentum, namely

$$\bar{s}_1 =< s_{1,t} >_t, \quad \bar{\sigma}_1 = \frac{\sqrt{< (s_{1,t} - \bar{s}_1)^2 >}}{\sqrt{< (H_{1,t} - \bar{H})^2 >}}, \tag{5.20}$$

$$\bar{s}_2 =< s_{2,t} >_t, \quad \bar{\sigma}_2 = \frac{\sqrt{< (s_{2,t} - \bar{s}_2)^2 >}}{\sqrt{< (H_{2,t} - \bar{H})^2 >}}. \tag{5.21}$$

Figure 5.6 illustrates the curves of $\bar{s}_{1,2}$ and $\bar{\sigma}_{1,2}$ as a function of the herding propensity κ for different values of f. The average values and the standard deviations are performed over 300 simulations of total length $T = 5000$ time steps. The plots of the average values confirm the theoretical analysis. Indeed, for $\kappa < \kappa_c$, the plots of $\bar{s}_1$ and $\bar{s}_2$ follow the trend predicted by the fixed point s. Nevertheless, for $f > 0.1$ the curves detaches from the theoretical predictions. We can argue that this behavior is due to the fact that for higher values of f, it is more probable that z enters in the unstable regime making more difficult the convergence to the stationary states. For $\kappa > \kappa_c$, the continuum of fixed points become unstable and the dynamics detaches completely from the s curve. This is the reason why in average the opinion indices reach the lower bound.
Eventually, we can notice that the standard deviations are enhanced at the critical value κ_c, but for higher value of f the peak shifts towards higher values of κ. This phenomenon can be explained by the theory presented in Harras et al. (2012). In the article, Harras and collaborators investigate the increasing of the fluctuations in a kinetic Ising system for an aperiodic external field. At odds with the stochastic resonance in case of a periodic external forcing, the fluctuations do not emerge as a consequence of an enhancement of the signal. Indeed, the opinion indices are constrained in the range $[-1,1]$, thus the high peak in the standard deviation cannot be explained as a divergence of the opinion indices. On the contrary, the amplification of the fluctuations can be compared with the divergence of the susceptibility that

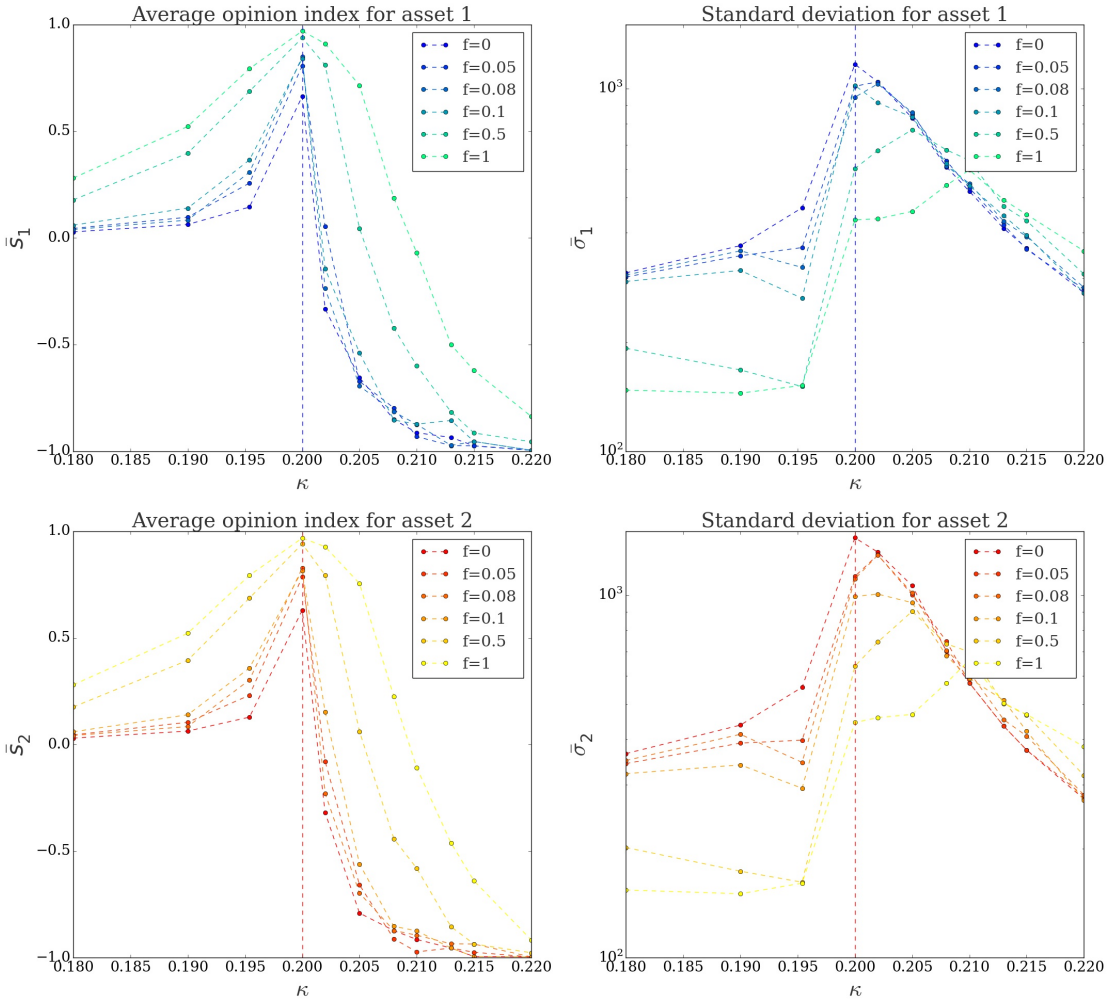

Figure 5.6: The first frame shows the mean values of $s_{1,t}$ and its scaled standard deviation as functions of the herding propensity κ. The second frames shows the analogous quantities for the second asset. In order to evidence the dependence on the parameter f, we have obtained the curves also for different values of f. The average and the standard deviations have been performed over 300 simulations.

happens during a phase transition. This phenomenon has been called in Harras et al. (2012) "noise-induced volatility".

To conclude, we can summerize our findings in the following lines. Simplifying the equations of the dynamics for the noise traders class, we have found the continuum of stable points $(s_1^* = s, s_2^* = s, z^*)$ and calculated the interval of z^* values that ensure the stability of the fixed points for $\kappa < \kappa_c$. In contrast, for $\kappa > \kappa_c$, the steady

states are always unstable and the mean values s_1 and s_2 diverges from the stable points. The theoretical results have been compared to the average values of the opinion indices obtained by simulated data. Figure 5.6 shows clearly the presence of two regimes separated by the critical value κ_c. For $\kappa < \kappa_c$, the average opinion index curve follows the theoretical prediction (eq. 5.17), whereas for $\kappa > \kappa_c$, the fixed points loose the stability and the opinion indices diverge exponentially. Therefore, we can conclude that the model presents a deep-rooted instability due to the herding behavior.
At this point, we can deduce that the time series with the Ornstein-Uhlenbeck herding propensity are characterized by the rapid passage of the system trough the stable and unstable regime. As a consequence of the stochastic process, the herding propensity κ_t can enter in the unstable regime, making the opinion indices diverge exponentially from the equilibrium value. The transient growing behavior of the opinion indices results in the faster-than-exponential growth of the prices as we can see in a zoom of the simulation with Ornstein-Uhlenbeck κ in correspondence of the bubbles at time $t \simeq 3600$ time steps and $t \simeq 3800$ (fig. 5.7). Furthermore, the model is further complicated by the presence of time varying momentum H_t that influences the decisions of the noise traders. In analogy to the explanation given by Kaizoji et al. (2015) for the original model, the momentum induces an additional sources of fluctuations in the dynamics and can enhance the formation of inherent instabilities, creating self-reinforcing loops that sustain the growth of longer bubbles even when κ_t reverts to the stable regime.

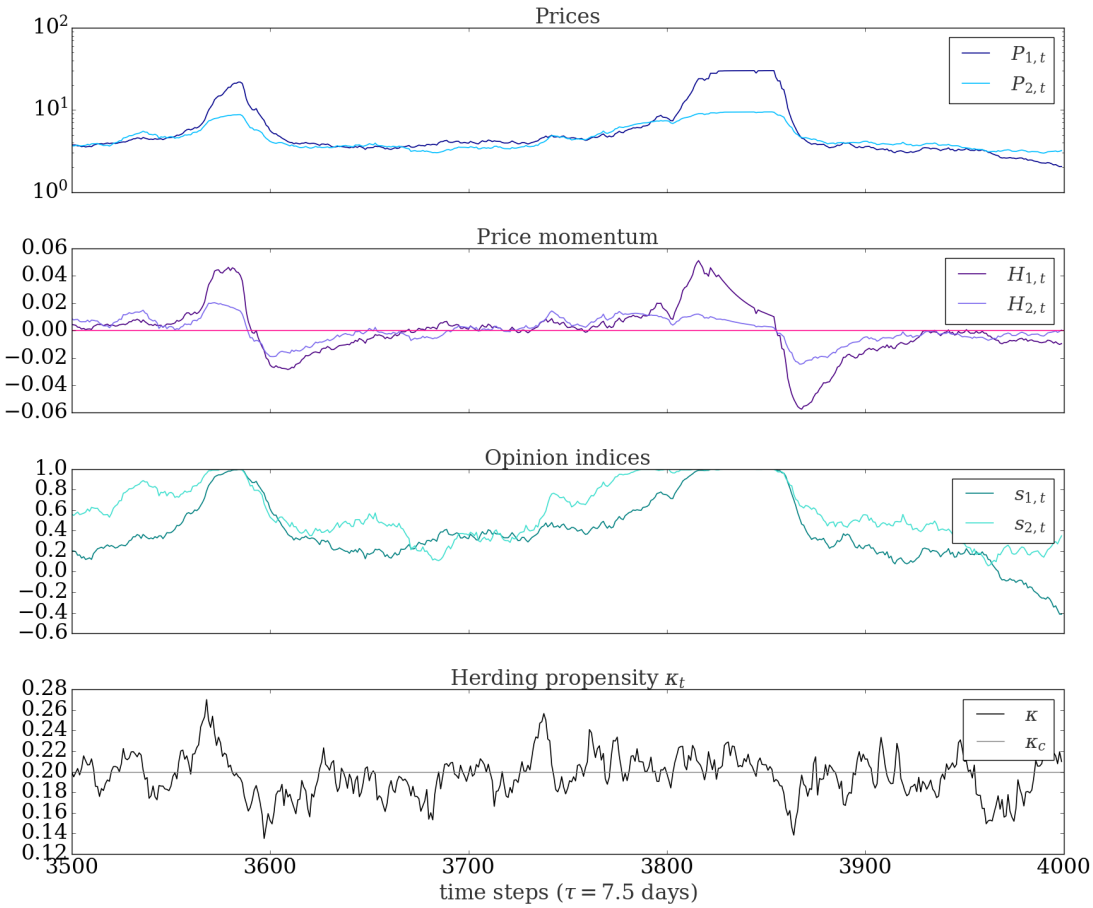

Figure 5.7: The plot shows a zoom of fig. 5.2 in correspondence of the bubbles in $t \simeq 3600$ and $t \simeq 3800$. The panels show the emergence of bubbles in the log-price trend. The plots confirm that the emergence of the transient faster-than-exponential behavior is triggered by the values of the herding propensity $\kappa > \kappa_c$ that causes the collective behavior of the noise traders and effecting the price. The growth of the price is sustained by the price momentum even in the occasion of the reversal of the herding propensity.

Eventually, we aim to confirm quantitatively the typical faster-than-exponential bubbles growth behavior in the simulations. As example, we concentrate on the bubble of previous simulation at time $t \simeq 3600$ (fig. 5.7). Following the same approach used in Kaizoji et al. (2015) in the case of a single risky asset, we argue that when $\kappa > \kappa_c$, the opinion indices increase exponentially in time

$$s_t = s_0 + ce^{\alpha t}, \tag{5.22}$$

and from visual inspection we argue that also log-prices grow exponentially:

$$log(P_t) = log(P_0) + de^{\beta t}. \tag{5.23}$$

Here, $s_0, \alpha, c, log(P_0), \beta, d$ represent the coefficients to be fitted. Figure 5.8 shows the fitted curves on the opinion indices and log-prices obtained by the models in eq.5.22 and 5.23, while the coefficients obtained by non linear regression are reported in tab. 5.2. From fig. 5.8 the faster-than-exponential behavior of the prices is confirmed. Moreover, the values of α found in tab.5.2 are in agreement with the range of values or at least the order of magnitude of the eigenvalues $\lambda_{2,3}$ that characterize the behavior of the mean-values $s_1(t)$ and $s_2(t)$ and determine the exponential growth in the unstable regime. The derivation of the eigenvalues is reported in Appendix B (eq. B.11).

Asset 1			
Opinion Index	$s_0 = 0.31 \pm 0.02$	$\alpha = 0.073 \pm 0.001$	$c = 0.14 \pm 0.01$
Log-price	$log(P_0) = 1.61 \pm 0.001$	$\beta = 0.199 \pm 0.0001$	$d = 0.027 \pm 0.0002$
Asset 2			
Opinion Index	$s_0 = 0.671 \pm 0.001$	$\alpha = 0.102 \pm 0.0005$	$c = 0.062 \pm 0.001$
Log-price	$log(P_0) = 1.497 \pm 0.0004$	$\beta = 0.155 \pm 0.0003$	$d = 0.041 \pm 0.0001$

Table 5.2: The table reports the values of the fitting of the models in eq. 5.23 and eq. 5.22 for both assets. The first line shows the parameters relative to the opinion index and the second line the parameters relative to the log-price.

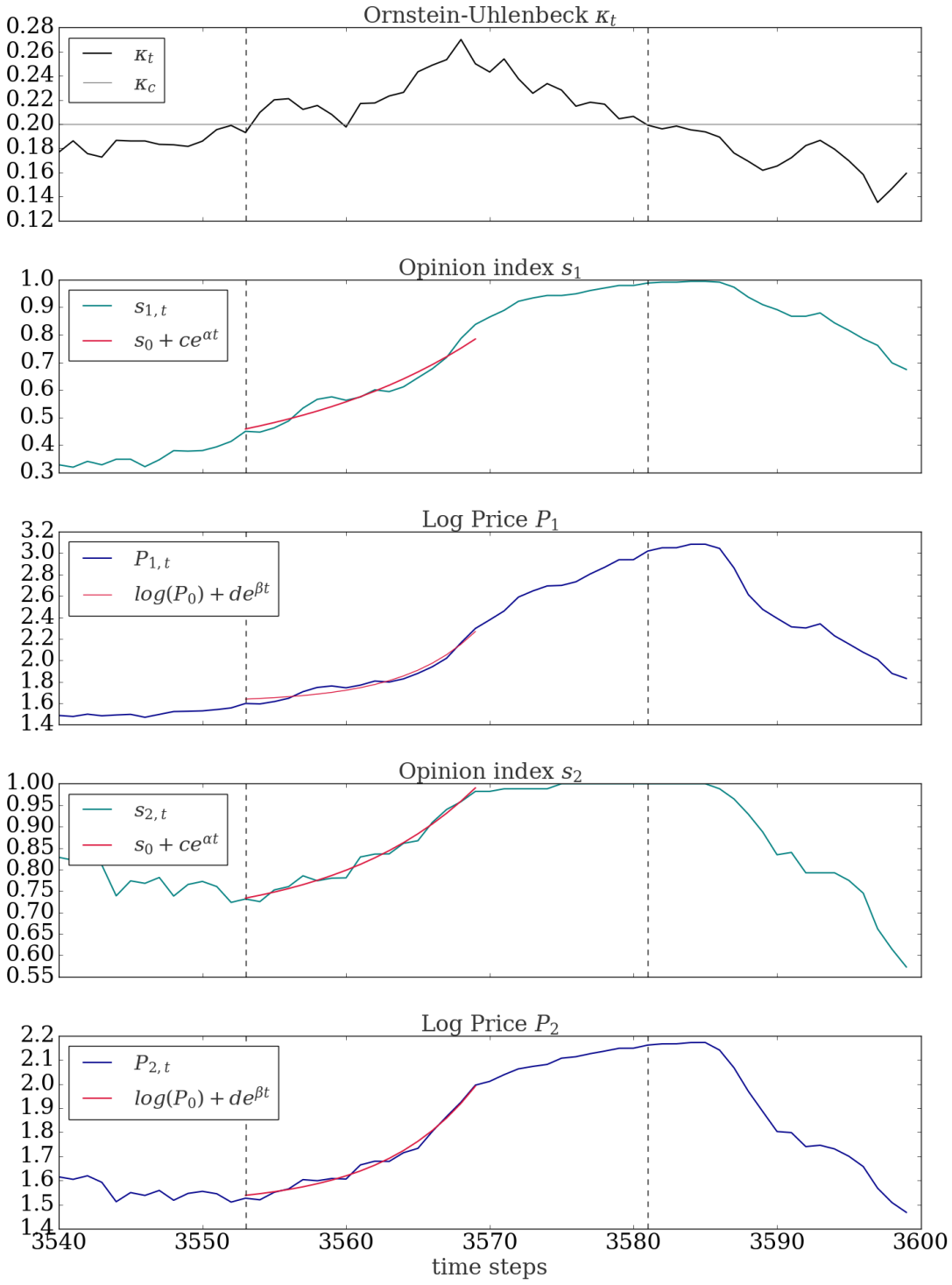

Figure 5.8: The figure shows a zoom of fig. 5.7 on the log-prices and the opinion indices. The figure shows also the fitting curves obtained by regression on the models in eq. 5.23 and 5.22. The dashed lines show the interval where $\kappa > \kappa_c$ and the opinion indices and the log-prices grow exponentially.

5.4 Correlations between the assets returns

In order to gain some insight into the dynamic behavior of the model, it is useful to analyse the co-movements of the returns of the two assets. The question is persued in two different directions:

- analysis of the relationship between the fundamentalists expectations on the correlations between the assets and the actual realized correlations,
- the impact of the noise traders on the formation of the correlation between the assets returns.

5.4.1 Dependence of the correlations on parameter ρ

We aim at the comprehension of the relationship between the expected correlation between the returns, represented by the exogenous parameter ρ and the realised correlations. As a matter of fact, the analysis of the relationship between the correlation imposed "a priori" and its realization a posteriori is significant to understand the role of fundamentalists in the enlarged model.

In figure 5.9 we have plotted the Person correlation coefficient calculated on the assets returns against different values of the correlation parameter ρ. The plot is obtained maintaining $f = 0$, in order to silent the effect of noise traders in this stage of the analysis. In the plot we have shown in dashed line the bisector of the frame in order to emphasize the difference between the imposed correlation and the realised correlation. First, we can notice that the trend of the plot is crescent and that in absence of a priori correlation between the two asset, i.e. for $\rho = 0$, the realised correlation is not zero ($\rho_{realised} \simeq 0.2$). Imposing $\rho = 0$ in eq. 4.36a and 4.36b, one obtains that the fundamentalist risky fractions are now uncorrelated and depend uniquely on the respective dividend-price process:

$$x^f_{1,t} = \frac{1}{\gamma \bar{\sigma_1}^2}\Big[\mathbb{E}_{rt,1} - r_f + \frac{d_{1,t}(1+r^d_1)}{P_{1,t}}\Big], \tag{5.24}$$

$$x^f_{2,t} = \frac{1}{\gamma \bar{\sigma_2}^2}\Big[\mathbb{E}_{rt,2} - r_f + \frac{d_{2,t}(1+r^d_2)}{P_{2,t}}\Big]. \tag{5.25}$$

However, the equations of the prices are not uncoupled. Indeed, inserting the value of $\rho = 0$ into the set of the parameters of the price equations (in app.A), one gets

$$b_{1,t}P_{2,t} + c_{1,t}P^2_{1,t} + d_{1,t}P_{1,t}P_{2,t} + e_{1,t}P_{1,t} + g_{1,t} = 0, \tag{5.26}$$

$$b_{2,t}P_{1,t} + c_{2,t}P^2_{2,t} + d_{2,t}P_{2,t}P_{1,t} + e_{2,t}P_{2,t} + g_{2,t} = 0. \tag{5.27}$$

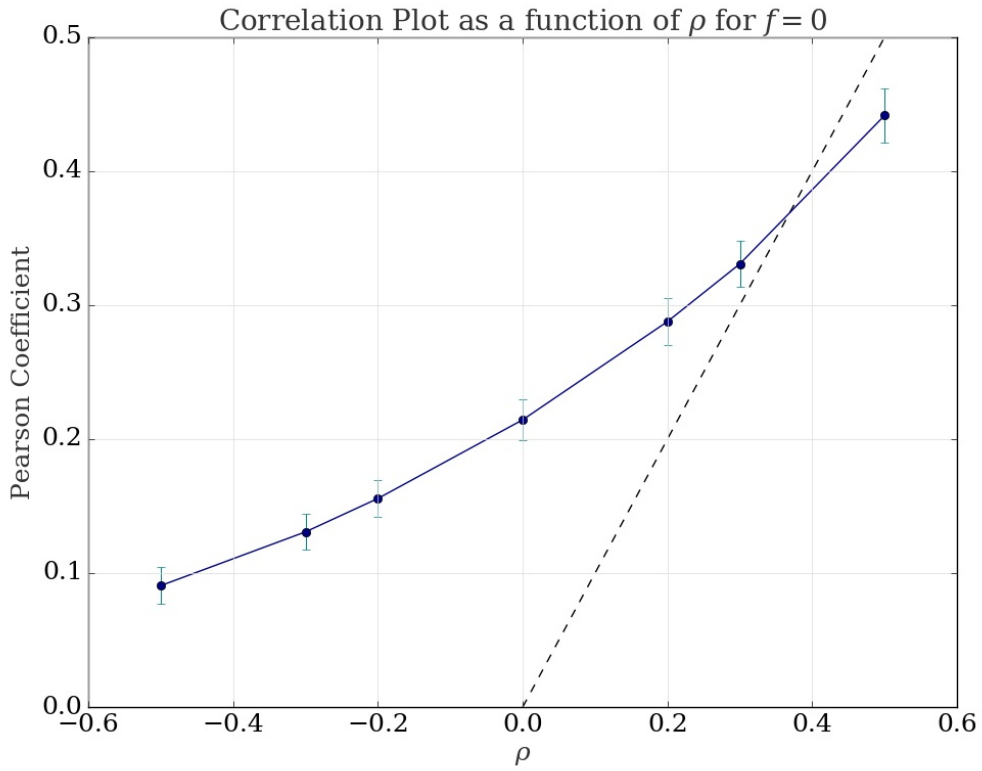

Figure 5.9: Plot of the Pearson coefficient of the asset returns as a function of the exogenous correlation coefficient ρ, computed over 300 simulations with different random seeds for $T > 100$ time steps. The simulation is obtained for $f = 0$, constant herding propensity κ and total length $T = 5000$ time steps. The dashed line represents the bisector line.

The two equations are still coupled and non-linear, which can explain the deviation of the realised correlation from the zero.
When $\rho > 0$, the fundamentalist risky fractions are coupled and both the dividend-price ratios give a contribution for the fundamentalist strategy (eq. 4.36a and eq. 4.36b). It is evident that the contribution of each asset enters in the equation with different weights: $1/(1-\rho^2)$ and $-\rho/(1-\rho^2)$. For instance, we focus on $x^f_{1,t}$ (eq. 4.36a), but the analogous argument applies to $x^f_{2,t}$.
When $\rho > 0$, the two terms become $1/(1-\rho^2) > 1$ and $-\rho/(1-\rho^2) < 0$. This means that for $x_{1,t}$ the dividend price ratio $d_{1,t}/P_{1,t}$ contributes positively, whereas the second one $d_{2,t}/P_{2,t}$ negatively. The consequence is that each risky fraction follows independent trends. The lag between the fundamentalist risky fractions $x_{1,t}$ and $x_{2,t}$ reflects also in the lag between the dividend-price ratios. This creates alternating

periods in which asset 1 is more volatile than asset 2 or vice-versa. This phenomenon increases the realised correlation in the assets returns.
On the other hand, when $\rho < 0$, the factor $-\rho/(1-\rho^2)$ becomes positive, whereas the first factor remains greater than one. Thus, both the dividend-price ratios give a positive contribution to the risky fractions. Consequently, the two risky fractions depend much more on both the dividend-price processes that now follow similar paths. The absence of the lag in the price trends is reflected also in a reduction of the correlation between the two assets. Nonetheless, even if the exogenous correlation coefficient is negative, the realised correlation is positive but almost zero.
The point ρ^* where the realised correlation and the correlation coefficient ρ meet has a relevant meaning. In general, there is a discrepancy between fundamentalists assumption on the covariance matrix and the realizations, except for this value. Thus, fixing $\rho = \rho^*$ would satisfy the problem of self-consistency and would give a natural justification to the correlations between the two assets.

5.4.2 Dependence of the correlations on the parameter f

The behavior of the correlation between the two assets returns does not depend uniquely on the correlation factor ρ, but also on the parameter f. The latter regulates the number of traders switching between the two noise traders sub-classes and its value is exogenously imposed at the beginning of the simulation. Since f regulates the flux of the traders and thus the opinion indices $s_{1,t}$ and $s_{2,t}$, the analysis will describe the impact of noise traders on the correlations between the asset returns.

Figure 5.10 shows the dependence of the Pearson coefficient against different values of f. The first property to notice is the presence of a minimum in $f \simeq 0.2 - 0.3$. It is the benchmark of two different behaviors for $\rho < 0.2$ and $\rho > 0.2$.
In order to gain some insight into the problem we have plotted the cross correlation function between the opinion indices $s_{1,t}$ and $s_{2,t}$ for different values of f. Figure 5.11 shows the cross-correlation coefficient obtained from the average over 100 simulations for different values of f. We remind that the cross-correlation coefficient of two time series x_t and y_t is computed as

$$r_{xy}(\tau) = \frac{\sigma_{xy}(\tau)}{\sqrt{\sigma_x(0)\sigma_y(0)}}, \tag{5.28}$$

$$\sigma_{xy}(\tau) = \frac{1}{N-1}\sum_{t=1}^{N}(x_{t+\tau} - \mu_x)(y_t - \mu_y). \tag{5.29}$$

Where, we intend as μ_x, μ_y the mean values of x_t and y_t. From the plot, we can immediately notice that the same discrepancy of behavior for $f < 0.2$ and $f > 0.2$ is still present, confirming the conjecture that the peculiar behavior of the returns

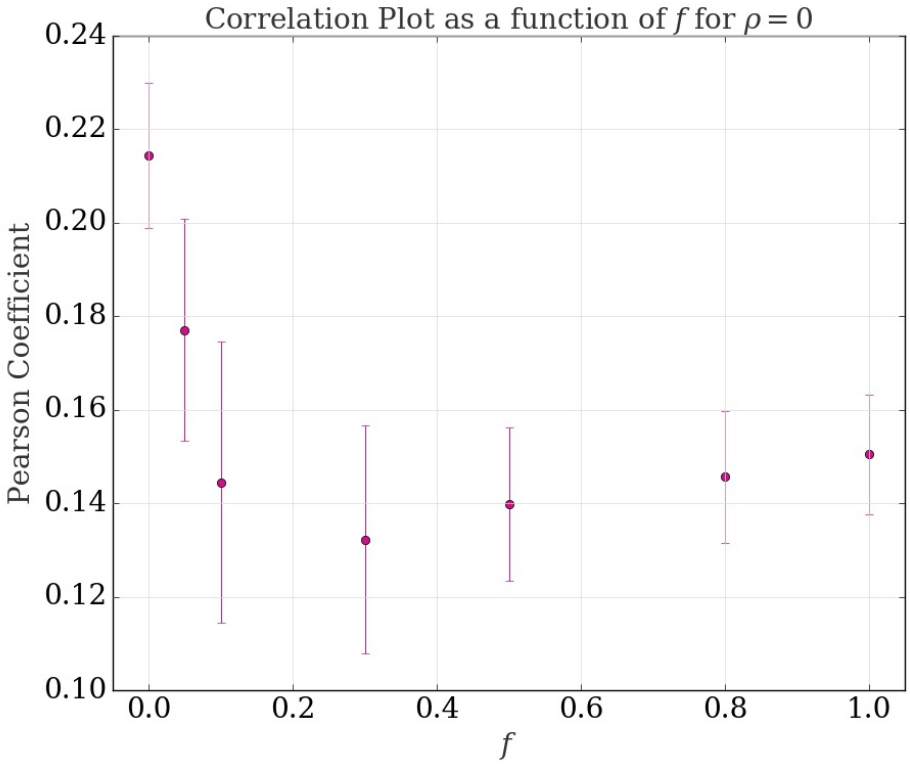

Figure 5.10: Plot of the Pearson coefficient of the asset returns as a function of the exogenous parameter f, computed over 300 simulations with different random seeds for $T > 100$ time steps. The simulation is obtained for $\rho = 0$, constant herding propensity κ and total length $T = 5000$ time steps. The errorbars are calculated as the standard deviation over 300 simulations.

correlations is an effect of the opinion index dynamics. In order to visualize the behavior of the opinion indices for the two different regimes, figure 5.12 shows two examples of opinion indices tracks for $f = 0.05$ and $f = 0.3$. The decreasing trend of the Pearson coefficient for $f < 0.2$ can be explained by the lack of correlation between the opinion index dynamics. The cross-correlation coefficient is nearly zero on average. Thus, the prices are the results of the balance between the fundamentalists and noise traders strategies. However, when f increases, the cross correlation between $s_{1,t}$ and $s_{2,t}$ is no more negligible. For $f > 0.2$ the cross-correlation reaches high values, indicating a larger correlation between the opinion indices. As we can see in figure 5.12 (lower panel) the opinion indices are not only correlated, but also near to the upper limit, which means that for most of the time the noise traders invest in the risky assets. The price dynamics is then led by the noise traders.

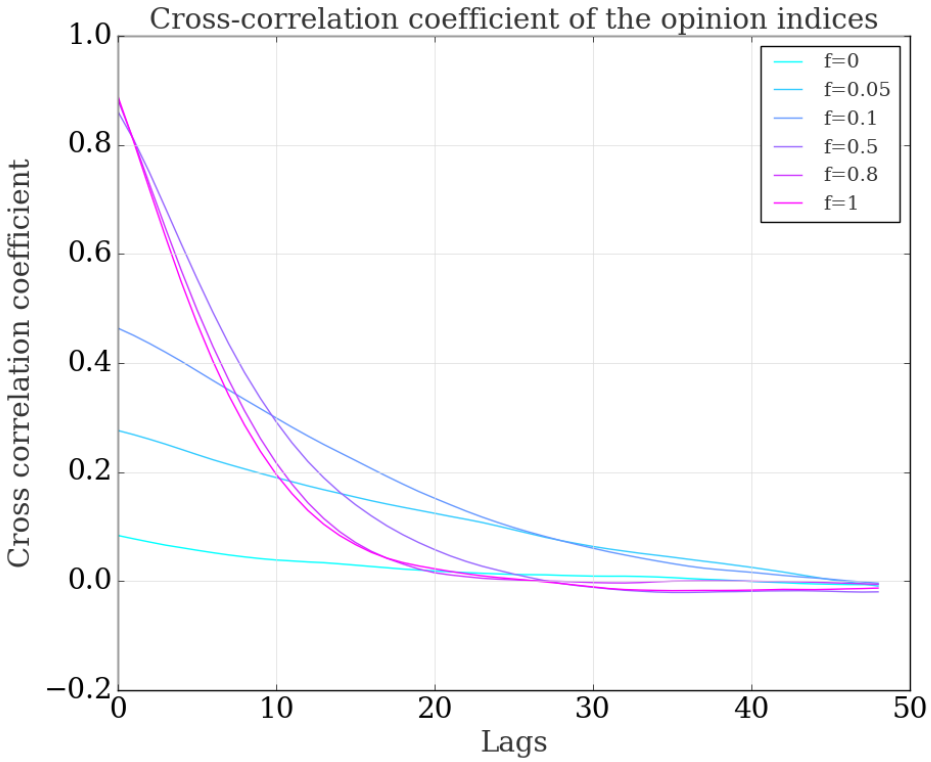

Figure 5.11: Plot of the cross-correlation coefficient of the opinion indices s_1 and s_2 for different time lags τ. The cross-correlation is computed as average over 100 simulations for each time lag.

On the contrary, for $f < 0.2$ the opinion indices are more oscillatory, but they are out of phases, causing the fact that from time to time one asset is more attracting than the other and more traders invest in it (fig. 5.12, upper panel). It follows that the assets alternate periods of tranquility to periods of high deviations as they are out of phase. For $f \simeq 0.2$, the signature of this behavior is more pronounced with the result that the two opposite trends compensate each other and thus the correlation reaches the minimum.

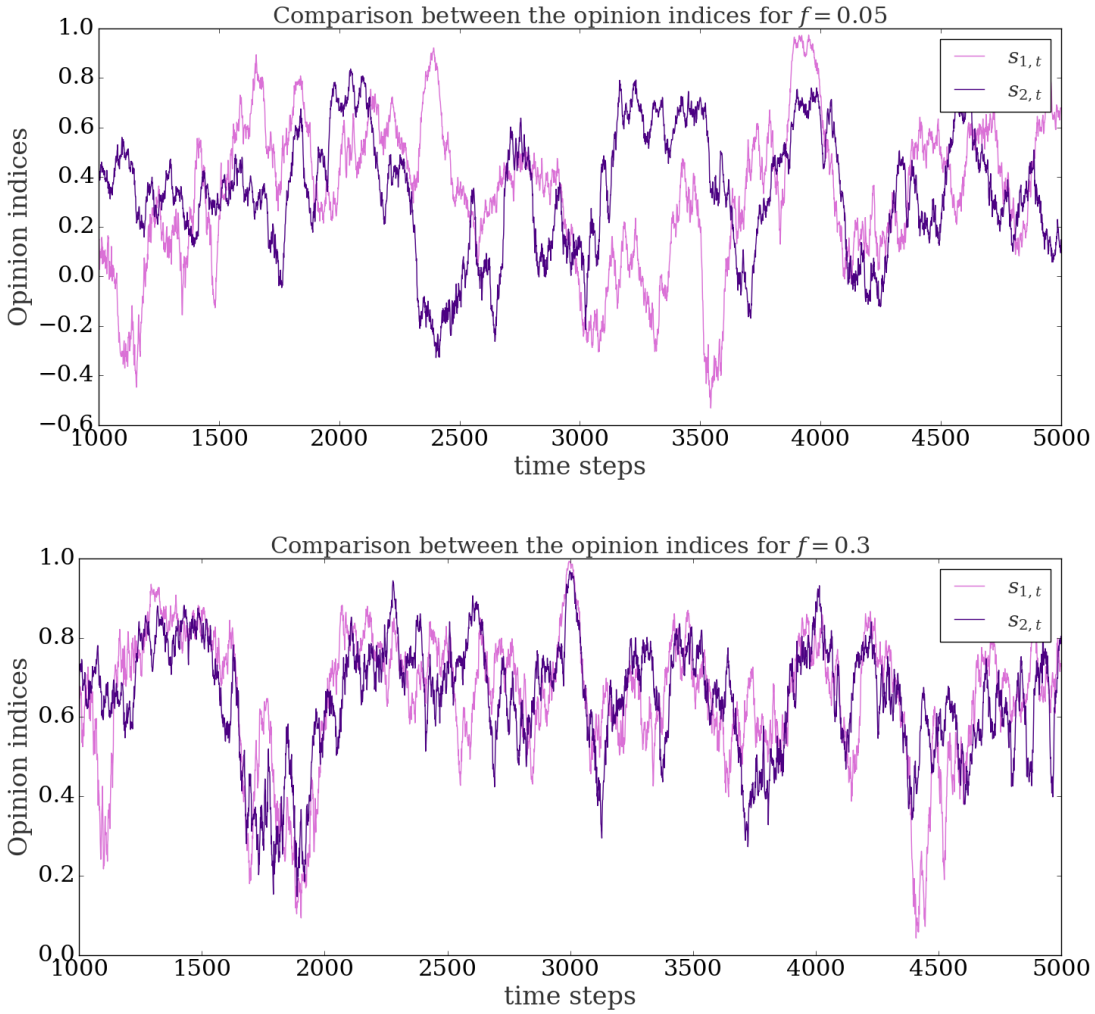

Figure 5.12: The figure shows in two different panels the comparison between the opinion indices $s_{1,t}$, $s_{2,t}$ for $f = 0.05$ and $f = 0.3$ (with constant κ and $\rho = 0.3$). The time series are obtained using $\rho = 0.3$ and the set of parameters listed in 5.1. The upper panel shows that for $f < 0.1$, there exists a lag between the opinion indices that determines correlations in the assets returns. On the contrary, the lower panel shows that for $f > 0.1$ the lag does not exist anymore and the opinion indices follows similar trends, increasing the correlations between the two assets.

5.5 The Stylized Facts of the financial market

The presence of ubiquitous statistical properties in financial data is well known. There exists a vast literature that tries to understand the emergence of these properties. A common thinking in a large part of the literature (Sornette (2014), Lux (1998)) is that, as in a complex system, from the micro-interactions among a large number of traders can emerge universal statistical properties, independent of the microscopic details of the interactions. Agent based models have furnished the natural framework for the implementation of the interactions among the investors and the analysis of the link between the micro-interactions and emergence of a collective behavior.

Our model is perfectly in line with this spirit. Reason why it is important to check if the model is able to reproduce some empirical statistical laws. In this section, we concentrate on a brief review of the most common "stylized facts" that can be reproduce by ABMs, adapted from Lux (2009):

1. *Fat tails of asset returns.*
   The shape of the distribution of the returns deviates from the shape of the Gaussian distribution. As a matter of fact, the empirical distribution of returns has fatter tails than the Gaussian distribution. From a probabilistic point of view, it means that rare events happens more often than what a Gaussian distribution could predict. From a statistical point of view, the difference can be grasped in the fourth moment of the distribution. The excess of kurtosis k is a measure of the fourth moment of a distribution:

   $$k = \frac{1}{T}\sum_{t=1}^{T}\Big(\frac{r_t - \bar{r}}{\sigma}\Big)^4 - 3. \tag{5.30}$$

   The Gaussian distribution is characterized by null kurtosis $k = 0$ and any distribution with $k > 0$, or excess forth moment is called 'leptokurtic'. The shape of a leptokurtic distribution has more mass in the centre and in the tails.

2. *Volatility clustering and long memory in the autocorrelation function of absolute returns.*
   The returns are not identical distributed RVs. A benchmark of this fact is the volatility clustering, or the phenomenon for which there exists periods of high peaks alternated by periods of tranquility. The burst-like phenomenon causes immediate nonhomogeneity in the distribution of higher moments. This effect is visible in the autocorrelation function of different powers of the asset returns

$|r_t|^\gamma$. At difference of signed returns, the powers of the absolute returns manifest long-memory properties. Indeed, for them, the autocorrelation function does not decays exponentially fast, but with an hyperbolic decay.

As pointed out by Lux (2009), even though such observations are ubiquitous in financial data, a straightaway explication is still missing. However, the literature investigating the emergence of these properties through adequate models is vast. After the initial studies of Mandelbrot (1963) on the fat tails of returns distributions, subsequently the first agent based models able to reproduce volatility clustering and long-memory in the autocorrelations appeared (Kirman (1993), Lux and Marchesi (2000), Lux and Marchesi (1999)). With the same spirit, in its original formulation, the model of Kaizoji et al. (2015) was able to reproduce the stylised facts of the financial data, but also a new interesting phenomenon: financial bubbles. Following the same spirit, our extension of the original market model is still able to reproduce bubbles, but it is necessary to check if it is able to recreate also the stylized facts.

First, we aim to demonstrate that the distributions of the returns of the two assets are fat tailed. This property can be highlighted by the cumulative distribution of the absolute returns. Indeed, as shown in Lux (2009), by extreme values theory, it can be proved that the decline of the tails can be approximated by a Pareto distribution

$$p(x) \sim x^{-1-\alpha}. \tag{5.31}$$

The tail parameter α in empirical observations is usually comprehended in the interval [2,4]. Figure 5.13 shows the cumulative distributions of the absolute returns for asset 1 and asset 2, defined as $F(x) = Prob(X \geq x)$ in log-log scale. Hence, the linear trend individuated in the plot is directly related to the power law distribution of the tails. Therefore, we have fitted the linear trend of the cumulative distribution in order to check if the tail parameter α is found in the empirical interval or not. As we can observe from fig. 5.13, the tail parameters fitted on the cumulative distributions are perfectly in agreement with the interval found in data. In order to be more quantitive, we have persued a statistical approach. Following the work of Lux and Marchesi (2000), the analysis is based on the estimation of the value of the tail index of the abolute returns time series using the Hill estimator (Hill (1975)). The Hill-estimates is obtained ordering the sample of data in descending order $x_1 \geq x_2 \geq ... \geq x_k \geq ... \geq x_1$, with k the number of data in the 'tail' of the distribution. The tail index is, thus, computed as

$$\alpha = \frac{1}{\frac{1}{k}\sum_{i=1}^{k}\Big[ln(x_i) - ln(x_{k+1})\Big]}. \tag{5.32}$$

We have estimated the tail indices for asset 1 and asset 2 on 100 different simulations of length $T = 5000$ time steps. The Hill-estimates have been computed over

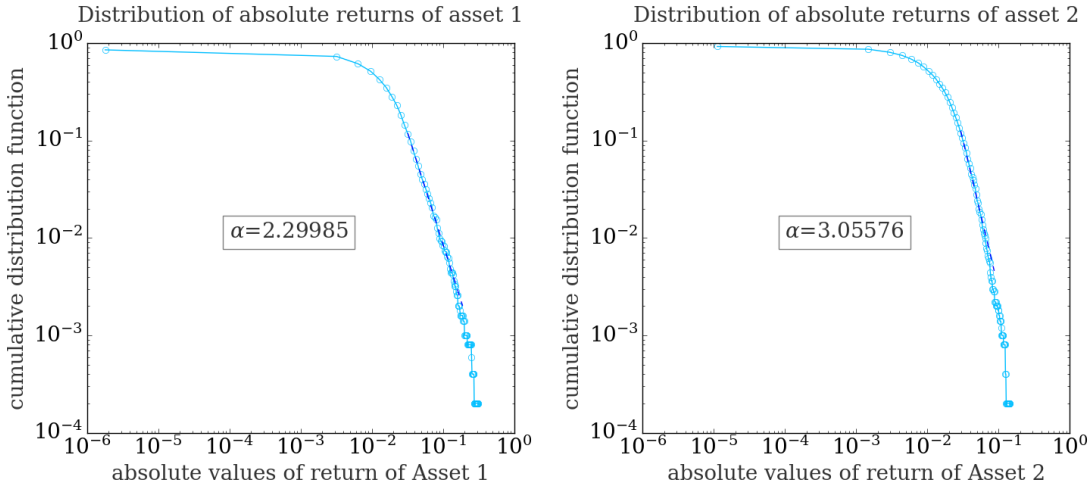

Figure 5.13: The figure shows the cumulative distribution function of the absolute returns for asset 1 and asset 2 for the simulation with the parameters used in tab.5.1, $\rho = 0.3$ and $f = 0.05$ and Ornstein-Uhlenbeck κ_t. The dashed lines represent the linear fit correspondent to the fat tails of the distribution, characterized by power law decay $p(x) \sim x^{-1-\alpha}$. The boxes report the values of the tail parameters α.

the 15% of the observations. In addition, we have added the computation of the mean of excess kurtosis k over 100 simulations. The results presented in table 5.3

	mean value	min value	max value	excess kurtosis
Asset 1	2.69	1.75	3.53	7.52 ± 7.68
Asset 2	2.83	1.95	3.43	7.32 ± 11.93

Table 5.3: The table reproduces the values of the tail indices for asset 1 and asset 2 calculated on 100 simulations with different random seed of length $T = 5000$ time steps. In table we report the mean value of the tail indices and the range of estimates (min value, max value) using the 15% of the absolute returns. In the last column, the table reports the mean-value of excess kurtosis for the distributions of the returns, computed over 100 simulations with its standard deviation. All the simulations use $f = 0.05$, $\rho = 0.3$ and Ornstein-Uhlenbeck κ_t.

are close to the empirical findings, according to which the range of the tail index is [2,4]. Moreover, the mean value of the excess kurtosis is positive, confirming the fact that the distribution of absolute returns is leptokurtic.

Eventually, we are interested in the long-memory properties in the distributions of powers of the absolute returns. Figure 5.14 shows the autocorrelation functions for signed and absolute returns for both assets, obtained as an average over 300 simulations with different random seeds and total length $T = 6000$ time steps, but considering only the values $t > 1000$ time steps.
For both assets, the signed returns decays to the zero exponentially fast. On the contrary, the absolute returns have a slower-than-exponential decay. The slower decay is said to be hyperbolic if it is a power law decay, namely

$$\rho(k) \sim Dk^{-\alpha}, \tag{5.33}$$

for some D and $\alpha > 0$. The hyperbolic decay is evidence of the long range dependence in volatility. Therefore, signed returns are almost uncorrelated, preventing traders from any possibility to arbitrage, whereas long-range dependence is found in the absolute returns.

Overall, our model is able to reproduce the typical stylised facts of the financial data as far as regards the long-memory in volatility and the presence of fat tails in the returns distributions.

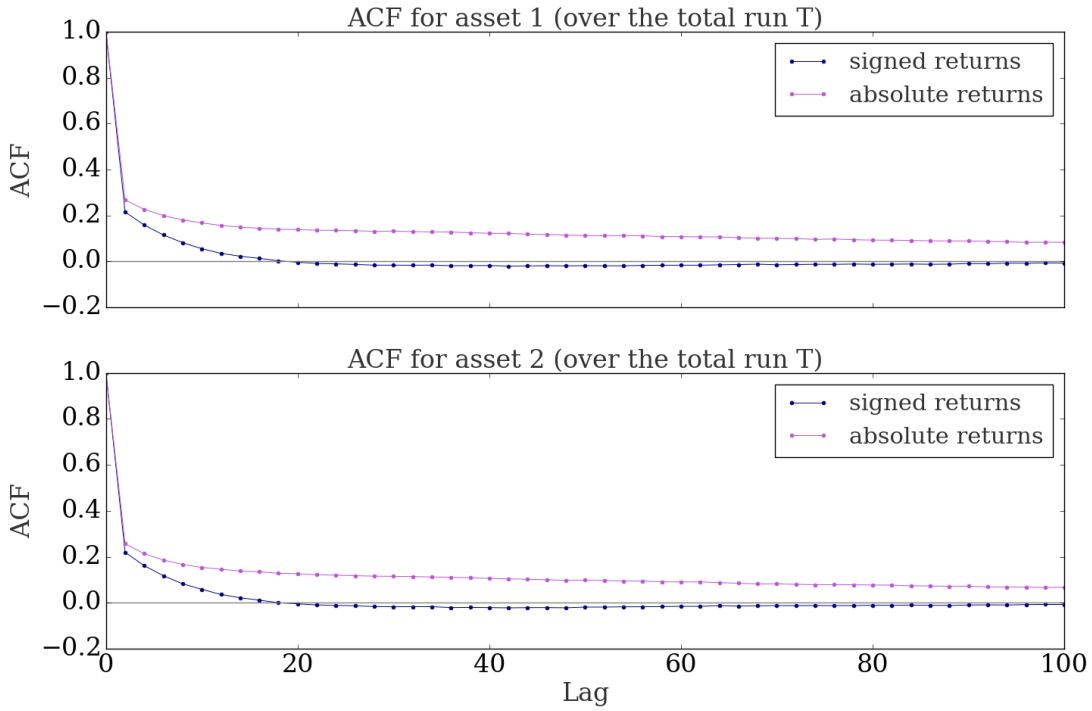

Figure 5.14: The figure shows the typical autocorrelation functions of signed and absolute returns for asset 1 and asset 2. The autocorrelation functions have been computed as an average over 300 simulations with different seed and Ornstein-Uhlenbeck κ_t and $T = 5000$ time steps. In order to compute a better estimation we have used the values for $t > 1000$ time steps. For the simulation, we have used the parameters in tab. 5.1, $\rho = 0.3$, $f = 0.05$.

Chapter 6

Conclusion

The goal of the present Thesis is to introduce the original market model formulated by Kaizoji et al. (2015) and extend it to the multi-assets framework. In the original version, the model was an equilibrium ABM of fundamentalists and noise traders that can invest in a risky asset or a risk-free asset. The major result obtained by the underlying model is the reproduction of faster-than-exponential price growth, typical of financial bubbles.

Chapter 2 and Chapter 3 have been dedicated to the description of the original model and the explanations of the major characteristics of the time series and a detailed theoretical analysis of the formation of the super-exponential growth of the price. In Chapter 3, we have introduced the extension of the original model to the multi-assets framework. Particular emphasis was given to the formulation of fundamentalists and noise traders strategies.
Fundamentalists invest the portion of the wealth into the risky assets that maximize the expected utility function on future wealth. Nevertheless, in the presence of more risky assets, fundamentalists have to form expectations on the future returns correlations, choosing a priori a correlation coefficient for the assets. Though, their choice may not be consistent with the realised correlations and their expectation on future relations can effect the market development.
As far as regards the noise traders class, it has been divided into two subgroups of traders holding only one type of risky asset. Any noise trader invests all his fortune into one type of asset at the time, but the switching between the two sub-classes allows to diversify the aggregate portfolio of the whole class. In Chapter 5 the main findings of the modified model have been presented. The most relevant result of the typical time series with Ornstein-Uhlenbeck herding propensity is the correlated build-up of bubbles in the prices trends. In order to deepen our theoretical insight into the model, we have adopted a mean-field approach and derived the mean-values equations regulating the opinion indices of the noise traders class. According to our

findings, there exists two different regimes according to the value of the herding propensity. When $\kappa > \kappa_c$, the system is unstable and the the opinion indices diverges from their stable equilibria. On the contrary, for $\kappa < \kappa_c$, the stability of the opinion indices depends on the composition of the noise traders sub-classes. The excess of traders investing on one risky assets or the other can cause inner instabilities. the presence of a inherent instabilities created by herding behavior has been confirmed also by the simulated data. Therefore, bubbles are triggered by the time-varying herding propensity. When the herding propensity overcome the threshold, the system enters in an unstable regime: the noise traders are influenced by the increasing number of traders holding the risky assets. The emergence of the collective agreement among noise traders influences the price dynamics and thus the price momentum tracks, which in turn conditions the number of risky assets holders. The reinforcing feedback loop is at the origin of the fact that the faster-than-exponential growth is sustained even when the herding propensity reverts to the stable range.
The second part of the analysis regards a deeper research on the correlations between the two assets and how they depend on fundamentalists expectations and on the exogenous parameter f controlling the switching of noise traders between the sub-classes. The most important aspect is the discrepancy between the formation of expectations by fundamentalists and the real correlations in time series. Fundamentalists are not always correct on the future development of the market and their beliefs can influence the price tracks. However, there exists a value of the correlation that matches with the realised correlation. The presence of the intersection opens to the possibilities of new strategies aiming to actually understand the real value of the correlations through a learning method based on previous data. In the present model, fundamentalists have constant expectations but they could actually update their beliefs in time learning from previous data. In this way, they could match the expected correlations with the realised correlations.
Eventually, we have showed that the model is able to retrieve many stylized facts of the financial market, such as fat tails in the returns distribution and the long-range memory in the auto-correlation function of the volatility.

In conclusion, we have achieved the goal to extend the original model and derived a modified version that takes account of two types of risky assets. The model is able to reproduce financial bubbles in the case of Orstein-Uhlenbeck propensity and the realised correlations between the assets have been explained in the light of fundamentalist expectations and noise traders behavior. Possible future research on the present work regards the possibility to change the setup of the noise traders class in presence of multiple choices and, as mentioned, the possibility to soften the fundamentalists expectations on future returns and the correlation coefficient.

Bibliography

T. Kaizoji, M. Leiss, A. Saichev, and D. Sornette. Super-exponential endogenous bubbles in an equilibroum model of fundamentalist and chartist traders. *Journal of Economic Behavior and Organization*, 112:289–310, 2015.

G. Harras, C. Tessone, and D. Sornette. Noise-induced volatility of collective dynamics. *Physical Review E*, 85(1), 011150, 2012.

D. Sornette. Physics and Financial Economics (1776-2014): puzzles, Ising and agent-based models. *Reports on Progress in Physics*, 77(6):062001, 2014.

A. Johansen, O. Ledoit, and D. Sornette. Crashes as critical points. *International Journal of Theoretical and Applied Finance*, 3:219–255, 2000.

T. Lux and M. Marchesi. Scaling and criticality in stochastic multiagent model of a financial market. *Nature*, 397:498–500, 1999.

T. Lux. The socio-economic dynamics of speculative markets: interacting agents, chaos, and the fat tails of return distribution. *Journal of Ecomomic Behavior and Organization*, 33:143–165, 1998.

C. Chiarella, R. Dieci, and X-Z. He. Heterogeneity, market mechanisms, and asset price dynamics. In *Handbook of Financial Markets: Dynamics and Evolution.*, chapter 5, pages 277–344. Elsevier, North-Holland, 2009.

E. Fama. Efficient capital markets: a review of theory and empirical work. *Journal of Finance*, 25:383–417, 1970.

T. Lux. Stochastic behavioral asset-pricing models and the stylized fact. In *Handbook of Financial Markets: Dynamics and Evolution.*, chapter 3, pages 161–215. Elsevier, North-Holland, 2009.

R. Dieci and X-Z. He. Heterogeneous agent models in finance. *Research Paper Series 389, Quantitative Finance Research Centre, University of Technology, Sydney.*, 2018.

C. Hommes and B. LeBaron. *Computational Economics: Heterogeneous Agent Modeling.* Elsevier, North-Holland, 2018.

D. Sornette and W-Z. Zhou. Importance of positive feedbacks and over-confidence in a self-fulfilling ising model of financial markets. *Physica A: Statistical Mechanics and its Applications*, 370(2):704–726, 2006.

S. Bornholdt. Expectation bubbles in a spin model of markets: intermittency from frustration across scales. *International Journal od Modern Physics C*, 12(5):667–674, 2001.

T. Kaizoji. Speculative bubbles and crashes in stock markets: an interacting-agent model of speculative activity. *Physica A: Statistical Mechanics and its Applications*, 287:493–506, 2000.

R. Khort. The market impact of exploiting financial bubbles. Master's thesis, ETH Zurich, Switzerland, 2016.

M. Ollikainen. Multiple market regimes in an equilibrium model of fundamentalist and noise traders. Master's thesis, ETH Zurich, Switzerland, 2016.

R. Westphal and D. Sornette. Market impact and performance of arbitrageurs od financial bubbles in an agent-based model. *Swiss Finance Institute*, Research Paper No. 19-29, 2019.

L. Walras. *Eléments d'Economie Politique Pure.* F. Rouge, 1926.

J. R. Conti. Long-term behavior of an artificial market, composed of fundamentalists and noise traders. Master's thesis, ETH Zurich, Switzerland, 2018.

C. Chiarella and X-Z. He. Asset price and wealth dynamics under heterogeneous expectations. *Quantative Finance*, 1:509–526, 2001.

M. Kelly. All their eggs in one basket: Portfolio diversification of US households. *Journal of Economic Behavior and Organization*, 27:87–96, 1995.

G. Harras and D. Sornette. How to grow a bubble: A model of myopic adapting agents. *Journal of Economic Behavior and Organization.*, 80:137–152, 2011.

D. Sornette. Sweeping of an instability: an alternative to self-organized criticality to get power laws without parameter tuning. *Journal de Physique I France*, 4: 209–221, 1994.

W. Brock and C. Hommes. Heterogeneous beliefs and routes to chaos in a simple asset-pricing model. *Quantative Finance Reseach Centre*, 22:1235–1274, 1998.

C. Chiarella and X-Z. He. Heterogeneous beliefs, risk and learning in a simple asset-pricing model. *Computational Economics*, 19:95–132, 2002.

C. Chiarella, R. Dieci, and X-Z. He. Heterogeneous expectations and speculative behavior in a dynamics multi-asset framework. *Journal of Economic Behavior and Organization*, 62:408–427, 2007.

V. Bohm and C. Chiarella. Mean-variance preferences, expectations formation and the dynamics of random asset prices. *Mathematical Finance*, 15(1):61–97, 2005.

H. Xu, W. Zhang, X. Xiong, and W. Zhou. Wealth share analysis with Fundamentalist/Chartist heterogeneous agents. *Abstract and Applied Analysis*, 8, 2014.

W. Samuelson and R. Zechauser. Status quo bias in decision making. *Journal of Risk and Uncertainty*, 1:7–59, 1988.

B. Mandelbrot. The variation of certain speculative prices. *The Journal of Business*, 36(4):394–419, 1963.

A. Kirman. Ants, rationality, and recruitment. *Quarterly J. Economics*, 108:137–156, 1993.

T. Lux and M. Marchesi. Volatility clustering in financial markets: a microsimulation of interacting agents. *International Journal of Theoretical and Applied Finance*, 3(4):675–702, 2000.

B. Hill. A simple general appraoch to inference about the tail of a distribution. *Annals of Statistics*, 3(5):1163–1174, 1975.

Appendix A

A.1 Derivation of the prices equations

In this section, we compute the derivation of the price dynamics proceeding from the excess demand equilibrium conditions for each stock (eq. 4.69):

$$\Delta D^{f,1}_{t-1\to t} + \Delta D^{n,1}_{t-1\to t} = x^f_{1,t} W^f_{t-1}\Big[(P_{1,t}+d_{1,t})\frac{x^f_{1,t-1}}{P_{1,t-1}} + (P_{2,t}+d_{2,t})\frac{x^f_{2,t-1}}{P_{2,t-1}} + (1-x^f_{1,t-1}-x^f_{2,t-1})R_f\Big]$$
$$- x^f_{1,t-1} W^f_{t-1}\frac{P_{1,t}}{P_{1,t-1}} + W^n_{1,t-1}x^n_{1,t}\left[(P_{1,t}+d_{1,t})\frac{x^n_{1,t-1}}{P_{1,t-1}} + (1-x^n_{1,t-1})R_f\right] - W^n_{1,t-1}x^n_{1,t-1}\frac{P_{1,t}}{P_{1,t-1}} = 0 \tag{A.1}$$

$$\Delta D^{f,2}_{t-1\to t} + \Delta D^{n,2}_{t-1\to t} = x^f_{2,t} W^f_{t-1}\left[(P_{1,t}+d_{1,t})\frac{x^f_{1,t-1}}{P_{1,t-1}} + (P_{2,t}+d_{2,t})\frac{x^f_{2,t-1}}{P_{2,t-1}} + (1-x^f_{1,t-1}-x^f_{2,t-1})R_f\right]$$
$$- x^f_{2,t-1} W^f_{t-1}\frac{P_{2,t}}{P_{2,t-1}} + W^n_{2,t-1}x^n_{2,t}\left[(P_{2,t}+d_{2,t})\frac{x^n_{2,t-1}}{P_{2,t-1}} + (1-x^n_{2,t-1})R_f\right] - W^n_{2,t-1}x^n_{2,t}\frac{P_{2,t}}{P_{2,t-1}} = 0 \tag{A.2}$$

Considering the definition of the fundamentalist risky fractions $x^f_{1,t}$ and $x^f_{2,t}$ in eq. 4.4:

$$x^f_{1,t} = \frac{A_{1,t}}{P_{1,t}} - \frac{B_{1,t}}{P_{2,t}} + C_{1,t},$$
$$x^f_{2,t} = \frac{A_{2,t}}{P_{1,t}} - \frac{B_{2,t}}{P_{2,t}} + C_{2,t},$$

where the parameters $A_{i,t+1}, B_{i,t+1}, C_{i,t+1}$ can be simply found to be

$$A_{1,t} = \frac{d_{1,t}(1+r_1^d)}{\gamma\bar{\sigma}_1^2(1-\rho^2)}, \tag{A.3a}$$

$$B_{1,t} = \frac{d_{2,t}\rho(1+r_2^d)}{\gamma\bar{\sigma}_1\bar{\sigma}_2(1-\rho^2)}, \tag{A.3b}$$

$$C_{1,t} = \frac{(\bar{\sigma}_2^2(E_{rt,1}-r_f)-\rho\bar{\sigma}_1\bar{\sigma}_2(\mathbb{E}_{rt,2}-r_f))}{\gamma\bar{\sigma}_1^2\bar{\sigma}_2^2(1-\rho^2)}, \tag{A.3c}$$

$$A_{2,t} = \frac{d_{2,t}(1+r_2^d)}{\gamma\bar{\sigma_2}^2(1-\rho^2)}, \tag{A.3d}$$

$$B_{2,t} = \frac{d_{1,t}\rho(1+r_1^d)}{\gamma\bar{\sigma}_1\bar{\sigma}_2(1-\rho^2)}, \tag{A.3e}$$

$$C_{2,t} = \frac{(\bar{\sigma}_1^2(\mathbb{E}_{rt,2}-r_f)-\rho\bar{\sigma}_1\bar{\sigma}_2(\mathbb{E}_{rt,1}-r_f))}{\gamma\bar{\sigma}_1^2\bar{\sigma}_2^2(1-\rho^2)} \tag{A.3f}$$

Consider the equilibrium condition for asset 1 (eq. A.1). After some algebra, one can collect all the terms depending on the prices and rewrite eq. A.1 as:

$$\begin{aligned}
&W_{t-1}^f(A_{1,t}P_{2,t} - B_{1,t}P_{1,t} + C_{1,t}P_{1,t}P_{2,t}) \\
&\Big[(P_{1,t}+d_{1,t})\frac{x_{1,t-1}^f}{P_{1,t-1}} + (P_{2,t}+d_{2,t})\frac{x_{2,t-1}^f}{P_{2,t-1}} + (1-x_{1,t-1}^f - x_{2,t-1}^f)R_f\Big] \\
&- x_{1,t-1}^f W_{t-1}^f \frac{P_{1,t}^2}{P_{1,t-1}} P_{2,t} + P_{1,t}P_{2,t}W_{1,t-1}^n x_{1,t}^n \left[\frac{x_{1,t-1}^n}{P_{1,t-1}}(P_{1,t}+d_{1,t}) + (1-x_{1,t-1}^n)(1+r_f)\right] \\
&- P_{2,t}W_{1,t-1}^n x_{1,t-1}^n \frac{P_{1,t}^2}{P_{1,t-1}} = 0.
\end{aligned}$$

$$\begin{aligned}
0 = {} & P_{1,t}^2\left(-B_{1,t}W_{t-1}^f\frac{x_{1,t-1}^f}{P_{1,t-1}}\right) + P_{2,t}\left(A_{1,t}W_{t-1}^f\frac{x_{2,t-1}^f}{P_{2,t-1}}\right) + P_{1,t}^2P_{2,t}\Big[W_{t-1}^f\frac{x_{1,t-1}^f}{P_{1,t-1}}(C_{1,t}-1) + \\
& W_{t-1}^n\frac{x_{1,t-1}^n}{P_{1,t-1}}(x_{1,t}^n-1)\Big] + P_{1,t}P_{2,t}\Big[x_{1,t}^nW_{1,t-1}^n\left(\frac{x_{1,t-1}^n}{P_{1,t-1}}d_{1,t} + (1-x_{1,t-1})(1+r_f)\right) + A_{1,t}W_{t-1}^f\frac{x_{1,t-1}^f}{P_{1,t-1}} \\
& - B_{1,t}W_{t-1}^f\frac{x_{2,t-1}^f}{P_{2,t-1}}\Big] + P_{1,t}P_{2,t}\left[C_{1,t}W_{t-1}^f\left(d_{1,t}\frac{x_{1,t-1}^f}{P_{1,t-1}} + d_{2,t}\frac{x_{2,t-1}^f}{P_{2,t-1}} + (1-x_{1,t-1}^f-x_{2,t-1}^f)(1+r_f)\right)\right] \\
& + P_{1,t}P_{2,t}^2\left(C_{1,t}W_{t-1}^f\frac{x_{2,t-1}}{P_{2,t-1}}\right) + P_{1,t}\Big[-B_{1,t}W_{t-1}^f\Big(1-x_{1,t-1}^f-x_{2,t-1}^f)(1+r_f) + d_{1,t}\frac{x_{1,t-1}^f}{P_{1,t-1}} + \\
& d_{2,t}\frac{x_{2,t-1}^f}{P_{2,t-1}}\Big)\Big] + P_{2,t}\left[A_{1,t}W_{t-1}^f\left((1-x_{1,t-1}^f-x_{2,t-1}^f)(1+r_f) + d_{1,t}\frac{x_{1,t-1}^f}{P_{1,t-1}} + d_{2,t}\frac{x_{2,t-1}^f}{P_{2,t-1}}\right)\right]
\end{aligned}$$

Which can be read in a simpler way as:

$$a_{1,t}P_{1,t}^2 + b_{1,t}P_{2,t}^2 + c_{1,t}P_{1,t}^2P_{2,t} + d_{1,t}P_{1,t}P_{2,t}^2 + e_{1,t}P_{1,t}P_{2,t} + f_{1,t}P_{1,t} + g_{1,t}P_{2,t} = 0, \quad \text{(A.4)}$$

Similarly, we can derived the equation for the second asset:

$$a_{2,t}P_{2,t}^2 + b_{2,t}P_{1,t}^2 + c_{2,t}P_{2,t}^2P_{1,t} + d_{2,t}P_{2,t}P_{1,t}^2 + e_{2,t}P_{1,t}P_{2,t} + f_{2,t}P_{2,t} + g_{2,t}P_{1,t} = 0. \quad \text{(A.5)}$$

The coefficients of the equations are found by direct comparison and they are listed in the following:

$$a_{1,t} = -B_{1,t}W_{t-1}^f \frac{x_{1,t-1}^f}{P_{1,t-1}}, \quad \text{(A.6a)}$$

$$b_{1,t} = A_{1,t}W_{t-1}^f \frac{x_{2,t-1}^f}{P_{2,t-1}}, \quad \text{(A.6b)}$$

$$c_{1,t} = W_{t-1}^f \frac{x_{1,t-1}^f}{P_{1,t-1}}(C_{1,t} - 1) + W_{t-1}^n \frac{x_{1,t-1}^n}{P_{1,t-1}}(x_{1,t}^n - 1), \quad \text{(A.6c)}$$

$$d_{1,t} = C_{1,t}W_{t-1}^f \frac{x_{2,t-1}^f}{P_{2,t-1}}, \quad \text{(A.6d)}$$

$$\begin{aligned} e_{1,t} = {} & x_{1,t}^n W_{1,t-1}^n \left[d_{1,t}\frac{x_{1,t-1}^n}{P_{1,t-1}} + (1 - x_{1,t-1}^n)(1 + r_f) \right] + A_{1,t}W_{t-1}^f \frac{x_{1,t-1}^f}{P_{1,t-1}} - B_{1,t}W_{t-1}^f \frac{x_{2,t-1}^f}{P_{2,t-1}} \\ & + C_{1,t}W_{t-1}^f \left[\frac{d_{1,t}x_{1,t-1}^f}{P_{1,t-1}} + d_{2,t}\frac{x_{2,t-1}^f}{P_{2,t-1}} + (1 - x_{1,t-1}^f - x_{2,t}^f)R_f \right], \end{aligned} \quad \text{(A.6e)}$$

$$f_{1,t} = -B_{1,t}W_{t-1}^f \left[(1 - x_{1,t-1}^f - x_{2,t-1}^f)(1 + r_f) + d_{1,t}\frac{x_{1,t-1}^f}{P_{1,t-1}} + d_{2,t}\frac{x_{2,t-1}^f}{P_{2,t-1}} \right], \quad \text{(A.6f)}$$

$$g_{1,t} = A_{1,t}W_{t-1}^f \left[(1 - x_{1,t-1}^f - x_{2,t-1}^f)(1 + r_f) + d_{1,t}\frac{x_{1,t-1}^f}{P_{1,t-1}} + d_{2,t}\frac{x_{2,t-1}^f}{P_{2,t-1}} \right], \quad \text{(A.6g)}$$

$$a_{2,t} = -B_{2,t} W^f_{t-1} \frac{x^f_{2,t-1}}{P_{2,t-1}}, \tag{A.7a}$$

$$b_{2,t} = A_{2,t} W^f_{t-1} \frac{x^f_{1,t-1}}{P_{1,t-1}}, \tag{A.7b}$$

$$c_{2,t} = W^f_{t-1} \frac{x^f_{2,t-1}}{P_{2,t-1}} (C_{2,t} - 1) + W^n_{t-1} \frac{x^n_{2,t-1}}{P_{2,t-1}} (x^n_{2,t} - 1), \tag{A.7c}$$

$$d_{2,t} = C_{2,t} W^f_{t-1} \frac{x^f_{1,t-1}}{P_{1,t-1}}, \tag{A.7d}$$

$$\begin{aligned} e_{2,t} = {} & x^n_{2,t} W^n_{2,t-1} \left[d_{2,t} \frac{x^n_{2,t-1}}{P_{2,t-1}} + (1 - x^n_{2,t-1})(1 + r_f) \right] + A_{2,t} W^f_{t-1} \frac{x^f_{2,t-1}}{P_{2,t-1}} - B_{2,t} W^f_{t-1} \frac{x^f_{1,t-1}}{P_{1,t-1}} \\ & + C_{2,t} W^f_{t-1} \left[\frac{d_{1,t} x^f_{1,t-1}}{P_{1,t-1}} + d_{2,t} \frac{x^f_{2,t-1}}{P_{2,t-1}} + (1 - x^f_{1,t-1} - x^f_{2,t-1}) R_f \right], \end{aligned} \tag{A.7e}$$

$$f_{2,t} = -B_{2,t} W^f_{t-1} \left[(1 - x^f_{1,t-1} - x^f_{2,t-1})(1 + r_f) + d_{1,t} \frac{x^f_{1,t-1}}{P_{1,t-1}} + d_{2,t} \frac{x^f_{2,t-1}}{P_{2,t-1}} \right], \tag{A.7f}$$

$$g_{2,t} = A_{2,t} W^f_{t-1} \left[(1 - x^f_{1,t-1} - x^f_{2,t-1})(1 + r_f) + d_{1,t} \frac{x^f_{1,t-1}}{P_{1,t-1}} + d_{2,t} \frac{x^f_{2,t-1}}{P_{2,t-1}} \right] \tag{A.7g}$$

Appendix B

B.1 Stability analysis of the line of fixed points

In this section, we want to analyze the conditions of the stability for the line of fixed points for the mean-value equations of z, s_1 and s_2, defined in section 5.3. The line of fixed points is $(s_1^* = s, s_2^*, z^*)$, where s is defined in eq. 5.17.
In order to study the stability of the continuum of fixed points we consider the entries of the Jacobian matrix J evaluated at the equilibrium:

$$a_{11} = \frac{d\dot{z}}{dz} = 0, \tag{B.1}$$

$$a_{12} = \frac{d\dot{z}}{ds_1} = \begin{cases} \frac{\kappa f}{4} z^*(1+s) & \text{if } s_2 - s_1 > 0 \\ \frac{\kappa f}{4}(1-z^*)(1+s) & \text{if } s_2 - s_1 < 0 \end{cases} \tag{B.2}$$

$$a_{13} = \frac{d\dot{z}}{ds_2} = \begin{cases} -\frac{\kappa f}{4} z^*(1+s) & \text{if } s_2 - s_1 > 0 \\ -\frac{\kappa f}{4}(1-z^*)(1+s) & \text{if } s_2 - s_1 < 0 \end{cases} \tag{B.3}$$

$$a_{21} = \frac{d\dot{s_1}}{dz} = 0, \tag{B.4}$$

$$a_{22} = \frac{d\dot{s_1}}{ds_1} = \begin{cases} -\left(\frac{p^- + p^+}{2}\right) + \kappa - \frac{(1+s)^2}{4}\kappa f & \text{if } s_2 - s_1 > 0 \\ -\frac{p^- + p^+}{2} + \kappa + \left(\frac{1-z^*}{z^*}\right)\frac{\kappa f}{4}(1+s)(1-s) & \text{if } s_2 - s_1 < 0 \end{cases} \tag{B.5}$$

$$a_{23} = \frac{d\dot{s_1}}{ds_2} = \begin{cases} \frac{\kappa f}{4}(1+s)^2 & \text{if } s_2 - s_1 > 0 \\ \frac{1-z^*}{z^*}\frac{\kappa f}{4}(1+s)(s-1) & \text{if } s_2 - s_1 < 0 \end{cases} \tag{B.6}$$

$$a_{31} = \frac{d\dot{s_2}}{dz} = 0, \tag{B.7}$$

$$a_{32} = \frac{d\dot{s_2}}{ds_1} = \begin{cases} \frac{\kappa f}{4}\frac{z^*}{1-z^*}(1+s)(s-1) & \text{if } s_2 - s_1 > 0 \\ \frac{\kappa f}{4}(1+s)^2 & \text{if } s_2 - s_1 < 0 \end{cases} \tag{B.8}$$

$$a_{33} = \frac{d\dot{s_2}}{ds_2} = \begin{cases} -\left(\frac{p^- + p^+}{2}\right) + \kappa + \left(\frac{z^*}{1-z^*}\right)\frac{\kappa f}{4}(1+s)(1-s), & \text{if } s_2 - s_1 > 0 \\ -\frac{p^- + p^+}{2} + \kappa - \frac{\kappa f}{4}(1+s)^2 & \text{if } s_2 - s_1 < 0 \end{cases} \tag{B.9}$$

The discontinuity in the derivatives is due to the condition of non-negativity imposed to the transition probabilities p_{12}^+ and p_{21}^+. Considering separately the cases $s_2 - s_1 > 0$ and $s_2 - s_1 < 0$, one can find the equations for the eigenvalues λ_i of the non-linear differential equations, finding the roots of $J - \lambda I = 0$:

$$(-\lambda)[(a_{22} - \lambda)(a_{33} - \lambda) - a_{23}a_{32}] = 0. \tag{B.10}$$

Thus an eigenvalue is simply $\lambda_1 = 0$, whereas the other two roots can be expressed as a function of the determinant and the trace of the sub-matrix J' obtained eliminating the first row and the first column from J. Namely, we have

$$\lambda_{2,3} = \frac{\tau}{2} \pm \frac{1}{2}\sqrt{\tau^2 - 4\Delta}, \tag{B.11}$$

where τ and Δ are defined as

$$\tau = a_{22} + a_{33}, \tag{B.12}$$

$$\Delta = a_{22}a_{33} - a_{23}a_{32}. \tag{B.13}$$

In order to ensure the stability of the fixed points, it is necessary that $\lambda_{2,3} < 0$. This conditions is reflected on the following conditions on the trace and the determinant:

$$(1) \;\; \tau < 0 \;\; \text{and} \;\; (2) \;\; \Delta > 0. \tag{B.14}$$

The insertion of the values of Jacobian entries in the first condition leads to

$$(1) \quad \begin{cases} -(p^- + p^+) + 2\kappa - \frac{\kappa f}{4}(1+s)^2 + \left(\frac{z^*}{1-z^*}\right)\frac{\kappa f}{4}(1+s)(1-s) < 0 & \text{if } \; s_2 - s_1 > 0, \\ -(p^- + p^+) + 2\kappa - \frac{\kappa f}{4}(1+s)^2 + \left(\frac{1-z^*}{z^*}\right)\frac{\kappa f}{4}(1+s)(1-s) < 0 & \text{if } \; s_2 - s_1 < 0. \end{cases} \tag{B.15}$$

The condition on the determinant determines the following if $\kappa < \frac{p^+ + p^-}{2} = \kappa_c$:

$$(2) \quad \begin{cases} -\frac{p^- + p^+}{2} + \kappa - \frac{\kappa f}{4}(1+s)^2 + \left(\frac{z^*}{1-z^*}\right)\frac{\kappa f}{4}(1+s)(1-s) < 0 & \text{if } \; s_2 - s_1 > 0, \\ -\frac{p^- + p^+}{2} + \kappa - \frac{\kappa f}{4}(1+s)^2 + \left(\frac{1-z^*}{z^*}\right)\frac{\kappa f}{4}(1+s)(1-s) < 0 & \text{if } \; s_2 - s_1 < 0. \end{cases} \tag{B.16}$$

If $\kappa > \kappa$ we have the opposite inequality. The four conditions can be satisfied simultaneously only in the case $\kappa < \kappa_c$. In this case, the line of fixed points is stable only if $z^* \in [z_b, z_a]$, where z_a and z_b are obtained by eq. B.16 as the range of values satisfying the conditions (2):

$$z_a(\kappa) = \frac{\frac{\kappa f}{4}(1+s)^2 + \frac{p^+ + p^-}{2} - \kappa}{\frac{\kappa f}{2}(1+s) + \frac{p^+ + p^-}{2} - \kappa}, \tag{B.17}$$

$$z_b(\kappa) = \frac{\frac{\kappa f}{4}(1+s)(1-s)}{\frac{\kappa f}{2}(1+s) + \frac{p^+ + p^-}{2} - \kappa}. \tag{B.18}$$

The critical lines for z^* are discussed in sec. 5.3.

B.2 Comparison between log-prices and moving window Pearson correlation

Figure B.1 shows four plots obtained from different simulations with different seeds. Each plot shows the comparison between the log-prices $log(P_{1,t}), log(P_{2,t})$ and the moving window Pearson correlation. As explained in sec. 5.2 during the bubbles regime the moving window Pearson coefficient reaches the maximum, indicating the synchronization betweeen the two assets, wheres during the stable regime the correlation is very fluctuation. With this illustrative example, we aim to pass the idea that the synchronization phenomenon is not limited to the example presented in sec. 5.2, but it is present in the simulated time series for different seeds.

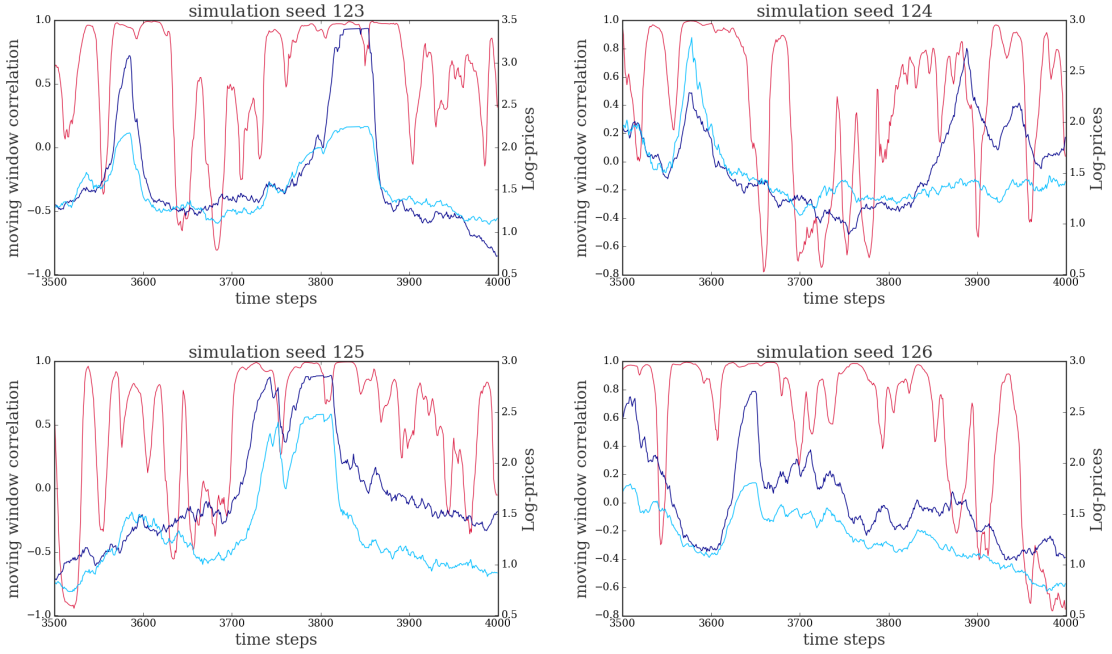

Figure B.1: The figure shows four different plots showing the comparison between the bubbles regime and the moving window Pearson coefficient, obtained for 4 different simulations with different seeds. The moving window Pearson correlation is computed over a time window of $w = 25$ time steps. The plots show two different scales: on the right the scale for the moving correlation and on the left for the log-prices.